Altering Reservoir Wettability to Improve Production from Single Wells

Final Report

Reporting Period Start Date: October 1, 2004

Reporting Period End Date: September 30, 2006

Principal Author: W.W. Weiss, Senior Engineer

Report Date: November 30, 2006

Cooperative Agreement Number: No. DE-FG26-4NT15527

Correlations Company
P.O. Box 730
115 Court Street
Socorro, NM 87801

Altering Reservoir Wettability to Improve Production from Single Wells

Table of Contents

	Pages
List of Figures	4
List of Tables	7
Executive Summary	8
Results of Work	9
Approach	11
Results and Discussion	11
Part A Laboratory	11
San Andres Furhman Masho Field	11
Brine Composition	12
Crude Oil Properties	12
Reservoir Core Properties	12
Surfactant and Interfacial Tension Measurements	17
Laboratory Procedures	20
Results	20
Summary	27
San Andres Eagle Creek Field	27
Laboratory Tests	27
Results	28
Cedar Creek Anticline Dolomite Field	33
Brine Composition	33
Crude Oil Properties	33
Reservoir Core Properties	35
Surfactant Solutions	38
Laboratory Procedure	39
Results	39
Nuclear Magnetic Resonance Carr-Meiboom-Gill Measurements	46
Summary	50
Part B Engineering	51
Overview	51
Cottonwood Creek Revisit	52
San Andres Dolomite Reservoirs	56
West Fuhrman Masho Unit	56
Eagle Creek San Andres Field	58
Fullerton San Andres Field	61
Matlab Neural Network Toolbox	69
AI Analysis of Cedar Creek NMR Dataset **References**	73

Cost and Schedule Status 84
Accomplishments 84
Actual Problems 84
Technology Transfer Activities 84
Conclusions 85
References 85

List of Figures

		Page
1.	Distribution of permeability and porosity of Fuhrman Masho cores.	15
2.	Distribution of permeability and porosity of Eagle Creek cores.	16
3.	Thin sections of Fuhrman Masho rock.	16
4.	Thin sections of Eagle Creek rocks	17
5.	Interfacial tensions of nonionic surfactant solutions and Soltrol.	18
6.	Interfacial tensions of cationic, anionic, and amphoteric surfactant solutions and Soltrol 220.	19
7.	Oil recovery by imbibition for Fuhrman Masho C zone rock/crude oil/FM brine and T91-8 solution ($S_{wi} = 0$).	21
8.	Oil recovery by imbibition for Fuhrman Masho C zone rock/crude oil/FM brine and T91-8 solution ($S_{wi} > 0$).	21
9.	Oil recovery by imbibition for Fuhrman Masho B zone rock/crude oil/FM brine and T91-8 solution ($S_{wi} = 0$).	22
10.	Oil recovery by imbibition for Fuhrman Masho B zone rock/crude oil/FM brine and T91-8 solution ($S_{wi} > 0$).	22
11.	Data set consists of both B & C zone core plugs.	23
12.	Data set consists of B zone plugs.	24
13.	Data set consists of C zone plugs.	24
14.	Summary of BVO versus oil recovery from both B and C zones.	25
15.	Examples of C zone cores with other surfactants ($S_{wi} = 0$).	26
16.	Examples of B zone cores with other surfactants ($S_{wi} = 0$).	26
17.	Examples of B zone cores with other surfactants ($S_{wi} > 0$).	27
18.	Oil recovery versus imbibition for Eagle Creek rock/oil/EC brine and T91-8 solution ($S_{wi} = 0$).	29
19.	Imbibition tests of Eagle Creek rock/oil/EC brine and T91-8 solutions ($S_{wi} > 0$).	29
20.	Imbibition oil recovery for FM oil/Eagle cores/seawater system.	30
21.	Imbibition oil recovery for FM oil/Eagle cores/seawater system (more surfactants).	31
22.	Imbibition oil recovery for Eagle cores/FM oil/seawater system.	31
23.	Imbibition oil recovery for Eagle cores/FM oil/seawater system (more surfactants).	32
24.	Stony Mountain Crude oil before (left) and after (right) sonic agitation and mixing.	34
25.	Heating followed by sonic mixing did not dissolve the precipitate.	35
26.	Left to right: 80, 50, and 20% 1-methylnaphthalene added to Stony Mountain crude oil.	35
27.	Permeabilities and porosities of all cores.	37
28.	Thin sections of Interlake dolomite.	37
29.	Thin sections of Stony Mountain dolomite.	38
30.	Thin sections of Red River dolomite.	38
31.	Interlake oil IFTs as a function of pH.	40

32.	Stony Mountain oil IFTs as a function of pH.	40
33.	Red River oil IFTs as a function of pH.	41
34.	Imbibition results for Sony Mountain cores when $S_{wi} = 0$.	42
35.	Imbibition results for Sony Mountain cores when $S_{wi} > 0$.	42
36.	Spontaneous imbibition of Red River cores for $S_{wi} = 0$.	43
37.	Spontaneous imbibition of Red River cores for $S_{wi} > 0$.	44
38.	Spontaneous imbibition of Interlake cores for $S_{wi} = 0$.	44
39.	Effect of permeability and BVO on oil recovery by imbibition.	45
40.	NMR scanning curves for Sony Mountain cores of $S_{wi} = 0$.	46
41.	NMR scanning curves for Sony Mountain cores of $S_{wi} > 0$.	47
42.	NMR scanning curves before and after imbibition for Red River cores.	48
43.	NMR scanning curves before and after imbibition for Interlake cores.	49
44.	Comparison of porosity between measured and NMR derived.	49
45.	Comparison of water saturation between measured and NMR derived.	50
46.	23-well composite performance through November 2005	53
47.	Cottonwood Creek well 218 performance through November 2005	54
48.	Cottonwood Creek fuzzy curve: before and after oil rates	55
49.	Results of the Cottonwood Creek neural network training	55
50.	Well 152 initial response	57
51.	Well 242 initial response	57
52.	Well 243 initial response	58
53.	Variation in water hardness	59
54.	Neural network training result	60
55.	Water-frac neural network training results	62
56.	Volume fuzzy curve	67
57.	Quantity of sand fuzzy curve	67
58.	Fullerton San Andres before/after oil rate fuzzy curve	68
59.	Matlab 3-3-1 NN training results with Cottonwood Creek dataset	69
60.	SNNS training result, 2-5-1 architecture	70
61.	Matlab NN toolbox training result, 2-5-1 architecture	71
62.	SNNS training result, 2-8-1 architecture	71
63.	Matlab NN toolbox training result, 2-8-1 architecture	72
64.	Calculated using NMR software vs. actual porosity	74
65.	T2 distribution of the two outliers shown in Figure 64	74
66.	Porosity training results with a 2-3-1 neural network	75
67.	All samples with Sw >0%, maximum and kurtosis as inputs	77
68.	All samples with Sw >0%, maximum and sum as inputs	78
69.	Statistical parameters generated from after-brine imbibition T2 scans dataset	80
70.	NORM Ccalc brine dataset with maximum and kurtosis to predict brine BVW	81
71.	Predicted after-surfactant imbibition versus measured BVW	82
72.	NMR calculated Sw following surfactant imbibition	82

73. 2-3-1 neural network prediction versus measured values of Swi 83
74. NMR calculated Swi versus measured Swi 83

List of Tables

		Page
1	Test brine composition and concentration (g/L)	12
2.	Crude oil properties	12
3.	Fuhrman Masho reservoir cores from C zone and properties	13
4.	Fuhrman Masho reservoir cores from B zone and properties	14
5.	Physical and chemical properties of four surfactants	17
6.	Physical and chemical properties of other surfactants	18
7.	IFTs between San Andres crude oil and surfactant solutions	19
8.	Crude oil properties and related IFTs (mN/m)	20
9.	Properties of Eagle Creek reservoir cores	27
10.	Water analysis from Encore Acquisition Co.	33
11.	Composition of laboratory synthetic formation water	33
12.	Crude oil properties	34
13.	Reservoir cores from Cedar Creek anticline	36
14.	Physical and chemical properties of anionic surfactants CD-128 and RA-246L	39
15.	IFT measurements of anionic surfactants CD-128 and RA-246L	39
16.	Neural network predicted response	56
17.	Optimum surfactant treatments	60
18.	Available water-frac data summary	61
19.	Fuzzy ranking of well log statistical parameters with water-frac production response, BOPD	62
20.	Neural network open hole log training results	63
21.	Cased-hole gamma ray log training	63
22.	GR-neutron log attributes used to predict water-frac response	64
23.	GR log attributes used to predict water-frac response	65
24.	Gamma ray log attributes used to predict water-frac response	65
25.	Fullerton Field forecasted surfactant stimulation results	69
26.	Statistical properties of T2 scans prior to imbibition normalized with core bulk volume	73
27.	Forty-six core samples with Sw > 0%	76
28.	Statistical parameters of 19 core samples, initial t2 scans	78
29.	Statistical parameters of 19 core samples after brine imbibition t2 scans	79
30.	Statistical parameters of 19 core samples after surfactant imbibition t2 scans	79
31.	Training results of the 13 network architectures	81

Executive Summary

Many carbonate reservoirs are naturally fractured and typically produce less than 10% original oil in place during primary recovery. Spontaneous imbibition has proven an important mechanism for oil recovery from fractured reservoirs, which are usually weak waterflood candidates. In some situations, chemical stimulation can promote imbibition of water to alter the reservoir wettability toward water-wetness such that oil is produced at an economic rate from the rock matrix into fractures. In this project, cores and fluids from five reservoirs were used in laboratory tests: the San Andres formation (Fuhrman Masho and Eagle Creek fields) in the Permian Basin of Texas and New Mexico; and the Interlake, Stony Mountain, and Red River formations from the Cedar Creek Anticline in Montana and South Dakota. Solutions of nonionic, anionic, and amphoteric surfactants with formation water were used to promote water-wetness. Some Fuhrman Masho cores soaked in surfactant solution had improved oil recovery up to 38%. Most Eagle Creek cores did not respond to any of the tested surfactants. Some Cedar Creek anticline cores had good response to two anionic surfactants (CD 128 and A246L). The results indicate that cores with higher permeability responded better to the surfactants. The increased recovery is mainly ascribed to increased water-wetness. It is suspected that rock mineralogy is also an important factor.

The laboratory work generated three field tests of the surfactant soak process in the West Fuhrman Masho San Andres Unit. The flawlessly designed tests included mechanical well clean out, installation of new pumps, and daily well tests before and after the treatments. Treatments were designed using artificial intelligence (AI) correlations developed from 23 previous surfactant soak treatments. The treatments were conducted during the last quarter of 2006. One of the wells produced a marginal volume of incremental oil through October. It is interesting to note that the field tests were conducted in an area of the field that has not met production expectations. The dataset on the 23 Phosphoria well surfactant soaks was updated. An analysis of the oil decline curves indicted that 4.5 lb of chemical produced a barrel of incremental oil. The AI analysis supports the adage “good wells are the best candidates.” The generally better performance of surfactant in the high permeability core laboratory tests supports this observation.

AI correlations were developed to predict the response to water-frac stimulations in a tight San Andres reservoir. The correlations maybe useful in the design of Cedar Creek Anticline surfactant soak treatments planned for next year.

Nuclear Magnetic Resonance scans of dolomite cores to measure porosity and saturation during the high temperature laboratory work were acquired. The scans could not be correlated with physical measurement using either conventional or AI methods.

Results of Work

Many carbonate reservoirs are naturally fractured and typically produce less than 10% original oil in place (OOIP) during primary recovery. Those reservoirs respond poorly to water injection, but spontaneous imbibition with water has proven to be effective. In some situations, chemical stimulation can promote imbibition of water to alter the reservoir wettability toward water-wetness such that oil can be produced at an economic rate. In this project, water-wetness was promoted with nonionic, anionic, and amphoteric surfactants. After preparing core samples using the corresponding reservoir crude oil and brine, spontaneous production of oil was measured in glass imbibition cells at reservoir temperature. After imbibition had ceased, the cores were transferred into surfactant solutions above the critical micelle concentration (CMC) to test for enhanced recovery by further imbibition.

The San Andres formation in the Permian Basin of Texas and New Mexico is one of the great oil-producing formations in the United States. An estimated 50,000 wells produce oil from this oil-wet carbonate reservoir. Thus, the San Andres was the largest target reservoir for the technology being developed through this project. Cores and reservoir fluids from Fuhrman Masho and Eagle Creek fields of the San Andres formation were used in the laboratory for low temperature (104°F) imbibition tests. Initially, the Interlake, Stony Mountain, and Red River dolomite reservoirs on the Cedar Creek Anticline were candidates for the surfactant soak process. These reservoirs are second to the San Andres in terms of surfactant soak potential. Cores and fluids from these high temperature reservoirs (200^{o}F) were used to conduct imbibition experiments in a laboratory equipped for high temperature work.

Reservoir brine used as the imbibition fluid in Fuhrman Masho cores generated oil recovery in the range of 0–4% of the OOIP. Immersion in T91-8 surfactant solution resulted in additional recovery up to 38% OOIP. The increased recovery is mainly ascribed to increased water-wetness. When synthetic reservoir brine was used as the imbibition fluid in Eagle Creek cores, oil recovery was up to 35% of the OOIP. Immersion in surfactant solutions did not improve oil recovery significantly; only one core had a 6% increase in oil, but most cores did not respond to any surfactant tested. Therefore, the Eagle Creek field is not a candidate for the spontaneous imbibition process with the proposed surfactants.

The high temperature imbibition tests with Cedar Creek Anticline cores demonstrated that surfactant generates additional oil in the Interlake and Stony Mountain reservoir systems. Surprisingly the Red River system appeared to be water-wet with very high imbibition oil recovery from cleaned cores. Surfactant did not improve oil recovery from these cores; however, improvement was seen in the non-cleaned cores.

Arbuckel formation core material and fluids from Kansas arrived late in the project life. Future plans are to conduct imbibition tests with this system.

The results of the laboratory work indicate that an initial wettability in the range of weakly water-wet to oil-wet can be altered to more water-wet by the use of surfactants to promote spontaneous imbibition. The success of the surfactant treatment may also depend on the pore structure and mineralogy.

The possible mechanisms of the improved imbibition of surfactant solutions in this project are as follows: cationic ions interact with the adsorbed anionic materials from the crude oil, resulting in the release of the adsorbed organic materials from the rock surface. The rock surface becomes more water-wet, and the imbibition rate is increased[1] due to an increase in capillary pressure resulting from alteration of the contact angle.

In the presence of surfactant, the interfacial tensions (IFTs) between the crude oil and the surfactant solutions are much lower than that of the crude oil and the synthetic brine. For a nonionic surfactant, the mechanism may be the decrease of the IFT between oil and brine. The corresponding increase in the Bond number, $N_a = \rho g r^2 / \sigma$, probably contributed to improved oil recovery through gravity segregation.[2] If the IFT is sufficiently low, capillary pressure P_c is also very small. Gravity segregation will then significantly contribute to oil recovery in cores.

Anionic surfactants can decrease the IFT and improve gravity segregation. For carbonate rock surfaces, anionic surfactants can alter the wettability to more water-wet.[3] The anionic surfactant may increase capillary pressure via adsorption.

Since displacement is not a factor, the single well surfactant soak process is dependent on the surface area of the formation exposed to the wettability altering surfactant. Thus, fractured wells are candidates. Adding the surfactant with hydraulic fracturing fluids is also feasible. A field-testing plan based on adding the nonionic surfactant to water-frac stimulations was developed. The plan called for test wells that had not been previously stimulated; hence, a direct before-and-after comparison of improved oil recovery due to imbibition is not possible. However an AI-based method was developed to establish a benchmark against which future water-frac wells plus surfactant can be evaluated. The before-and-after responses of approximately 80 water-fraced wells were examined. Suitable neural network correlations were found to predict water-frac results given the current oil producing rate, and the gamma ray and the neutron log response patterns through the fractured zone. The AI method can be applied to either open-or cased-hole logs. The operator of a tight San Andres dolomite reservoir elected not to conduct the tests due to excessive service company costs.

Well logs and production history of producing wells in the Eagle Creek San Andres field on the northwest flank of the Permian Basin were acquired to predict surfactant soak responses. The predictions were based on AI correlations developed from field tests conducted in a Phosphoria dolomite reservoir in the Big Horn basin of Wyoming. While the correlation suggested that the process should be tested, the laboratory work failed to support a field test.

The operator of the Cedar Creek Anticline reservoirs is considering surfactant soak tests in the Interlake and Stony Mountain reservoirs. The AI correlations will be utilized in the stimulation designs. Field tests are expected during the first quarter of 2007.

The Phosphoria 23-well surfactant soak dataset was revisited and updated. The increase in the producing time since the well treatments were conducted facilitated more accurate analyses of the oil decline rate. It is evident that these initial experimental treatments generated 15,000 bbl of incremental oil. The recovery can be expressed as 4.5 lb of surfactant per barrel of incremental oil. The wells were treated during last half of 2002 and early 2003 when the cost of surfactant was about $0.80/lb. Today the surfactant cost is over $1.00/lb.

Late in the project life Range Resources conducted three very well monitored tests in the West Fuhrman Masho field. While not complete, one test appeared to be marginally successful. No response was observed at the others.

As available, the laboratory results were presented to Encore Acquisition, ConocoPhillips, Yates Petroleum, Range Resources, Texland Petroleum, Cano Petroleum, and Kinder Morgan. Results of the San Andres laboratory work geared toward service company needs were also presented to Tiorco and Gel-Tec, small niche-type service companies located in Denver, Colorado, and Midland, Texas.

Approach

The project approach consisted of laboratory testing with reservoir systems followed by field tests if supported by laboratory results. The resulting field tests will be included in a database that will be used to design and improve future field treatments. This report is divided into a laboratory section and an engineering section to follow the approach used.

Results and Discussion

Part A Laboratory

Spontaneous imbibition can be especially important to oil recovery from fractured reservoirs. However, spontaneous imbibition does not take place if rocks are oil-wet or neutral-wet. Spontaneous imbibition only occurs when the pore surfaces are effectively water-wet so that the water imbibes into the rock matrix, and oil is produced into the fractures. The oil can be flushed along the fractures toward the production wellbore. This project investigated the use of chemicals to modify the wettability of reservoir rock to a more water-wet state in order to produce additional oil via spontaneous imbibition. The significance of spontaneous imbibition as a recovery mechanism was first recognized for the naturally fractured water-wet Spraberry field of west Texas in the early 1950s,[4] and oil recovery by spontaneous imbibition from the Spraberry field is still being promoted.[5] Improved oil recovery with surfactants has been studied for over 40 years. Craig[6] showed that surfactants can alter the rock surface from oil-wet to surfactant-wet and then the oil can be displaced from the pores. Stone et al.[7] improved displacement-type oil recovery by altering the rock surface to oil-wet. Extensive laboratory research on improved oil recovery from carbonate cores by imbibition of cationic and nonionic surfactant solutions has been reported by Spinler et al.[8] and Austad et al.[9] The surfactant interacts with and removes the adsorbed organic materials from the rock surface, which then becomes water-wet, and imbibition is enhanced. Chen et al.[2] reported the use of nonionic surfactants to stimulate oil wells in the Yates San Andres reservoir. The average oil-production rate for one well increased from 35 to 67 barrels per day for an incremental 17,000 barrels of oil at the time of publication. Improved recovery was ascribed to altering the rock surface wettability and/or gravity segregation of oil and water between the fracture and the matrix. Anecdotal evidence suggests that a number surfactant soak field tests were conducted in the Yates field. Chen et al. reported the results of a single test. Hirasaki and Zhang[3] proposed the use of anionic surfactant with sodium carbonate.

Past laboratory work conducted by the Correlations Company suggests that altering the wettability of core samples from the Phosphoria formation with either a non-ionic or a cationic surfactant produces incremental oil.[10] A possible mechanism of improved imbibition recovery from the use of surfactant solutions may be the release of the adsorbed organic materials from the rock surface, which becomes more water-wet, so that the imbibition rate is increased. Surfactants also lower the IFT, therefore decreasing the capillary pressure. The corresponding increase in the Bond number, $N_a = \rho g r^2 / \sigma$, probably contributed to improved oil recovery through gravity segregation.

San Andres Fuhrman Masho Field

The San Andres formation in the Permian Basin consisted of about half of the laboratory part of the project. Encore Acquisition Company (Ft. Worth, Texas) provided the cores and fluids from the W. Boner Well No. 40, B and C zones in the Fuhrman-Masho field in Andrew

County, Texas. Yates Petroleum Corporation (Artesia, New Mexico) provided an additional 1200 ft of whole San Andres core from the Eagle Creek field in Eddy County, New Mexico. Two crude oil/reservoir rock/brine systems were tested:

1. Crude oil, reservoir core samples, and synthetic reservoir brine or synthetic seawater from the Fuhrman Masho San Andres field;
2. Crude oil, reservoir core samples, and synthetic reservoir brine from the Eagle Creek San Andres field, or crude oil from the Fuhrman Masho San Andres field and synthetic seawater as the fluids.

Brine Composition

The laboratory testing included seven different surfactants. Cationic, nonionic, anionic, and amphoteric surfactants were tested.

The following brines were used in the laboratory tests: synthetic reservoir brine based on the composition of Fuhrman Masho reservoir water, and designated as FM brine; synthetic reservoir brine, which represents the average Eagle Creek reservoir brine concentration, and designated as EC brine; and synthetic seawater based on North Sea water composition, designated as SW brine. Since the salinities of FM brine and EC brine were high, surfactants except for T91-8 could not fully dissolve in those brines at the designated concentrations. SW brine was used in the tests to make surfactant solutions. All brine compositions are listed in Table 1.

Table 1. Test brine composition and concentration (g/L)

Composition	FM brine	SW brine	EC brine
NaCl	61.773	28	64.3
KCl		0.935	0
$CaCl_2$	5.944	1.19	8.8835
$MgCl_2$	1.788	5.368	5.88
Na_2SO_4	6.284	0	3.0
$NaHCO_3$	2.093	0	0
Total dissolved solids, ppm	77,882	35,493	82,064

Crude Oil Properties

The properties of the two crude oils used in the lab tests are shown in Table 2. The reservoir temperature of the San Andres field was 40°C. Before use the oils were filtered to remove any physical debris such as scale or corrosion products and then degassed to avoid component change during the course of experiments.

Table 2. Crude oil properties

Crude oil	Density at 20°C, g/ml	API°	Viscosity at 40°C, cp	Asphaltene content, wt%	Wax content, wt%
Fuhrman Masho	0.892	27.13	9.9	1.0	0.6
Eagle Creek	0.844	36.15	4.2	-	-

Reservoir Core Properties

The properties of the reservoir cores from the Fuhrman Masho San Andres field are listed in Tables 3 and 4. All cores were 1.5” in diameter and about 3” in length. The porosity and

permeability of Fuhrman Masho reservoir cores ranged from 8–17% and 3–623 md, respectively. Porosity and permeability distributions are plotted in Figure 1.

Table 3. Properties of Fuhrman Masho reservoir cores from C zone

Core	kg, md	S_{wi}, %	ϕ, %	Brine	R by FM imb. % OOIP	Surfactant, C	R by surf. imb. % OOIP
4378	560.0	0	16.5	FM	1.6	T91-8, 1500 ppm	32.5
4390.3	91.0	0	13.9	FM	3.0	T91-8,3500 ppm	38.8
4389.9	98.0	0	14.3	FM	1.5	T91-8, 1500 ppm	27.9
4378.8	154.0	0	13.0	FM	1.5	T91-8,3500 ppm	23.5
4377.9	483.0	0	16.3	FM	2.0	T91-8,3500 ppm	45.6
4378.2b	407.0	0	16.0	FM	1.1	T91-8, 1500 ppm	16.7
4391b	623.0	0	20.0	FM	1.7	T91-8, 1500 ppm	38.0
4391a	359.0	0	16.6	FM	1.5	T91-8,3500 ppm	32.9
4384.3	5.1	59.1	19.6	FM	0.0	T91-8,3500 ppm	9.4
4384.2	5.4	38.2	18.9	FM	0.0	T91-8, 1500 ppm	10.0
4390b	48.0	31.9	15.0	FM	0.0	T91-8,3500 ppm	21.8
4390a	80.0	25.4	13.9	FM	0.0	T91-8, 1500 ppm	16.6
4378.3	19.6	0	14.7	SW	6.9	MCB, 3000 ppm	26.0
4379.8	55.0	17.7	10.3	SW	1.0	MCB, 3000 ppm	2.4
4379.3	100.0	21.1	10.1	SW	0.0	MCB, 3000 ppm	6.9
4379.4	6.3	0	9.9	SW	3.0	C-50, 3000ppm	36.7
4378.2a	58.0	22.2	10.3	SW	0.0	T91-8, 3000 ppm/FM	19.0
4377.8	524.0	17.3	17.1	SW	0.0	T91-8, 3000 ppm/FM	48.2
4383.9	887.0	13.4	17.4	SW	0.0	T91-8, 3000 ppm/SW	31.1
4378.9	144.0	13.6	12.3	SW	0.8	Iw-o	
4379.7	25.2	17.8	9.8	SW	0.0	RCD128, 3000 ppm	0.7
4379.5	6.4	0	9.6	SW	5.9	RA246, 3000 ppm	0.0
4379.1	147.0	20.2	12.6	SW	0.0	RA246, 3000 ppm	5.0
4379.2	141.0	19.94	11.7	SW	1.2	RA246, 3000 ppm	0.0
4385.2a	3.4	0	14.8	FM	13.2	T91-8, 3000 ppm	12.4
4384.6b	1.7	0	14.5	FM	34.8	T91-8, 3000 ppm	2.6
4384.5b	2.3	0	15.9	FM	27.1	T91-8, 3000 ppm	7.8
4385.4b	17.4	0	15.2	FM	22.0	T91-8, 3000 ppm	12.6
4385.4a	19.3	0	15.2	FM	11.8	T91-8, 3000 ppm	15.0

Table 4. Properties of Fuhrman Masho reservoir cores from B zones							
Core #	kg, md	S_{wi}, %	ϕ, %	Brine	R, FM imb. brine,% OOIP	Surfactant	R, surf. imb. % OOIP
4340.5	14.0	0	11.8	FM	3.0	T91-8,3500 ppm	5.5
4340.6	27.0	0	12.6	FM	2.2	T91-8, 1500 ppm	4.8
4341.3	0.3	0	5.6	SW	0.0	T91-8, 3000 ppm	0.0
4341.6	0.2	0	1.1	SW	0.0	T91-8, 3000 ppm	0.0
4341.7	0.2	0	0.5	SW	0.0	T91-8, 3000 ppm	0.0
4341.2	3.6	0	7.3	SW	5.4	MCB, 3000 ppm	0.0
4340.4	7.5	0	10.8	SW	5.6	RA246, 3000 ppm	0.0
4340.9	3.5	0	15.6	SW	6.8	C-50, 3000 ppm	0.0
4349.3	13.1	0	9.0	FM	7.6	T91-8, 3000 ppm	0.0
4329.9	3.4	21.1	7.8	FM	0.8	T91-8,3500 ppm	0.0
4329.8a	12.0	11.9	8.8	FM	0.0	T91-8, 1500 ppm	0.0
4329.8b	10.5	0	8.8	SW	6.9	T91-8, 3000 ppm	0.0
4328.3	5.0	0	7.4	SW	6.2	L-64, 3000 ppm	0.0
4328.0	3.7	0	6.8	SW	9.8	T91-8, 3000 ppm	0.0
4327.8	2.9	0	5.4	SW	5.9	RCD128, 3000 ppm	0.0
4328.4	4.1	0	7.2	SW	8.3	L-64, 3000 ppm	0.0
4329.1	13.9	0	9.8	SW	8.3	RCD128, 3000 ppm	0.0
4328.7	25.0	0	9.8	SW	8.5	Iw-o	
4327.9	5.2	19.0	7.0	SW	0.0	T91-8, 3000 ppm	0.0
4329.6	5.0	25.2	8.6	SW	0.0	L-64, 3000 ppm/SW	0.0
4328.9	10.4	20.9	8.5	SW	1.6	L-64, 3000 ppm/SW	1.1
4328.8	25.1	19.2	9.5	SW	0.4	RCD128, 3000 ppm/SW	0.0
4327.7a	0.6	0	4.7	FM	8.1	T91-8, 3000 ppm	0.0
4327.1a	3.4	0	5.2	FM	4.0	T91-8, 3000 ppm	0.0
4327.8b	8.4	0	6.8	FM	5.5	T91-8, 3000 ppm	0.0
4327.1b	5.5	0	6.3	FM	4.1	T91-8, 3000 ppm	0.0
4329.7	14.0	0	9.1	FM	5.7	MCB, 3000 ppm	1.0
4327.6b	0.3	0	2.9	FM	2.5	MCB, 3000 ppm	0.0
4327.2a	4.8	0	6.0	FM	3.0	MCB, 3000 ppm	0.0
4327.6a	1.3	0	4.4	FM	10.4	MCB, 3000 ppm	0.0
4329.9b	1.0	0	6.1	FM	4.4	T91-8, 3000 ppm	0.0
4329.7b	13.1	0	9.7	FM	7.4	T91-8, 3000 ppm	0.0

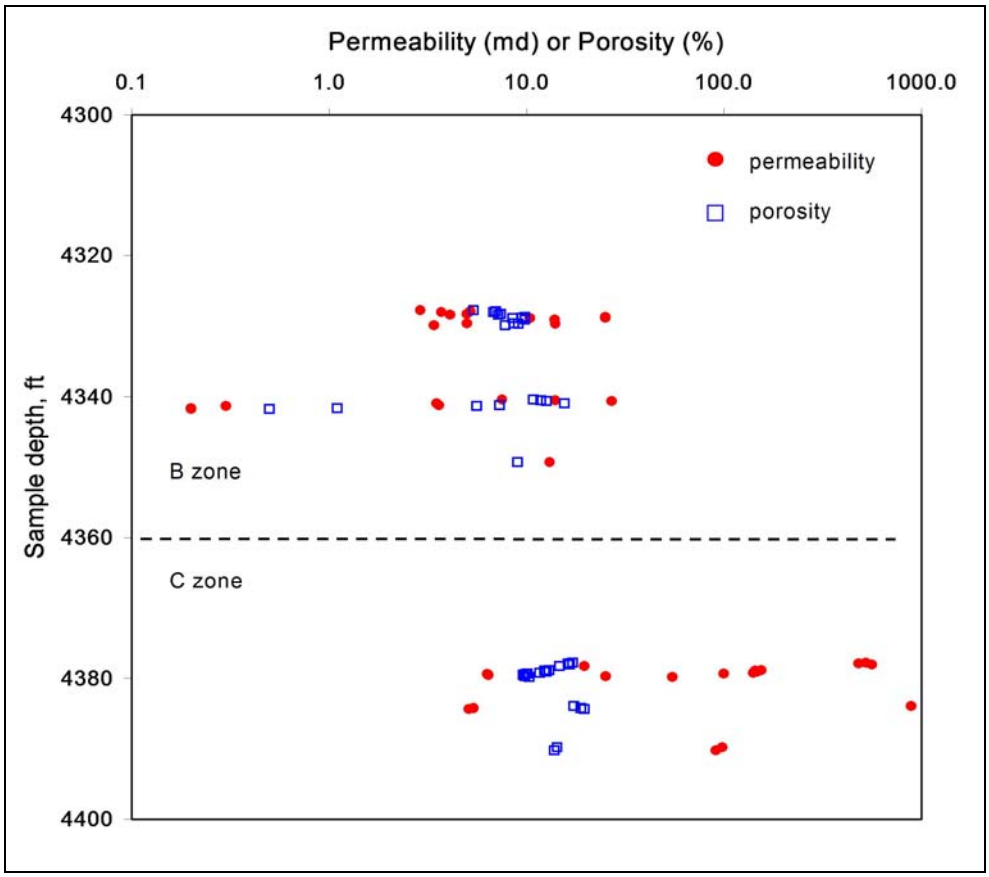

Figure 1. Distribution of permeability and porosity of Fuhrman Masho cores.

The porosities of most cores from the B and C zones were around 10%. The permeabilities of most cores from the C zone were higher than those from the B zone. B zone permeability ranged from 0.2–25 md, and C zone permeability ranged from 5–880 md.

Properties of the reservoir cores from the Eagle Creek San Andres field are listed later in Table 9. All the cores were 1.5" in diameter and about 3" in length. Comparably, Eagle Creek cores were tighter and less permeable; the porosity and permeability ranged from 3–14% and 0.1–26 md, respectively (Figure 2).

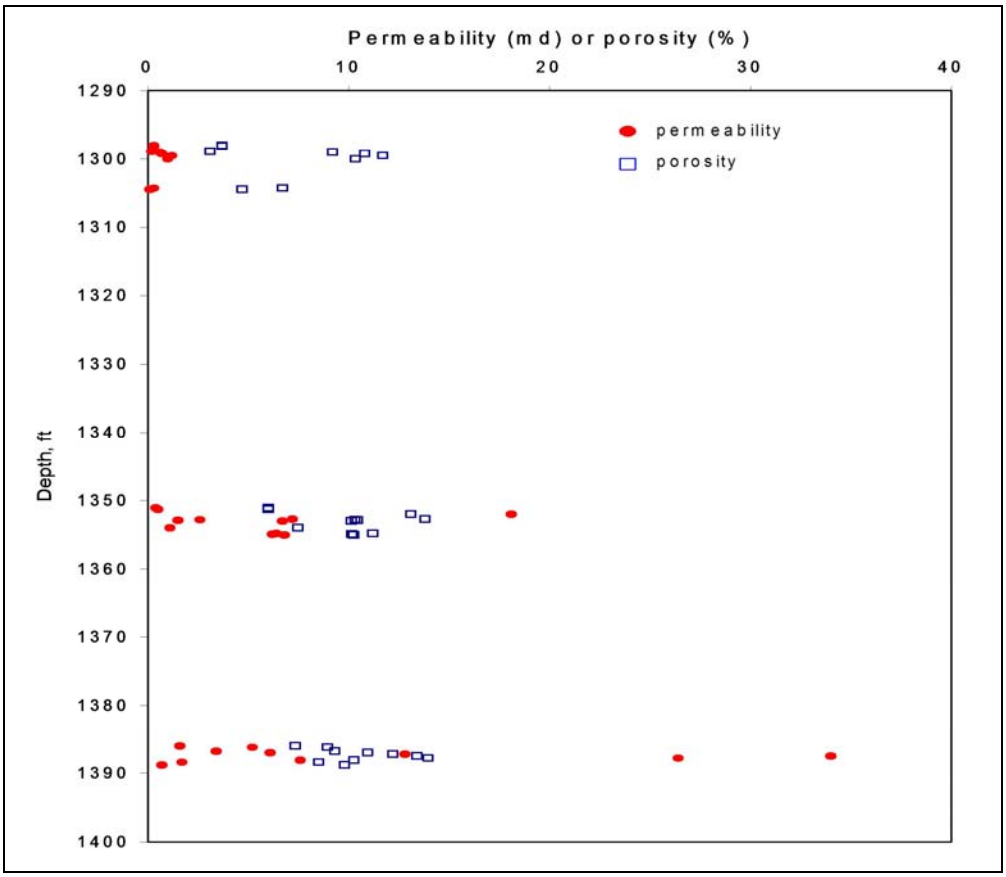

Figure 2. Distribution of permeability and porosity of Eagle Creek cores.

Thin sections of Fuhrman Masho and Eagle Creek rocks are shown in Figures 3 and 4.

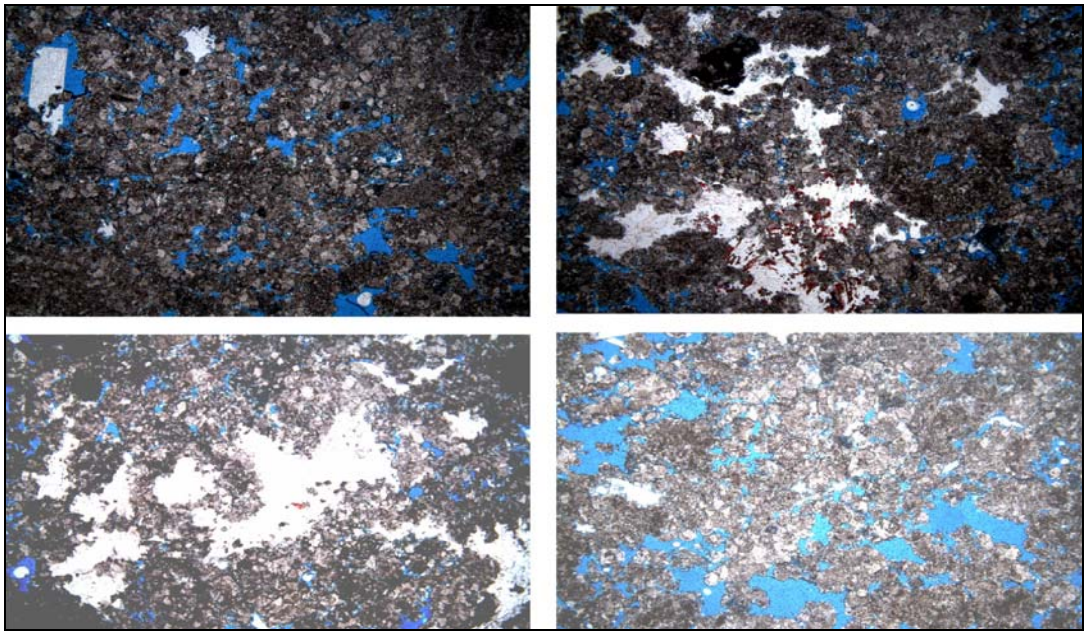

Figure 3. Thin sections of Fuhrman Masho rock.

Mineralogy analysis of the rock by thin section demonstrates that the Furman Masho rock consisted of grainstone dolomite containing minor anhydrite and calcite (Figure 3); the Eagle Creek rock consisted of wackestones or packstones containing dolomite, calcite, and some anhydrite (Figure 4).

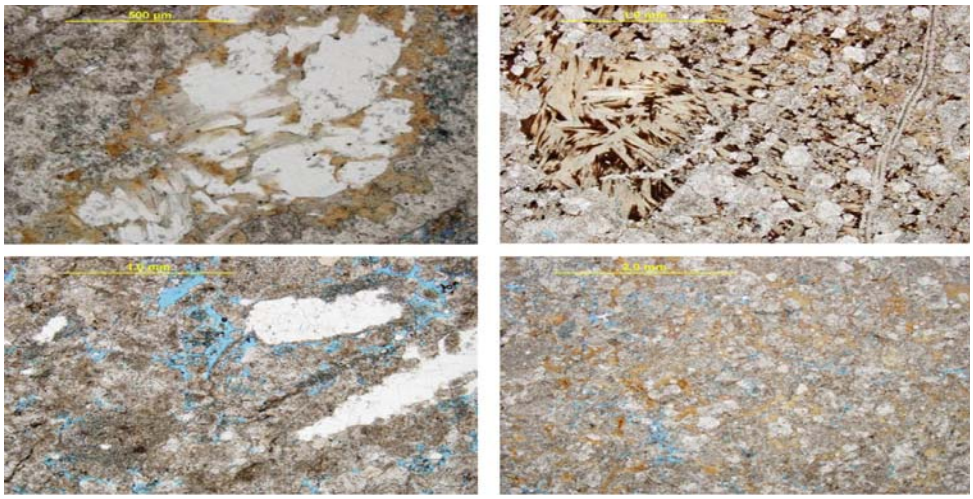

Figure 4. Thin sections pictures of Eagle Creek rocks.

Cedar Creek thin sections indicate that the Interlake rock contained dolomite crystals and small clay particles with good connection between pores. Stony Mountain rock is clay-rich and heterogeneous, and contained smaller dolomite crystals than the Interlake rock. Red River rock also contained small dolomite crystals, anhydrite particles, a clay-rich band, fossils, and moldic pores. The photomicrographs are presented later in the report.

Surfactant and Interfacial Tension Measurements

All of the chemicals and related properties are listed in Tables 5 and 6.

Table 5. Physical and chemical properties of four surfactants

Properties	L64 (Pluronic, Antarox)	Arquad C-50*	Tomadol 91-8	Triton X100
Chemical name	Ethylene and propylene oxide	Cocoalkyltrime-thyl ammonium chloride	Poly (2.5 or 6 or 8) oxyethylene $C_{9\text{-}11}$ alcohol	Alkylaryl polyether alcohol
Type	nonionic	cationic	nonionic	nonionic
Simplified as	L64	C-50	T91-8	X100
Chemical formula	$HO(C_2H_4O)_a(C_3H_6O)_b(C_2H_4O)CH$	$RN(CH_3)_3Cl$ R = cocoalkyl	$ROCH_2CH_2O)_nH$ R = $C_9/C_{10}/C_{11}$	$C_{14}H_{22}O(C_2H_4O)_n$ (n = 9 or 10)
Chain length	14	12–16	9–11	~ 9.5
Equivalent weight	2900	278	524	250
pH	5.0–7.5	6–7	-	6–8 (5% solution)
Surface tension at 0.1 mol, dynes/cm	43	31 (0.1% aqueous)	30	-
Cloud point, °C	58 (1% aqueous)	-	80	66 (1% aqueous)
Hydrophilic and lipophilic balance value (HLB)	15	23	13.9	13.5
CMC at 30°C	soluble	< 1 m mol or 278 ppm	about 1 m mol at 25°C, or 524	0.22–0.24 m mol or 138

			ppm	- 150 ppm
Commercial concentration, (wt%)*	~ 100	~ 45–55	~ 100	~ 97

*Commercially supplied Arquad C-50 contains about 30–35% of CH_3-CH_3-CHOH and 10–20% of water besides the surfactants.

Table 6. Physical and chemical properties of other surfactants			
Product name	Rhodacal A 246 L	Rhodapex CD 128i	Mirataine CB
Chemical name	Sodium alpha-olefin sulfonate	Ammonium C6-10 alkyl ether sulfate	Cocamidopropyl betaine
Designated as	RA-246L	CD-128	MCB
Type	Anionic	Anionic	Amphoteric
Properties	Emulsifier	Foam stablizer agent	-
Carbon chain length	14 - 16	-	-
Commercial concentration, (wt%)*			

The first step in the laboratory tests was to determine the CMCs of the surfactants. This was achieved by measuring IFTs between surfactant North Sea water (SW) brine solutions with a series of concentrations and Soltrol 220 mineral oil at room temperature. The IFTs of the various surfactants are plotted in Figures 5 and 6.

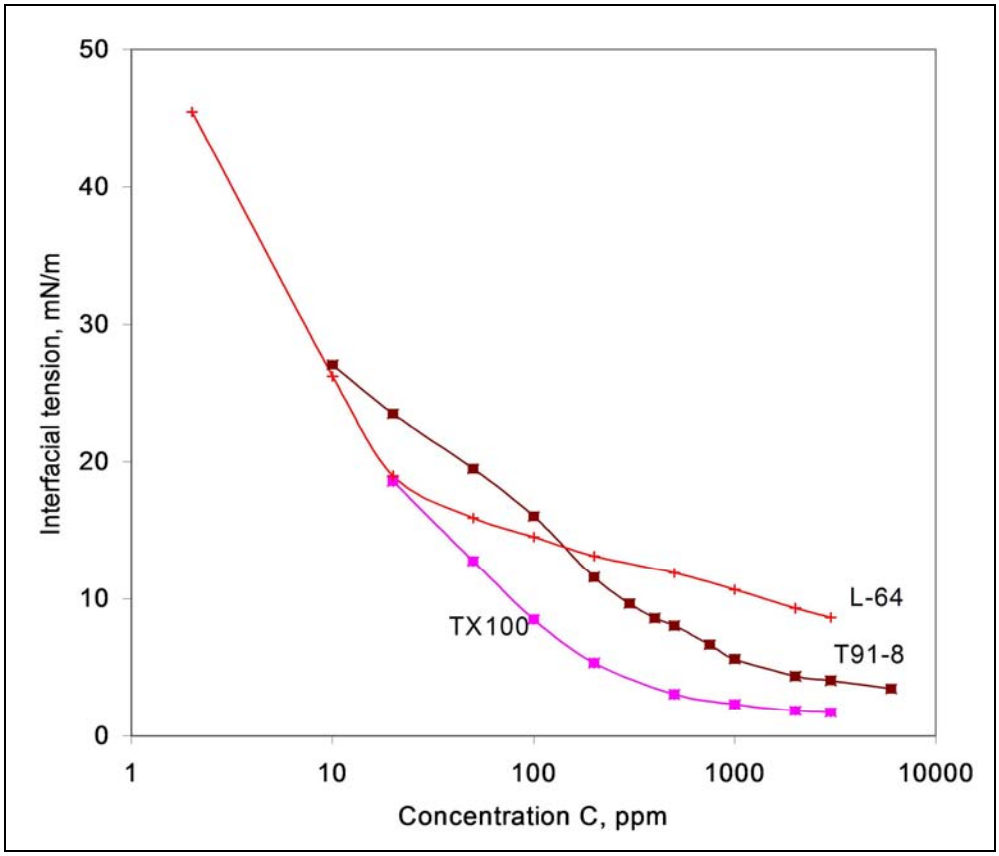

Figure 5. Interfacial tensions of nonionic surfactant solutions and Soltrol.

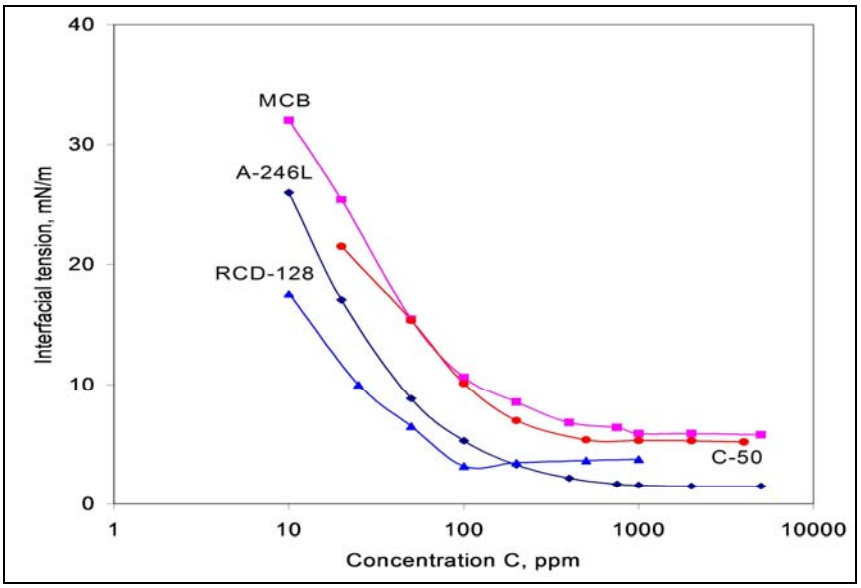

Figure 6. Interfacial tensions of cationic, anionic, and amphoteric surfactant solutions and Soltrol 220.

After CMCs of all the surfactants were examined, proper surfactants and concentrations were selected for the spontaneous imbibition tests for reservoir rock/crude oil/brine systems.

According to the IFT measurements and previous laboratory and field experience, the nonionic surfactants T91-8 and L-64, anionic surfactants RA-246L and CD-128, and the amphoteric surfactant MCB were selected for oil recovery improvement. The surfactant solutions were the mixture of the designated synthetic reservoir brine with each surfactant at concentrations of 1,500–3,500 ppm. The San Andres reservoir temperature of 40°C was used for the test temperature. The related IFTs between crude oil and surfactant solutions are listed in Table 7 and 8.

Table 7. IFTs between San Andres crude oil and surfactant solutions

	IFT, mN/m						
Concentration	L64	RA-246L	C-50	T91-8	CD-128	TX100	MCB
0	49.55						
2	45.47						
10	26.23	26		27.06	17.5		32
20	18.98	17	21.49	23.50		18.58	25.4
25					10		
50	15.92	8.8	15.31	19.50	6.5	12.76	15.4
100	14.53	5.3	10.09	16.03	3.2	8.50	10.6
200	13.15	3.3	6.97	11.57	3.49	5.36	8.5
300				9.65			
400		2.2		8.60			6.8
500	11.88		5.37	8.05	3.66	3.10	
750		1.7		6.68			6.4
1000	10.65	1.6	5.31	5.65	3.78	2.36	5.9
2000	9.31	1.5	5.30	4.41		1.87	5.9
3000	8.65			4.08		1.74	
4000			5.20				
5000		1.5					5.8
6000				3.50			

Table 8. Crude oil properties and related IFTs (mN/m)			
Crude oil	Eagle Creek crude oil	Fuhrman Masho crude oil	
Measurement temperature, °C	40	40	
Brine	EC brine	FM brine	SW brine
Brine with no surfactant added	30.2	17.2	20.9
Brine with 3000 ppm T91-8 added	3.6	2.0	2.6
Brine with 3000 ppm L-64 added	-	-	0.2
Brine with 3000 ppm RCD-128 added	-	-	1.5
Brine with 3000 ppm MCB added	-	-	1.6
Brine with 3000 ppm RA-246L added	-	-	0.28

Laboratory Procedures

Reservoir cores with different permeabilities and initial water content S_{wi} were tested for spontaneous imbibition, both in synthetic reservoir brine and surfactant solutions. The test procedure for initial water saturation $S_{wi} > 0$ is listed as follows:

1) Saturate the cores with brine and allow cores to sit in brine for at least 7 days for ionic equilibrium;
2) Displace the brine from the core with crude oil until designated initial water saturation S_{wi} is reached or no water can be displaced;
3) Age the cores for 10 days at 40°C;
4) Displace the aged crude oil from the aged core with fresh crude oil at 40°C;
5) Immerse the cores in test brine for imbibition until no oil is produced;
6) Immerse the cores in surfactant brine solution for imbibition.

For $S_{wi} = 0$, the cores were saturated with crude oil directly by vacuum and then the above procedure was followed starting from step 3.

Results

Fuhrman Masho rock/crude oil/FM brine and/or synthetic seawater

T91-8 surfactant

Fuhrman Masho (FM) cores from the C and B zones were tested with T91-8 formation water solutions; concentrations ranged from 1500–3500 ppm. Shown in Figures 7 and 8 are the oil recovery versus spontaneous time of FM cores from the C zone with FM brine and surfactant T91-8.

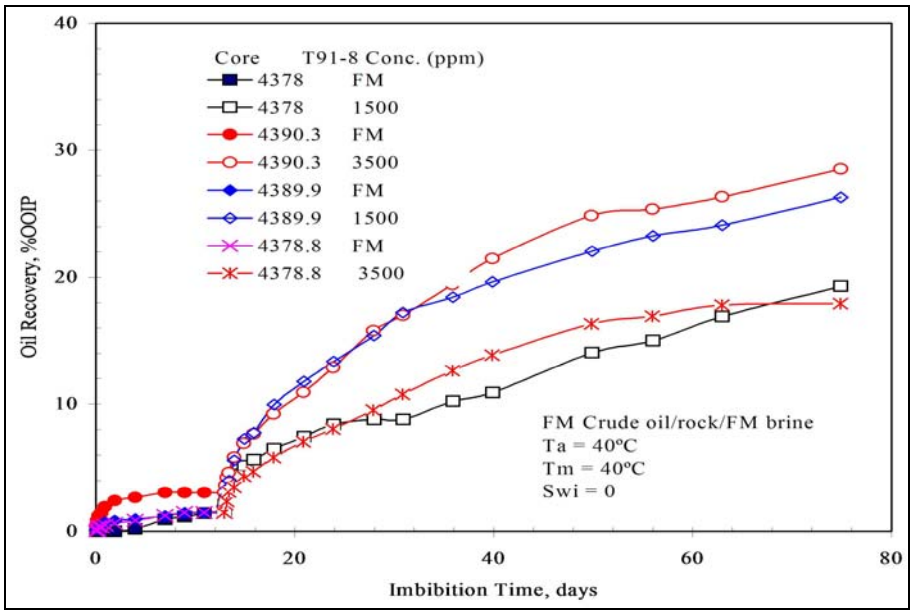

Figure 7. Oil recovery by imbibition for Fuhrman Masho C zone rock/crude oil/FM brine and T91-8 solution (S_{wi} = 0).

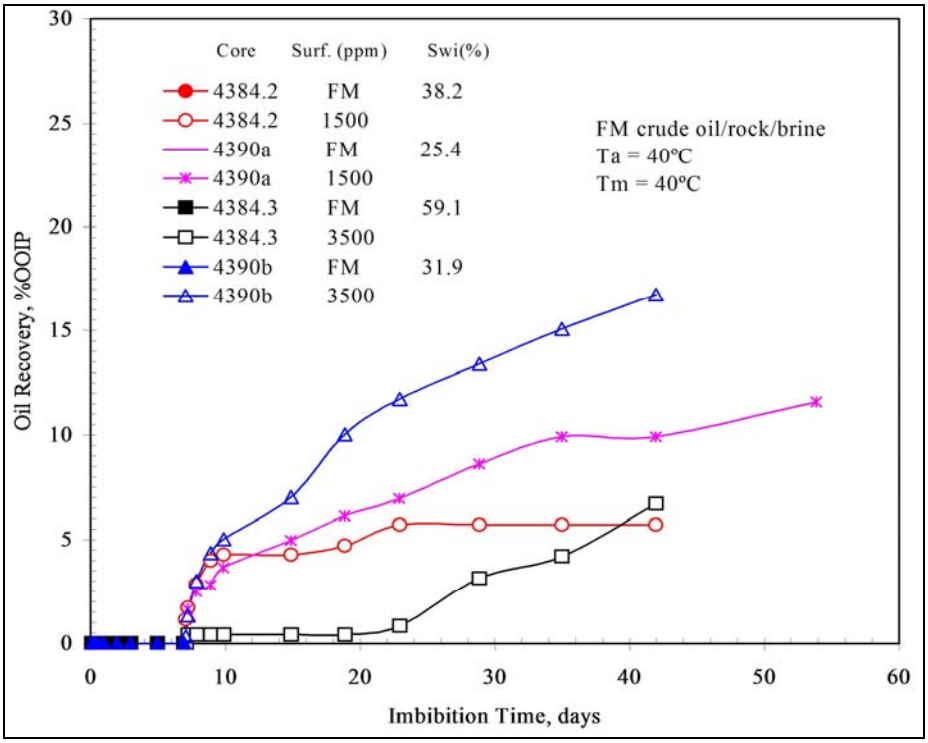

Figure 8. Oil recovery by imbibition for Fuhrman Masho C zone rock/crude oil/FM brine and T91-8 solution (S_{wi} >0).

Cores from the B zone are plotted in Figures 9 and 10.

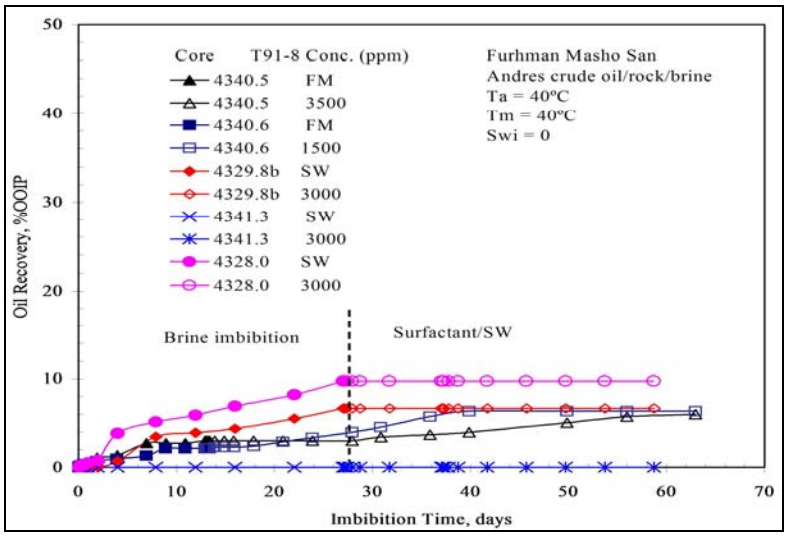

Figure 9. Oil recovery by imbibition for Fuhrman Masho B zone rock/crude oil/FM brine and T91-8 solution (S_{wi} = 0).

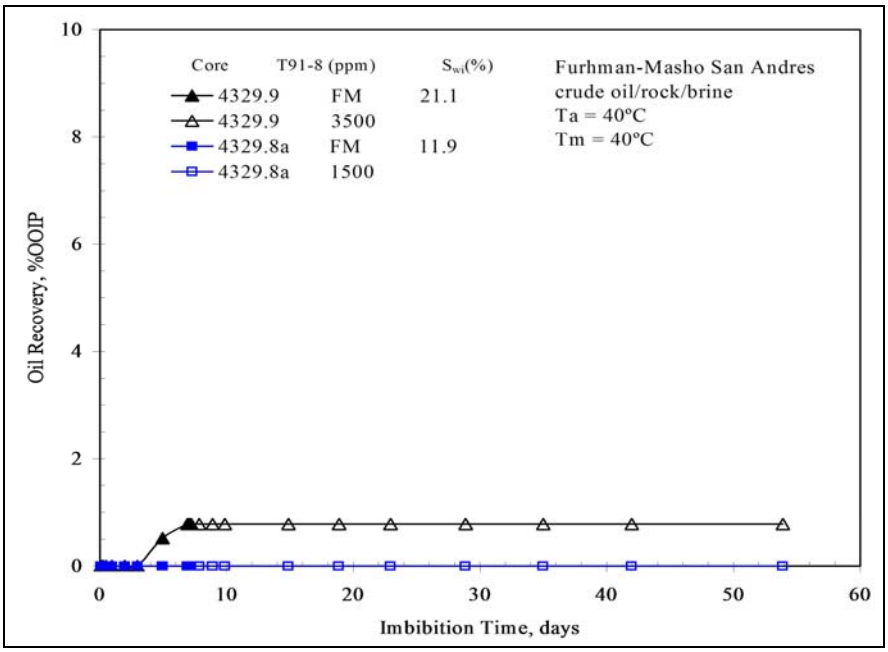

Figure 10. Oil recovery by imbibition for Fuhrman Masho B zone rock/crude oil/FM brine and T91-8 solution (S_{wi} > 0).

These figures show that the maximum oil recovery by imbibition from brine for this batch of cores from the B zone was only about 3%. After the cores were soaked in a T91-8 brine solution, cores from the C zone produced more oil. Oil recovery by imbibition was improved by up to 35%, demonstrating a sound response to surfactant treatment (see Table 3). Furman Masho rock consists of grainstone dolomite containing minor anhydrite and calcite. As indicated from previous studies,[10] T91-8 effectively enhances oil recovery from dolomite rocks.

However, for cores from the B zone, it appears that the effect of the T91-8 concentration was poor. All of the oil recoveries by brine and improved by surfactants are listed in Table 4. The mineralogy of cores from both B and C zones is similar, but the effect of the surfactant is

obviously different. The permeability of cores from the B zone is much lower than that from the C zone. The permeability may be the most important factor in the surfactant mechanism of improved oil recovery in these tests, as reported previously.[10]

Shown in Figure 11 are the incremental oil values (termed enhanced oil recovery on the graph) versus bulk volume oil (BVO) for the 16 plugs, from both B and C zones. BVO is defined as the product of porosity ϕ, and oil saturation $1 - S_{wi}$,

$$BVO = \phi(1 - S_{wi}) * 100 .$$

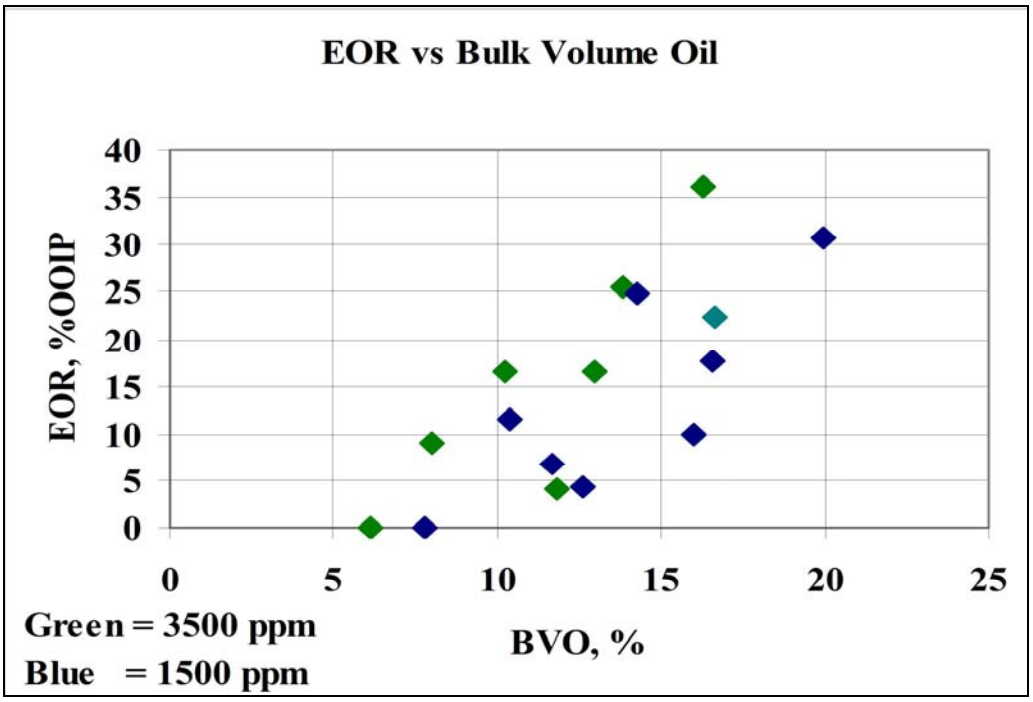

Figure 11. Data set consists of both "B" & "C" zone core plugs.

The trend suggests that the higher the BVO (more oil available), the greater the oil recovery. Overall the higher concentration of surfactant solution (1500 or 3500 ppm) resulted in slightly higher oil recovery with a few exceptions. The data for the B and C zone samples are presented in Figures 12 and13, respectively. A summary of the oil recovery versus BVO is shown in Figure 14.

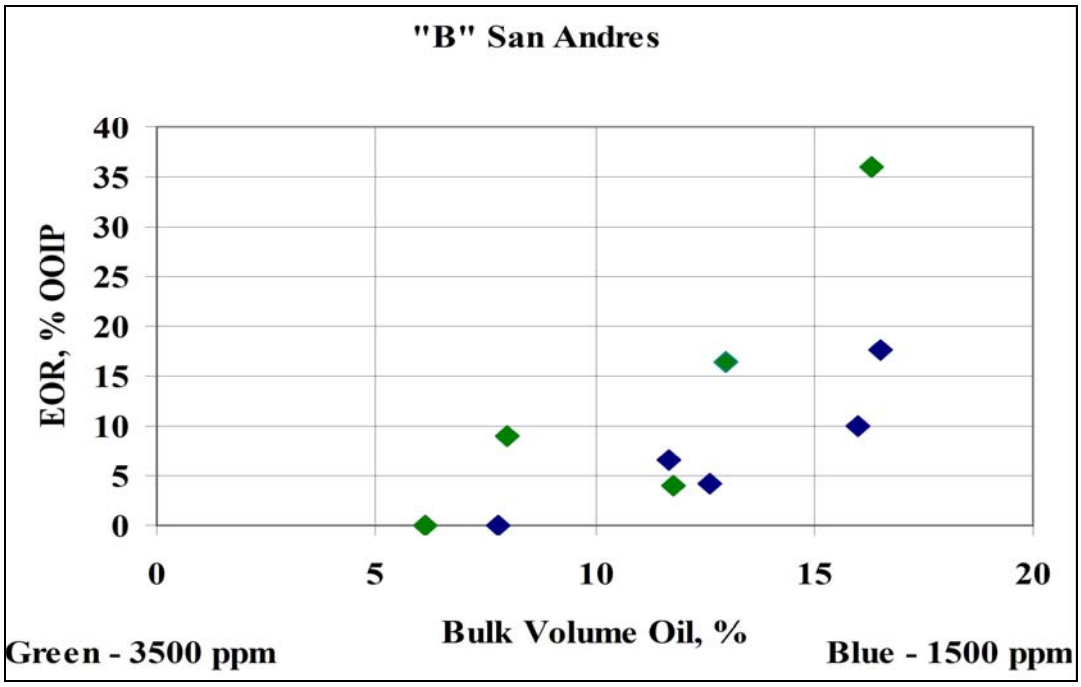

Figure 12. Data set consists of B zone plugs.

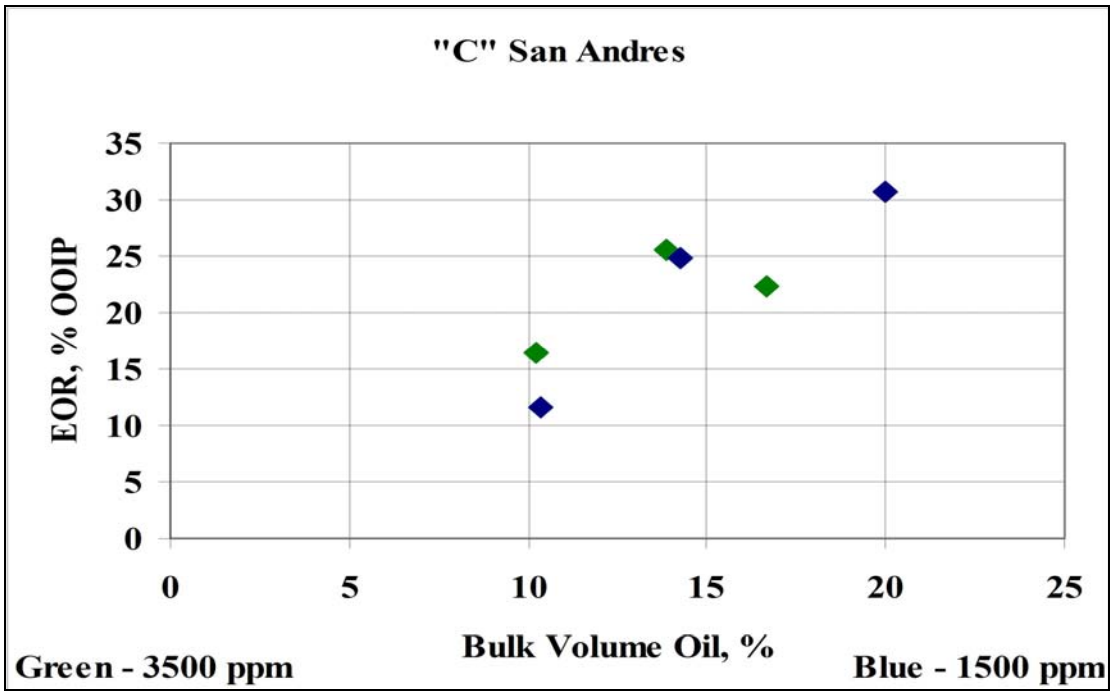

Figure 13. Data set consists of C zone plugs.

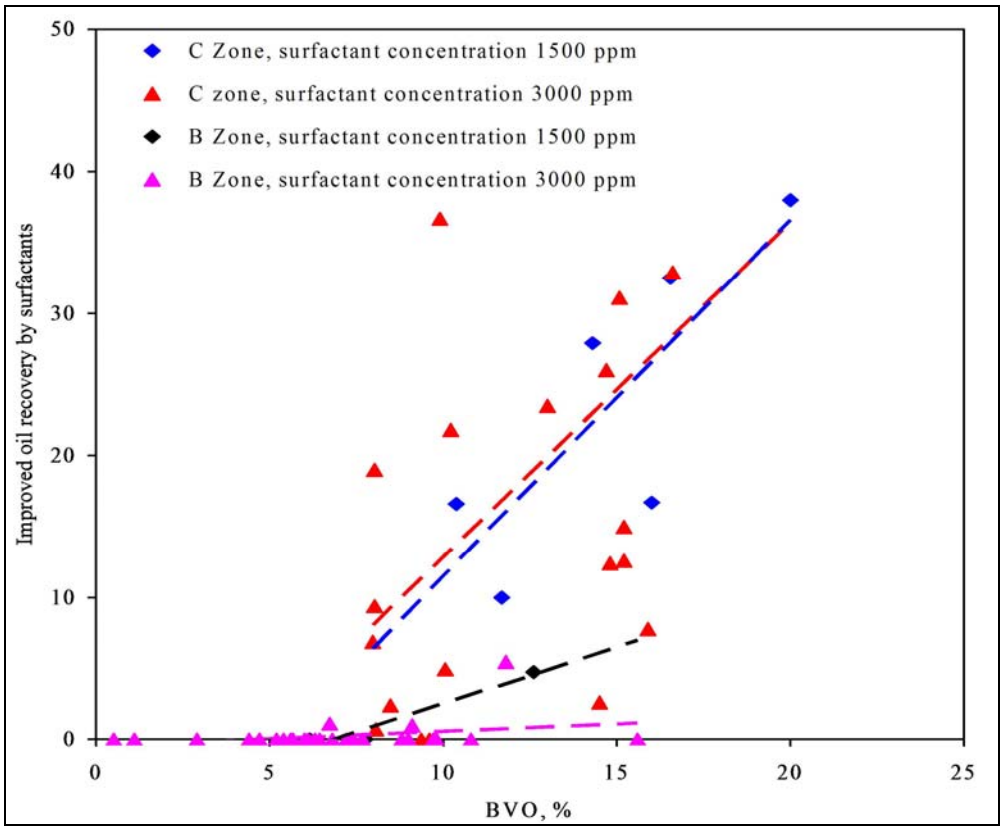

Figure 14. Summary of BVO versus oil recovery from both B zone and C zones.

Other surfactants

Our objective was to investigate the effect of the proposed surfactants, including T91-8, on oil recovery by imbibition of dolomite rocks. Other surfactants included a cationic surfactant C-50, anionic surfactants CD-128 and RA246, a nonionic surfactant L-64, and an amphoteric surfactant MCB.

As shown in Figure 15, all the surfactants had positive effects on the C zone cores; C-50 and MCB improved oil recovery up to 25%.

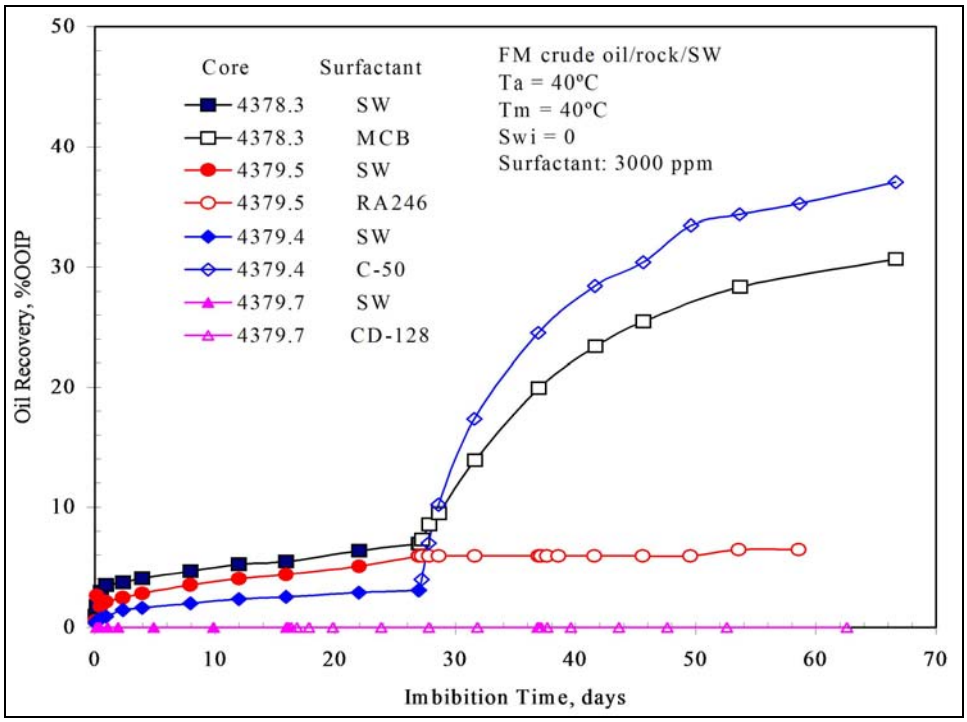

Figure 15. Examples of C zone cores with other surfactants (S_{wi} = 0).

Except for L-64, all other surfactants did not improve oil recovery in any of the B zone cores (Figures 16 and 17). Since the permeability of the B zone cores is low, there may not have been enough surfactant solution to reach the pores in order to expel the oil.

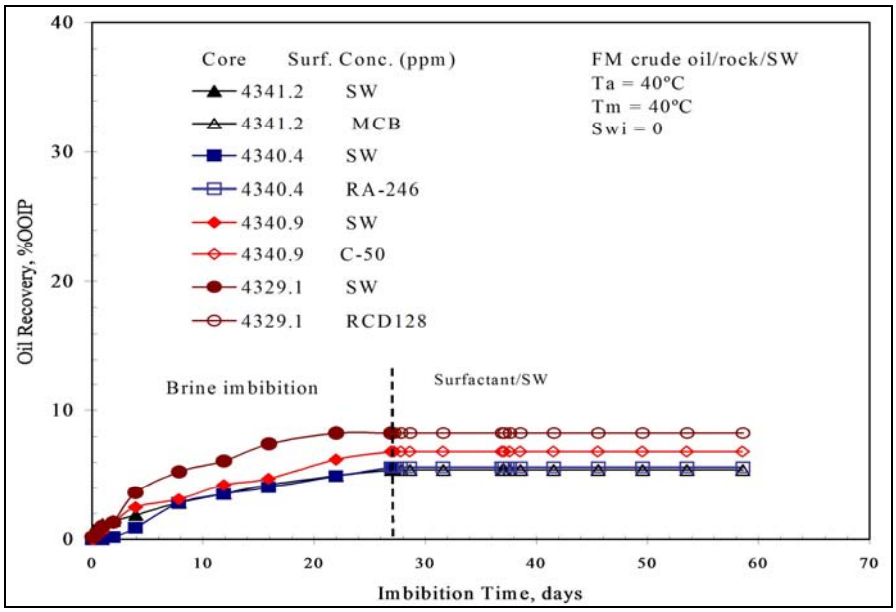

Figure 16. Examples of B zone cores with other surfactants (S_{wi} = 0).

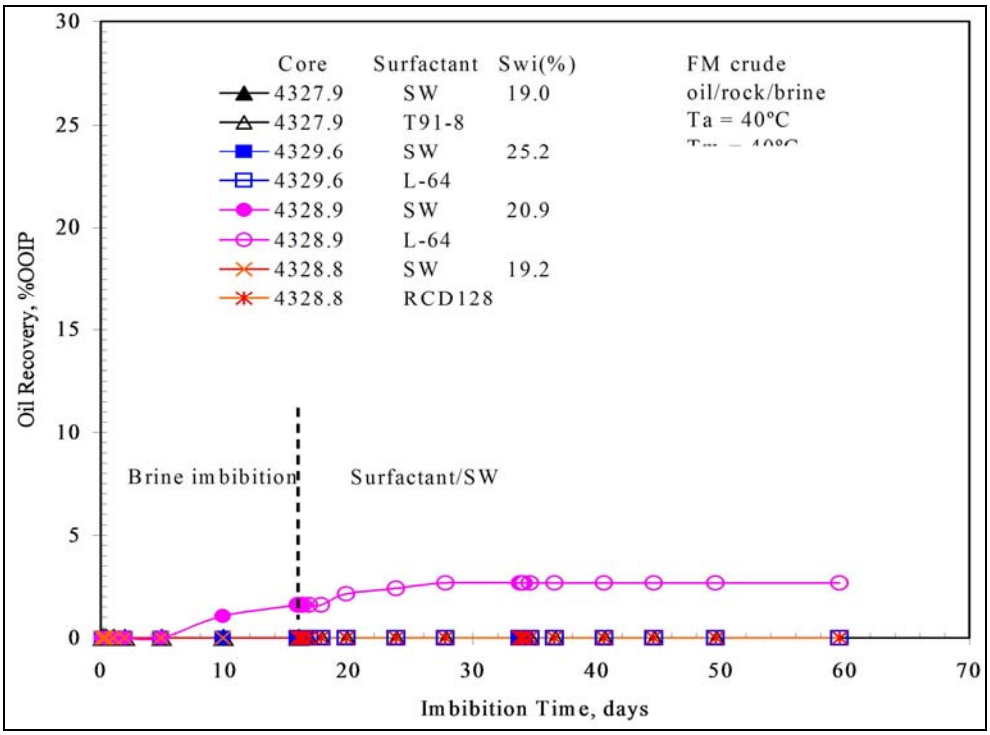

Figure 17. Examples of B zone cores with other surfactants (S_{wi} > 0).

Researchers from the Austad group indicate that sulfate ions in brine can have positive effect on how much surfactant improves oil recovery.[11] To verify this, Na_2SO_4 was added to the surfactant solutions during the imbibition tests. No obvious effect was observed.

Summary

The brine imbibition oil recovery from Fuhrman Masho cores ranged from 0–4% of the OOIP. Immersion in a T91-8 surfactant solution resulted in additional recovery of up to 38% of the OOIP. The laboratory results imply that both zones are candidates for the surfactant soak process with the C zone showing much better response.

San Andres Eagle Creek Field

The San Andres at Eagle Creek is on the northwest edge of the Permian Basin near Artesia, New Mexico. The dolomitized section of the reef is found at about 1400 ft as opposed to the Fuhrman Masho that is located deeper in the Basin at about 4400 ft.

Laboratory Tests

The fluid Eagle Creek fluid properties were described earlier, and the core properties are shown in Table 9.

Table 9. Properties of Eagle Creek reservoir cores

Core #	k_g, md	S_{wi}, %	ϕ, %	Brine used	Oil used	R, imb. brine, % OOIP	Surfactant (3000 ppm)	R, surf. imb. % OOIP
1300	1	0	10.33	EC	EC	19.44	T91-8	0
1352.8	2.6	0	10.31	EC	EC	25	T91-8	0
1387.0	6.1	0	10.94	EC	EC	3.47	T91-8	0

1387.2	12.8	0	12.19	EC	EC	3.47	T91-8	0
1387.5	34	0	13.37	EC	EC	3.03	T91-8	0
1299.5	1.2	48.4	11.7	EC	EC	1.3	T91-8	0
1352.0	18.1	13.0	13.1	EC	EC	0	T91-8	0
1354.8	6.4	8.5	11.2	EC	EC	0	T91-8	0
1354.9	6.2	8.2	10.2	EC	EC	0	T91-8	0
1354.0	1.1	15.5	7.5	EC	EC	0	T91-8	0
1351.1	0.4	0	6	SW	FM	3.96	T91-8	1.66
1351.3	0.5	0	6	SW	FM	1.9	T91-8	1.27
1388.8	0.7	0	9.8	SW	FM	13.77	L-64	6.07
1298.1	0.3	0	3.7	SW	FM	0	L-64	1.79
1299.0	0.6	0	9.2	SW	FM	29.46	RCD-128	0.63
1298.9	0.2	0	3.1	SW	FM	1.26	RCD-128	1.73
1299.2	0.7	0	10.8	SW	FM	33.79	MCB	0
1298.0	0.3	0	3.7	SW	FM	2.25	MCB	0
1304.5	0.1	0	4.7	SW	FM	7.67	RA-246L	0
1304.3	0.3	0	6.7	SW	FM	0	RA-246L	0
1387.8	26.4	6.6	13.95	SW	FM	0	T91-8	0
1352.9	1.5	30.8	10.44	SW	FM	5.78	T91-8	0
1355.0	6.8	8.1	10.25	SW	FM	0	L-64	0
1386.0	1.6	9.8	7.34	SW	FM	0	L-64	0
1386.8	3.4	7.5	9.31	SW	FM	0	RCD-128	0
1388.4	1.7	15.4	8.5	SW	FM	0	RCD-128	0
1388.1	7.6	6.0	10.26	SW	FM	0	MCB	0
1386.2	5.2	3.4	8.95	SW	FM	0	MCB	0
1353.0	6.7	9.5	10.13	SW	FM	2.06	RA-246L	0
1352.7	7.2	16	13.8	SW	FM	0	RA-246L	0

Results

EC crude oil/EC brine and T91-8 solution (3000 ppm)

The initial water saturation S_{wi} was zero for all cores shown in Figure 18. The oil recovery from brine imbibition ranged from 3–20%. Spontaneous imbibition in a 3000 ppm T91-8 solution did not result in any extra oil recovery.

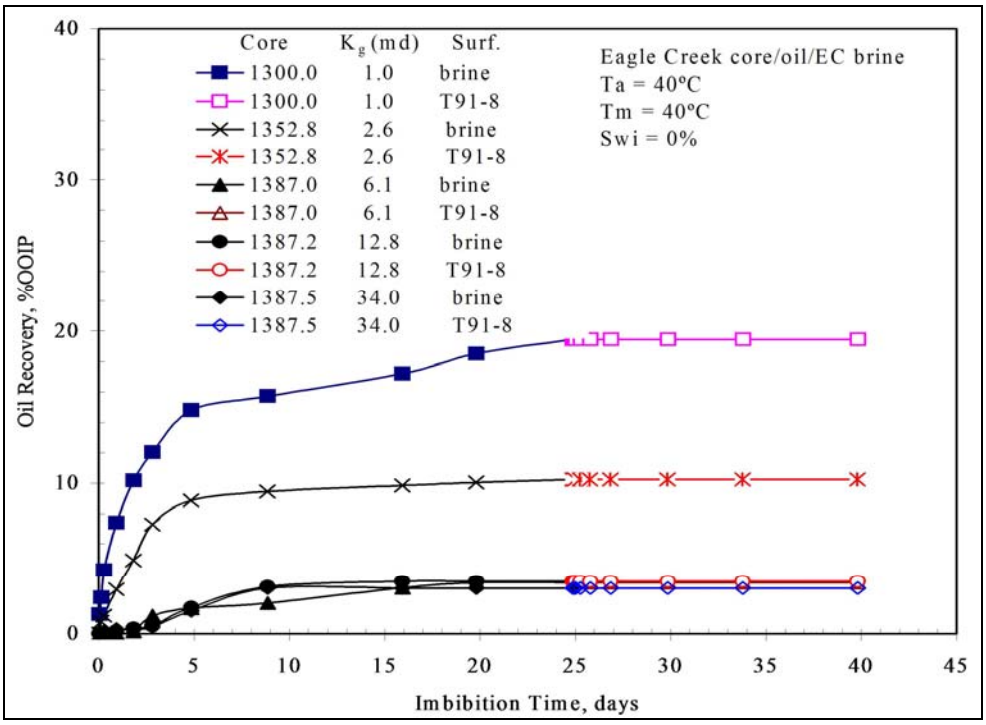

Figure 18. Oil recovery versus imbibition for Eagle Creek rock/oil/EC brine and T91-8 solution (S_{wi} = 0).

Cores with $S_{wi} > 0$ are shown in Figure 19. After 10–15 days of imbibition in brine, only core #1299.5 produced about 1.5% of the OOIP; no oil was produced from the other cores. No oil was produced from any of the five cores after soaking in 3000 ppm of the T91-8 solution.

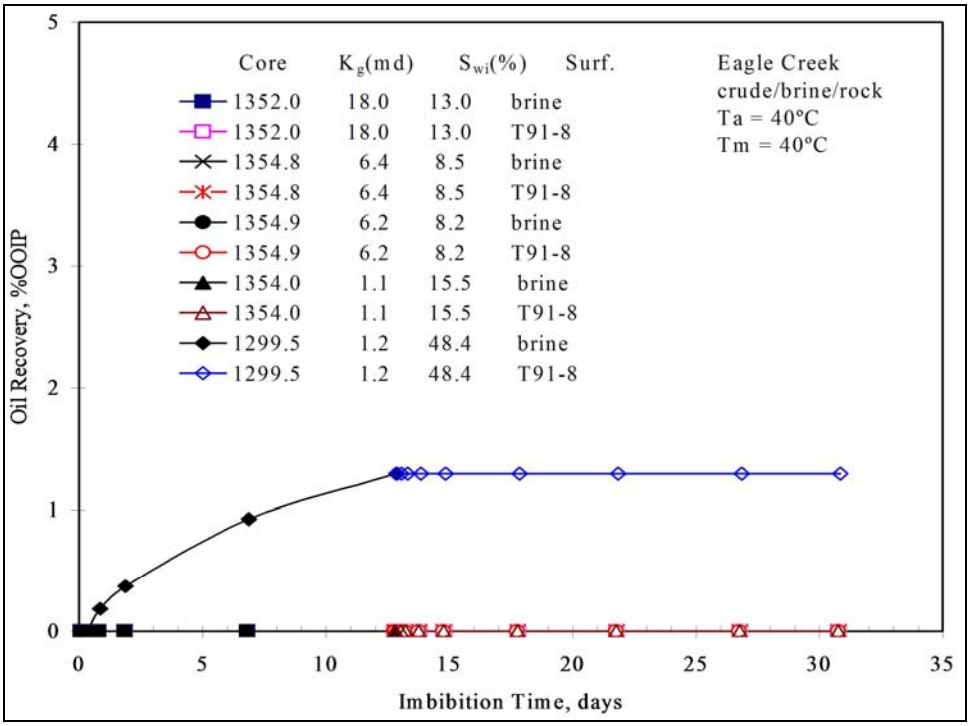

Figure 19. Imbibition tests of Eagle Creek rock/oil/EC brine and T91-8 solutions (S_{wi} > 0).

Apparently, T91-8 did not affect the oil recovery of the Eagle Creek system. We have encountered a similar situation; T91-8 improved oil recovery for dolomite cores but had no effect on cores with calcite.[10] Eagle Creek rock consists of wackestones or packstones containing dolomite, calcite, and some anhydrite, and the permeability is generally low. Most of the cores are less than 20 md in permeability.

Methanol is used in well treatment fluids and may change the wettability of the rock to more water-wet. Hence, alcohol was evaluated in the Eagle Creek system on the outside chance that the surfactant imbibition performance could be improved. After the imbibition tests in surfactant solutions, Eagle Creek cores were submersed in a series of different concentrations (10%, 20%, 30%, 40%, 50%, and 80%) of ethanol/Eagle Creek brine solutions. Ethanol was used to replace methanol for safer and easier operation. No oil was produced after more than 10 days of soaking, further indicating the unfavorable wettability.

EC rock/FM crude oil/SW brine and surfactant solutions

The Eagle Creek reservoir rock/Fuhrman Masho crude oil/seawater system utilized five different surfactants (Tables 5 and 6) to improve the oil recovery by spontaneous imbibition. The properties of the core samples were shown earlier in Table 9. Ten core samples were originally saturated with crude oil (S_{wi} = 0); another 10 samples had connate water saturation S_{wi} = 3.4–30.8%. Four core samples were used for each surfactant.

Oil recovery versus imbibition times for $S_{wi} = 0$ and $S_{wi} > 0$ are plotted in Figures 20–23, respectively.

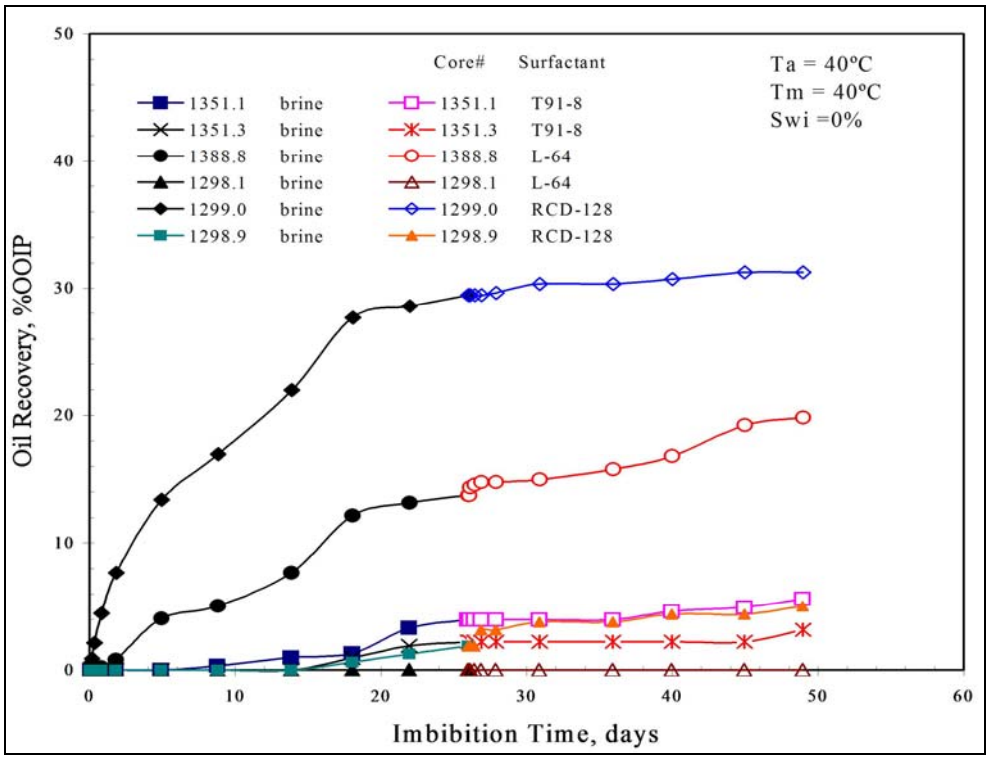

Figure 20. Imbibition oil recovery for FM oil/Eagle cores/seawater system.

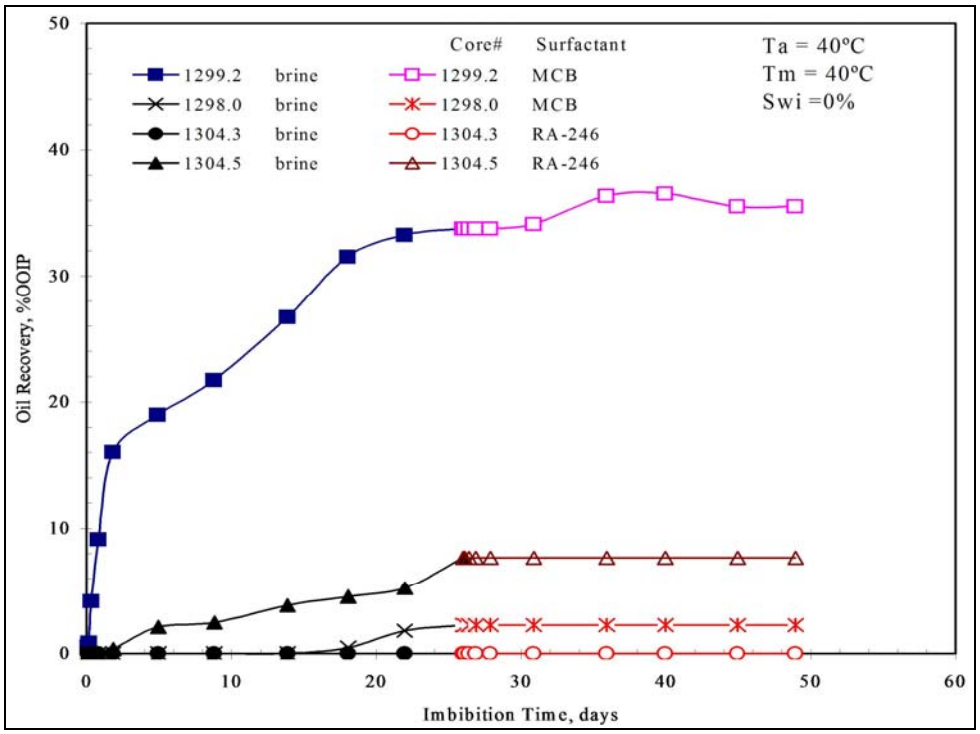

Figure 21. Imbibition oil recovery for FM oil/Eagle cores/seawater system (more surfactants).

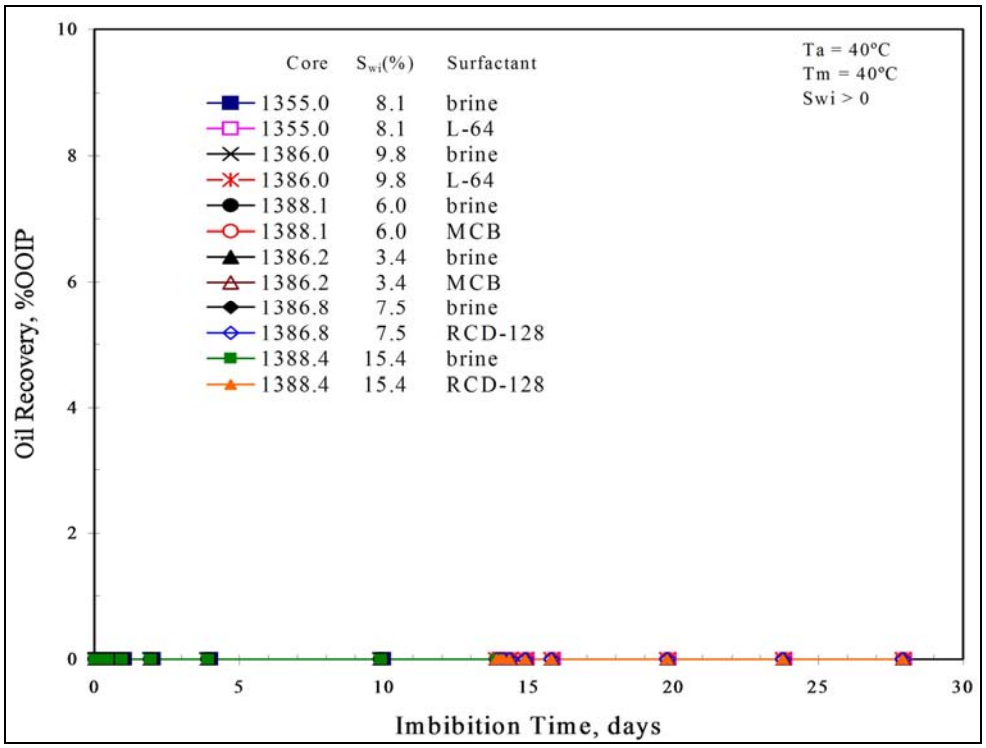

Figure 22. Imbibition oil recovery for Eagle cores/FM oil/seawater system.

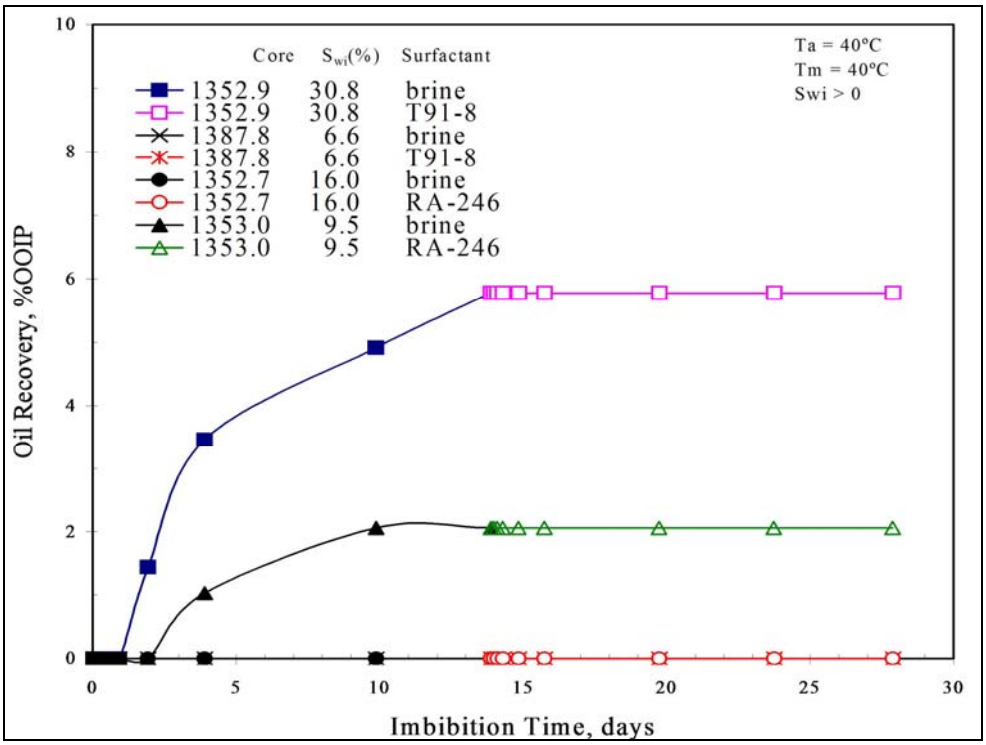

Figure 23. Imbibition oil recovery for Eagle cores/FM oil/seawater system (more surfactants).

For $S_{wi} = 0$, some cores had an oil recovery up to 33% by seawater imbibition and an additional 6% oil recovery by surfactant imbibition. But some cores had no oil recovery by imbibition either in seawater or surfactant solutions, indicating the heterogeneous nature of the carbonate rocks. Using core #1388.8 as an example, oil recovery by seawater imbibition was 13.16%; additional oil recovery by imbibition in an L-64 solution was about 6%. However, for core #1298.1, neither soaking in seawater nor L-64 surfactant solution resulted in any oil production.

For $S_{wi} > 0$, only cores #1352.9 and #1353.0 produced oil by seawater imbibition, though the recovery was very small. None of the other cores produced any oil by either seawater or surfactant imbibition. In these cases, none of the five surfactants improved oil recovery.

In an effort to determine the poor imbibition oil recovery in the Eagle Creek system, the Amott index wettability of the cores was measured. The Amott index of one core, #1387.5 after soaking in T91-8, was measured, $I_{w-o} = -0.49$, meaning that the core was medium oil-wet. The index indicates that soaking in T91-8 did not alter the oil-wetness of the core. This core imbibed water while it was soaked in brine and behaved like it was oil-wet after soaking in a T91-8 solution. Therefore, oil recovery in Eagle Creek cores by the surfactants was not improved. The heterogeneity of the rock increased the complexity of the problem. Another aspect of the ineffectiveness of the surfactant may be related to the rock lithological properties. The Eagle Creek rock consisted of wackestones or packstones containing dolomite, calcite, and some anhydrite. Perhaps the rock minerals interfered with surfactant reaction on dolomite so the wettability of the rocks remained unchanged.

None of the tested surfactants had a positive effect on Eagle Creek reservoir cores. For Eagle Creek crude oil/EC brine and Fuhrman Masho crude oil/seawater, oil recovery by spontaneous imbibition was poor both in water and in various surfactant solutions. At least one

core appeared oil-wet after soaking in a surfactant T91-8 solution. The surfactants tested in this project were not suitable for improving oil recovery in the Eagle Creek field.

Cedar Creek Anticline Dolomite Fields

In terms of oil producing rate on the Cedar Creek Anticline, the Red River formation is the #1 producer, the Stony Mountain is the #2 followed by the Interlake formation. The dolomite formations are highly heterogeneous. The laboratory objective was to find surfactants to improve oil recovery by spontaneous imbibition. The reservoir temperature is high at 200°F, and the usual surfactants are not stable at high temperature in high salinity water. The anionic surfactants Rhodapex CD 128i (CD-128) and Rhodacal A 246 L (RA-246L) were used for the laboratory tests. The high temperature imbibition tests were performed at the ConocoPhillips Technical Center (Bartlesville, Oklahoma).

Brine Composition

The produced water from all formations varied considerably due to 50 years of waterflood operations. The representative water analysis for the three formations obtained from Encore Acquisition Co. is listed in Table 10. The synthetic laboratory brine composition listed in Table 11 was the modification of the formation water analysis. HCO_3^- was removed to avoid the precipitation of bi-carbonate salts.

Table 10. Water analysis from Encore Acquisition Co.

Constituent	Interlake water, mg/L	Stony Mountain water, mg/L	Red River water, mg/L
Ca^{++}	421	2611	2363
Mg^{++}	85	453	560
Na^{+}	4610	9871	16398
K^{+}	35	70	400
$HCO3^{-}$	439	235	261
$SO4^{--}$	700	1600	1080
Cl^{-}	7365	19914	30523
Total dissolved solids, ppm	13655	34755	51585

Table 11. Composition of laboratory synthetic formation water

Composition	Interlake water, g/L	Stony Mountain water, g/L	Red River water, g/L
$CaCl_2$	1.168	7.246	6.557
$MgCl_2$	0.333	1.777	2.196
KCl	0.067	0.134	0.763
Na_2SO_4	1.035	2.127	1.598
NaCl	10.873	23.766	40.391
TDS, ppm	13476	35050	51504

Crude Oil Properties

Crude oils were from the same Cedar Creek Anticline dolomite reservoir. Operators in general have had difficulty obtaining representative oil samples from these producing formations. Oil samples from the wells were obtained just prior to the end of the chemical treatment cycle. Before use all oils were filtered to avoid any debris such as corrosion or scale products and degassed to avoid component change during the course of experiments (Table 12).

Table 12. Crude oil properties				
Crude oil	density at 22°C, g/ml	API gravity, °	viscosity at 22°C	note
Interlake	0.8902	27.5	51.4	Shallowest formation
Stony Mt.	0.8854	28.3	21.9	Middle formation/crude precipitation
Red River	0.8727	30.6	18.6	Deepest formation

Crude oils from Interlake and Red River formations were stable during the experiments. The crude oil from the Stony Mountain formation precipitated at room condition. Other researchers have observed the precipitation of Stony Mountain oil even after filtering by core plugs. It was not obvious that the precipitates were asphaltenes.

Initially a technique consisting of ultrasonic agitation to dissolve the precipitates was applied to samples of the Stony Mountain crude oil. The photomicrographs from before and after agitation as shown in Figure 24 demonstrate that vibration alone did not solubilize the precipitates.

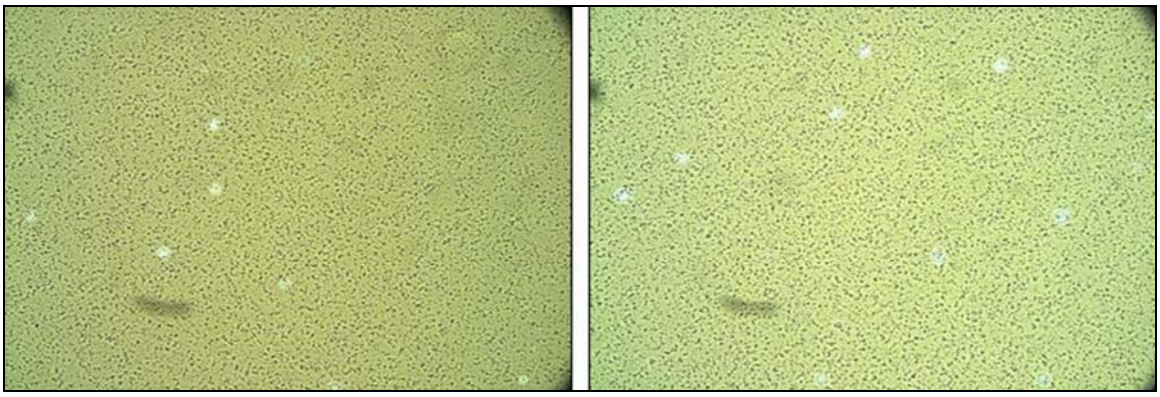

Figure 24. Stony Mountain Crude oil before (left) and after (right) sonic agitation and mixing.

The crude was then heated and maintained at 75^{o}C for 2 hours before ultrasonic mixing. This procedure did not affect the precipitates as shown in Figure 25.

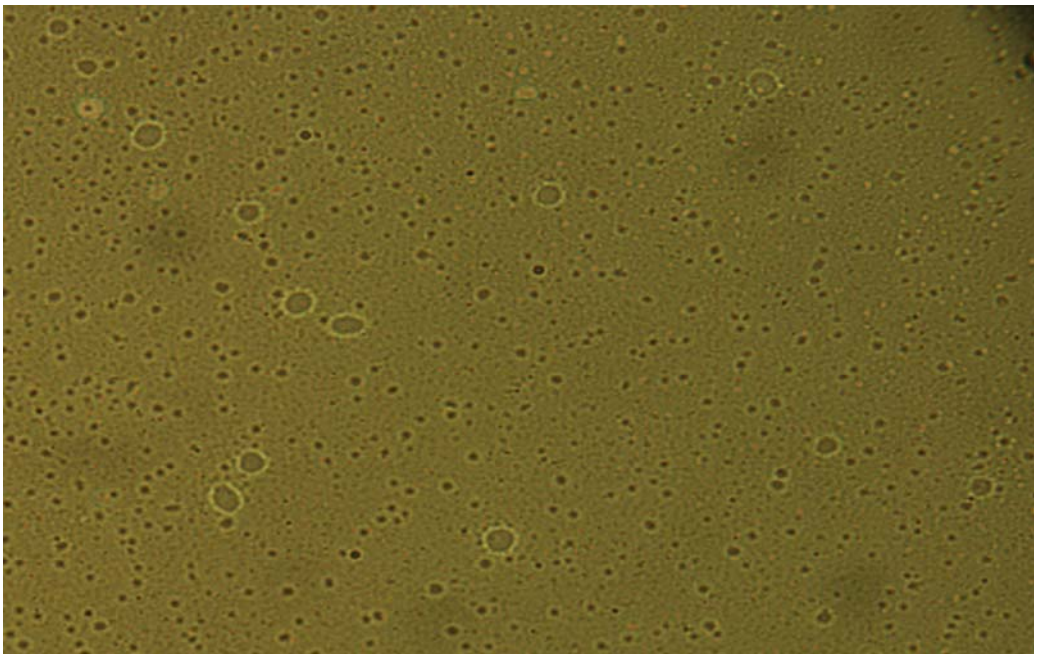

Figure 25. Heating followed by sonic mixing did not dissolve the precipitate.

Since asphaltene is soluble in naphthalene, xylene, and toluene, 20%, 50%, and 80% by volume of 1-methylnaphthalene was added to the crude as a means of identifying the precipitate. Figure 26 shows that the precipitates dissolved at all concentrations of solvent. Thus, the conclusion is that the particles are indeed asphaltenes.

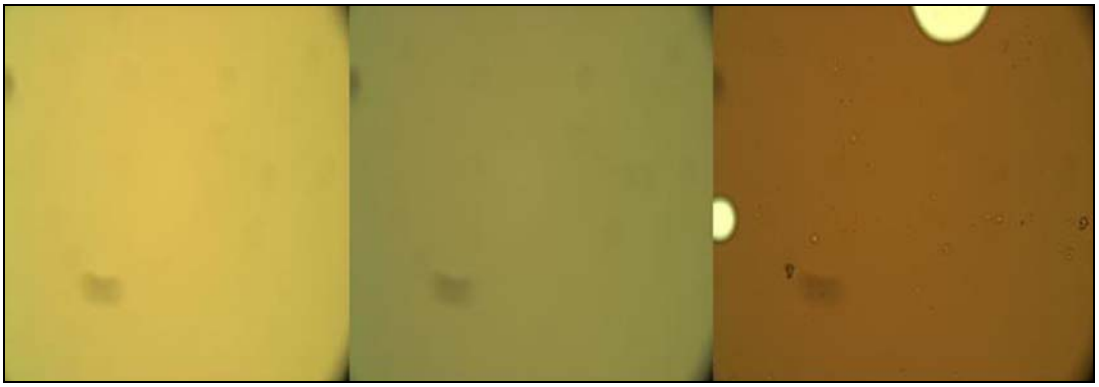

Figure 26. Left to right 80, 50, and 20% 1-methylnaphthalene added to Stony Mountain crude oil.

Reservoir Core Properties

The reservoir cores were obtained from the BEG core repository in Midland, Texas, and the plugs were cut by SCAL, Inc. The core samples from those dolomite formations were 1" in diameter. Some cores remained as non-cleaned; other cores were cleaned with toluene and CO_2. Gas permeability and porosity were measured for all cores. For non-cleaned cores, porosity and gas permeability were measured again after the cores were fully used and tested. Porosity ranged from 3–24%; permeability by SCAL, Inc., ranged from 0.02–148 md (Table 13). Porosities from the three zones were similar, but the permeabilities of Stony Mountain and Red River cores were much lower than that of the Interlake cores.

Table 13. Reservoir cores from Cedar Creek anticline							
Core#	If clean	L, cm	Kg, md	Kg after use, md	ϕ, %	ϕ after use, %	Initial water saturation Swi, %
Red River cores							
RR13	Cleaned by CO_2/C_7H_8	3.72	3.48	-	24.35	-	13.2
RR14	Cleaned by CO_2/C_7H_8	3.745	3.96	-	23.62	-	12.8
RR15	Cleaned by CO_2/C_7H_8	3.757	4.11	-	17.3	-	8.0
RR20	Cleaned by CO_2/C_7H_8	3.47	13.01	-	6.8	-	0.9
RRU 8719.75	Oil residue	4.71	0.27	0.35	10.83	10.85	0
RRU 8713.5	Oil residue	3.8	0.3	0.55	12.3	12.4	0
RRU 8715.35	Oil residue	5.12	1.47	1.8	17.21	17.3	0
Stony Mountain cores							
St 8188B	Looked clean	4.858	0.31	-	9.62	-	0
St 8801B	Looked clean	4.69	0.2	-	10.26	-	0
St 8801A	Looked clean	5.137	0.1	-	8.7	-	0
St 8800	Looked clean	5.35	0.14	-	11.46	-	0
St 8785	Looked clean	5.439	0.02	-	2.98	-	0
St 8831A	Looked clean	4.618	0.92	-	11.22	-	0
St 8293	Looked clean	5.503	0.92	-	9.43	-	4.6
St 8831B	Looked clean	4.981	0.49	-	7.09	-	2.8
St 8845A	Looked clean	4.125	4.41	-	14.52	-	5.6
St 8848A	Looked clean	3.714	1.88	-	13.07	-	5.8
Interlake cores							
IL 8230.65	Oil residue	5.5	148	148	11.69	11.69	0
IL 8286.35	Oil residue	4.68	21.5	22.1	7.62	7.4	0

Permeabilities and porosities are shown graphically in Figure 27.

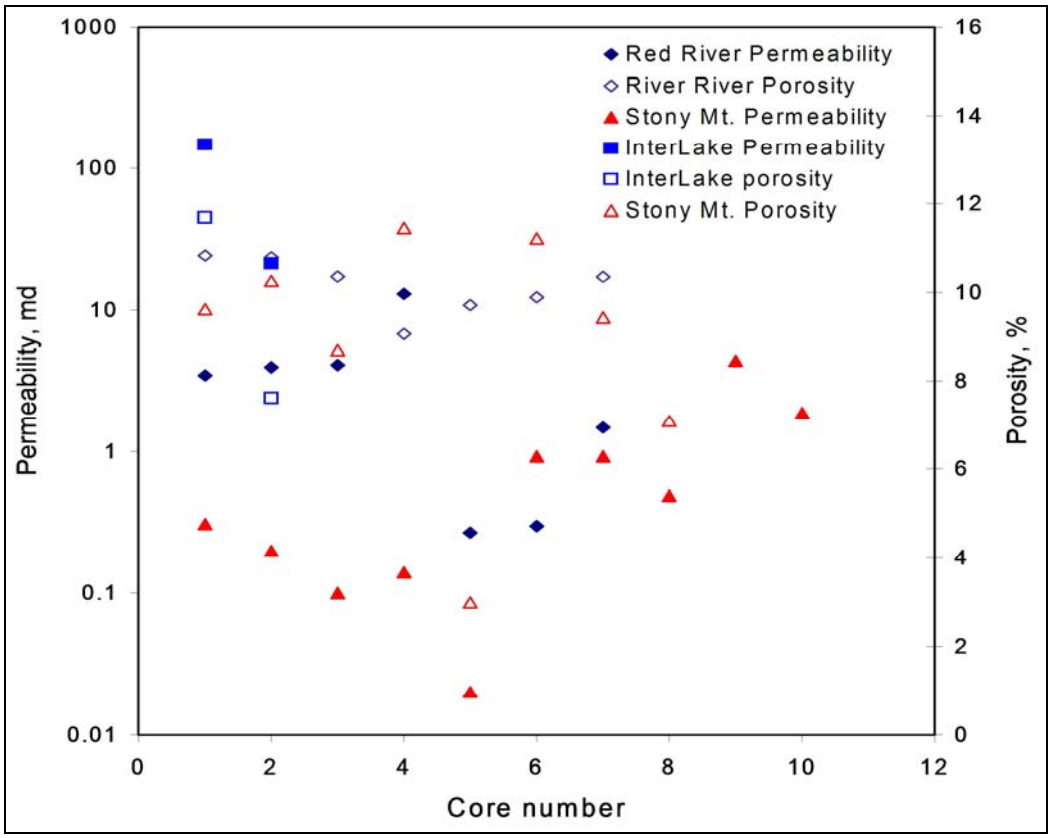

Figure 27. Permeabilities and porosities of all the cores.

Thin sections for rock samples indicated that the Interlake rock contained dolomite crystals and small clay particles (Figure 28) with good connection between pores.

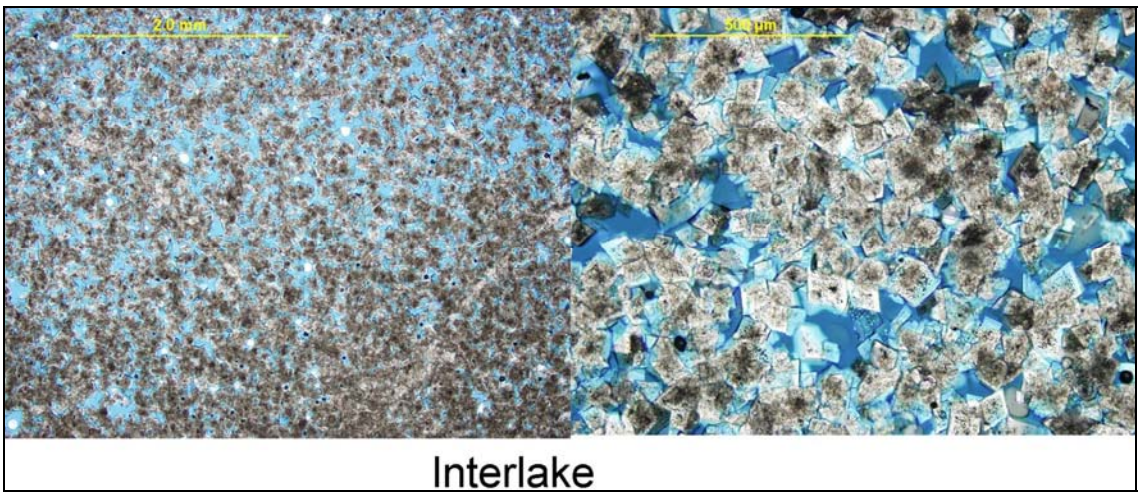

Figure 28. Thin section of Interlake dolomite.

Stony Mountain rock was clay-rich and heterogeneous and contained smaller dolomite crystals than the Interlake rock (Figure 29).

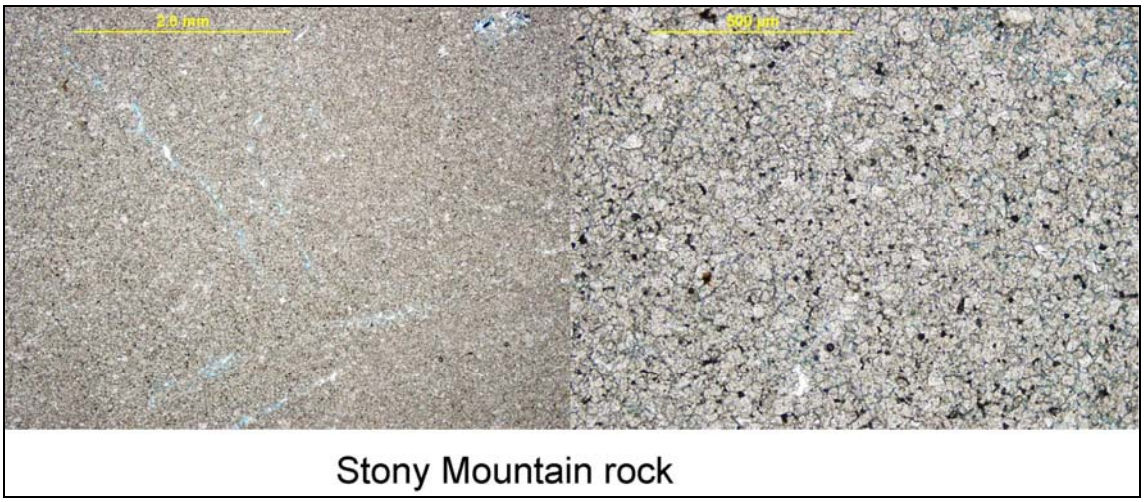

Figure 29. Thin section of Stony Mountain dolomite.

Red River rock also contained small dolomite crystals, anhydrite particles, a clay-rich band, fossils, and moldic pores (Figure 30).

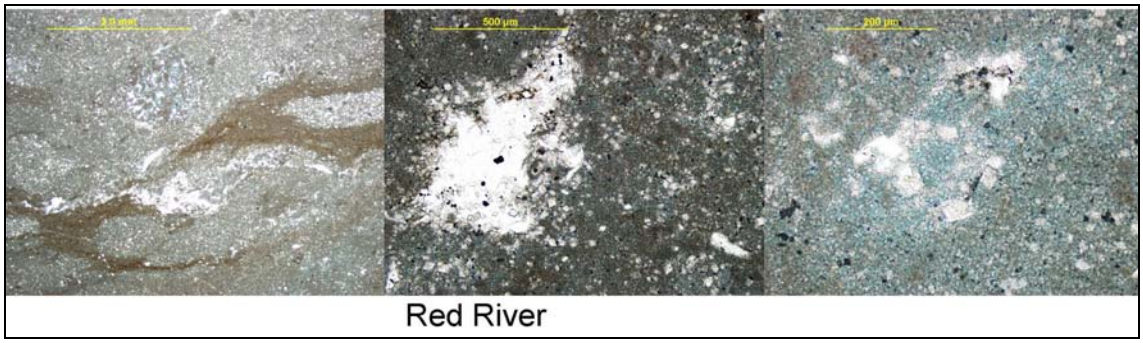

Figure 30. Thin section of Red River dolomite.

Surfactant Solutions

ConocoPhillips' previous experience with the anionic surfactants Rhodapex CD 128i (CD-128) and Rhodacal A 246 L (RA-246L) demonstrated improved oil recovery in chalk at a test temperature of over 212°F (100°C). These two surfactants (Table 14) were selected as the chemical agents to improve recovery of imbibition oil for carbonate rocks from the three Cedar Creek Anticline formations. However, Porter[12] pointed out that anionic sulfates contain a C-O-S bond that may not be chemically stable at temperatures higher than 122°F (50°C). To ensure chemical stability, CD-128 and RA-246L at a concentration of 1000 ppm were diluted with the formation waters. This concentration was used for all surfactant solutions in the spontaneous imbibition tests. The solutions were aged for 24 hours at 200°F. IFTs were measured by the drop volume method for both original and aged solutions at room temperature (71°F) except for RA-246L solutions, which were measured at 104°F. The RA-246L Interlake water solution was clear since the salinity of the Interlake water was relatively low. Precipitation appeared in RA-246L with Stony Mountain and Red River waters at room temperature, and the solutions became clear when the solution temperature reached 104°F (40°C) or higher. The IFTs are listed in Table 15. It appeared that the CD-128 was thermal stable since the IFTs only increased slightly

after aging. The IFTs of the RA-246L solutions were too small to be measured by the drop volume method (The accuracy of the drop volume method is ± 0.1 dynes/cm).

Table 14. Physical and chemical properties of anionic surfactants CD-128 and RA-246L		
Product name	Rhodapex CD 128i	Rhodacal A 246 L
Chemical name	Ammonium C6-10 alkyl ether sulfate	Sodium alpha-olefin sulfonate
Simplified as	CD-128	RA-246L
pH	7 at 10 wt%	-
Commercial concentration, (wt%)	~ 56–60	39

Table 15. IFT measurements of anionic surfactants CD-128 and RA-246L				
Brine / Crude oil	Formation water (71°F)	CD-128 solution (71°F)	Aged CD-128 solution (71°F)	RA-246L solution and aged solution (104°F)
Interlake (IL)	26.5	2.1	4.0	< 0.1
Stony Mt. (ST)	26.2	0.9	2.1	< 0.1
Red River (RR)	32.8	1.8	2.4	< 0.1

Laboratory Procedure

Clean cores were first saturated with formation water. After at least 10 days of soaking, the cores were set on porous plates for water displacement to establish initial water saturation. Then the cores were weighed, and crude oil from the same formation was introduced by vacuum. Cores with oil residue were directly saturated with the crude oil. Imbibition tests at 200°F with a backpressure of 12 psi were performed at the ConocoPhillips Technical Center after the wettability was restored by aging all cores in crude oil at 200°F. The cores were first soaked in formation waters to imbibe. After the brine imbibition stopped, the cores were transferred to surfactant solutions for further spontaneous imbibition.

Nuclear Magnetic Resonance (NMR) Carr–Purcell–Meiboom–Gill (CPMG) measurements[13] were performed on all cores before brine imbibition, before surfactant imbibition, and after surfactant imbibition. The objective was to verify the indirect NMR measurements of porosities and water saturations of the cores at various imbibition stages with direct physical measurements.

Results

The effect of brine pH and ionic strength on the IFTs

The effect of brine pH and ionic strength on the IFTs between brine and crude oil from the Interlake, Stony Mountain, and Red River formations were investigated. Brine with pH values from 2–12 and Na^+ ionic strengths from 0.01 M–1 M was used in the measurements. The results were compared with that of a standard oil–n-decane. To make Na^+ buffer solutions with different pH values and different ionic strengths, the following chemicals from strong acids to strong bases were used: HCl, CH_3COOH, CH_3COONa, Na_2HPO_4, NaH_2PO_4, Na_2CO_3, $NaHCO_3$, NaOH, and NaCl.

The IFTs between three oils and brines with different pH values and ionic strength are shown in Figures 31–33. All the IFTs had the similar trend in comparison with that of decane. When pH = 5–11, only the pH and ionic strength affected the IFTs slightly. On the acidic side (pH < 5), the IFTs decreased with the decrease of the pH value; an ionic strength of 1 M had the

lowest IFTs. On the basic side, pH also decreased when the pH value increased; the effect of ionic strength was not obvious.

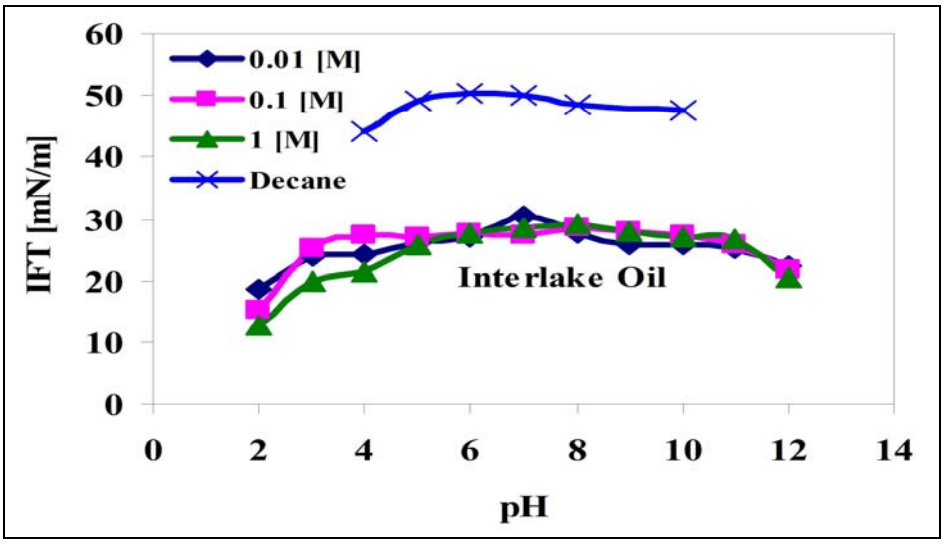

Figure 31. Interlake oil IFTs as a function of pH..

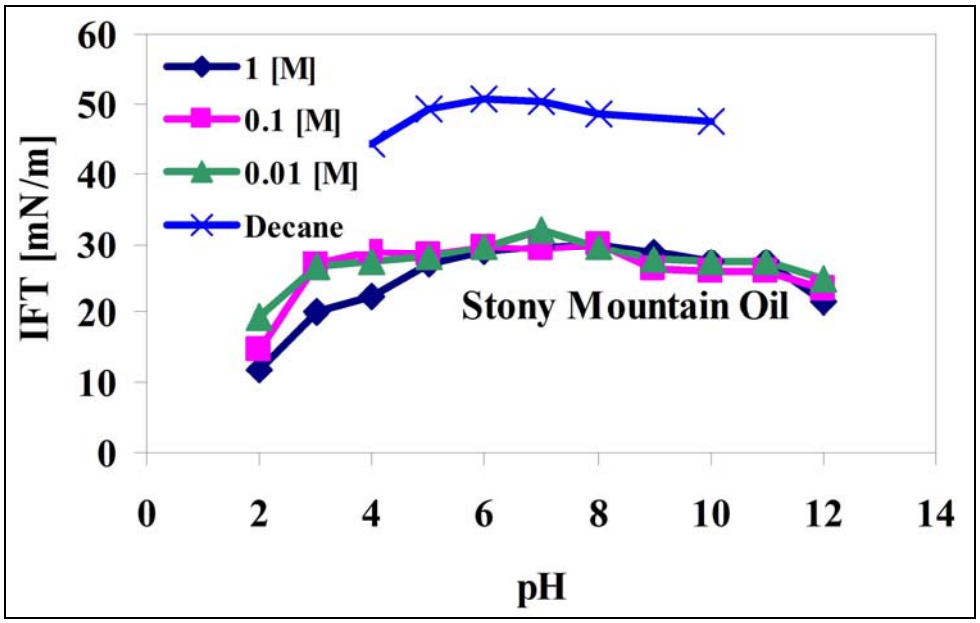

Figure 32. Stony Mountain oil IFTs as a function of pH..

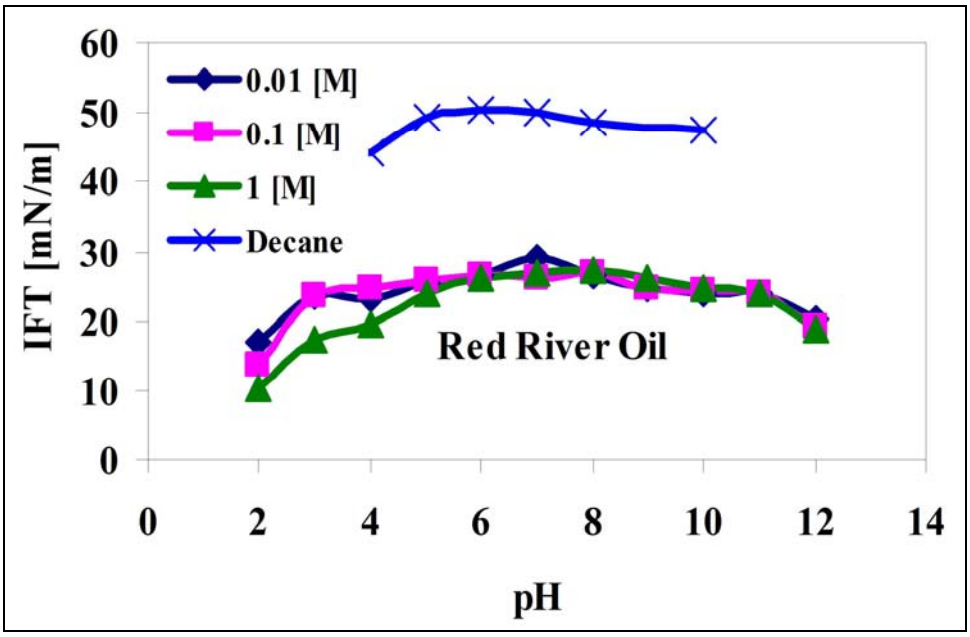

Figure 33. Red River oil IFTs as a function of pH..

Spontaneous Imbibition

Stony Mountain Cores

Core plugs were cut from whole core from wells 22-32C (LAMP), 12-15A (Pine Unit), and 14-14A (Pine Unit) in the Stony Mountain formation. Oil recovery by spontaneous imbibition versus imbibition time for Stony Mountain cores is plotted in Figures 34 and 35.

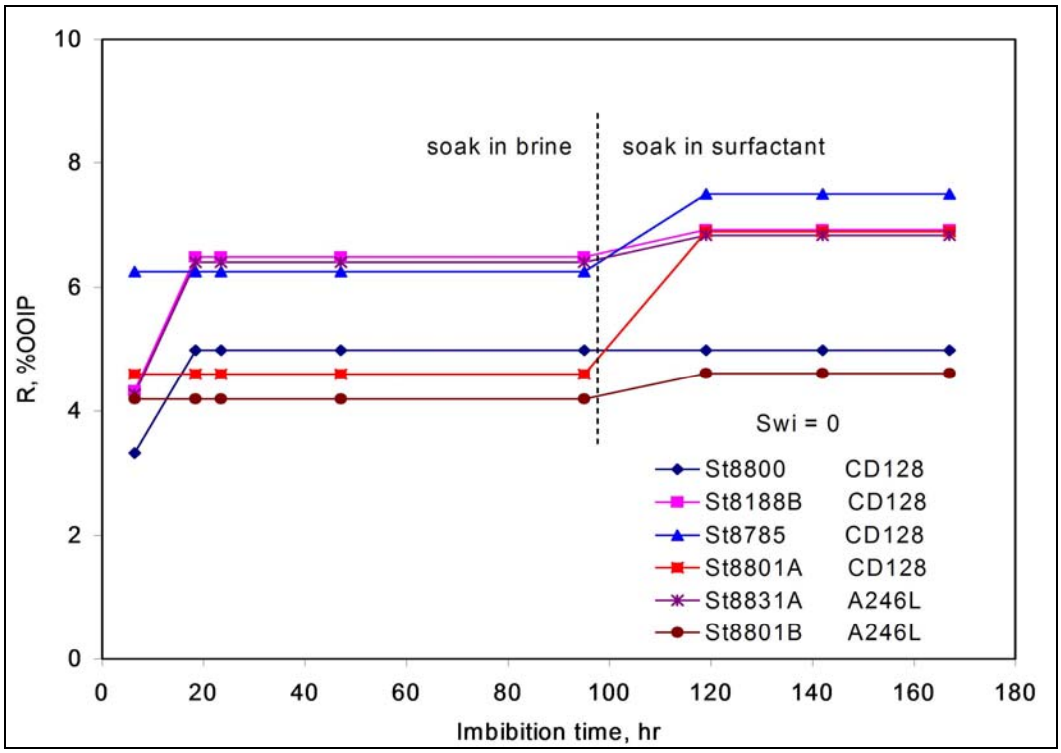

Figure 34. Imbibition results for Stony Mountain cores when S_{wi} = 0.

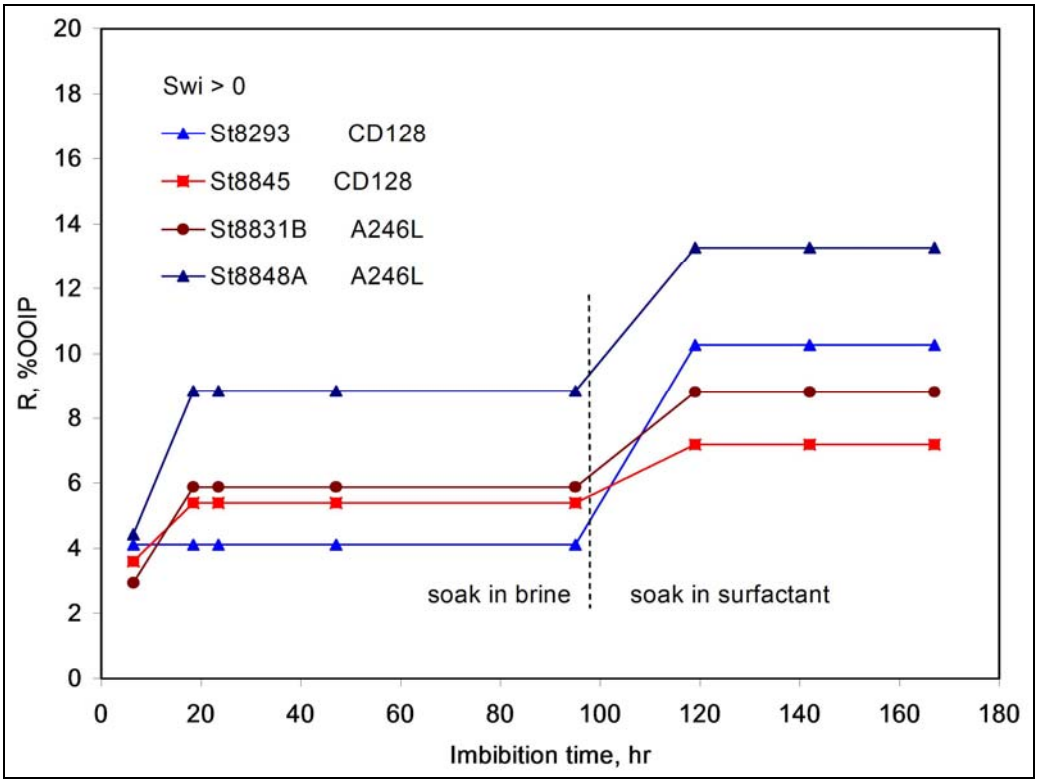

Figure 35. Imbibition results for Stony Mountain cores when S_{wi} > 0.

Oil recovery by spontaneous imbibition in Stony Mountain water was less than 15%. When S_{wi} = 0 (Figure 34), oil recovery was improved up to 2% by the CD-128 solution, and less

than 1% by the RA-246L solution. When $S_{wi} > 0$, 2–6% more oil was produced with the CD-128 solution, and 3–5% more oil with the RA-246L solution (Figure 35). Note that that thermal expansion may have been responsible for part of the oil recovered at the beginning of the imbibition process when the cores were in brine solution.

Since the permeability of the Stony Mountain cores was very low (gas permeability of most cores was less than 1 md), it was understandably difficult for the surfactant to penetrate far enough to have much effect on oil recovery during the laboratory time scale. Nevertheless, the two anionic surfactants improved oil recovery by imbibition.

Red River Cores

The non-cleaned Red River core plugs came from the Coral Creek well 23X-10 whole core (Red River U4 zone) as did the cleaned cores, which were cleaned three times with CO_2-toluene. Imbibition tests were conducted on both clean and non-cleaned cores. For the three non-cleaned cores with initial water saturation $S_{wi} = 0$, oil recoveries by spontaneous imbibition were 51, 54, and 77%, respectively. Those recoveries were very high for spontaneous imbibition, indicating the strongly water-wet nature of the cores. Imbibition of the CD128 solution increased oil recovery by another 4%, but the A246L solution did not improve oil recovery (Figure 36).

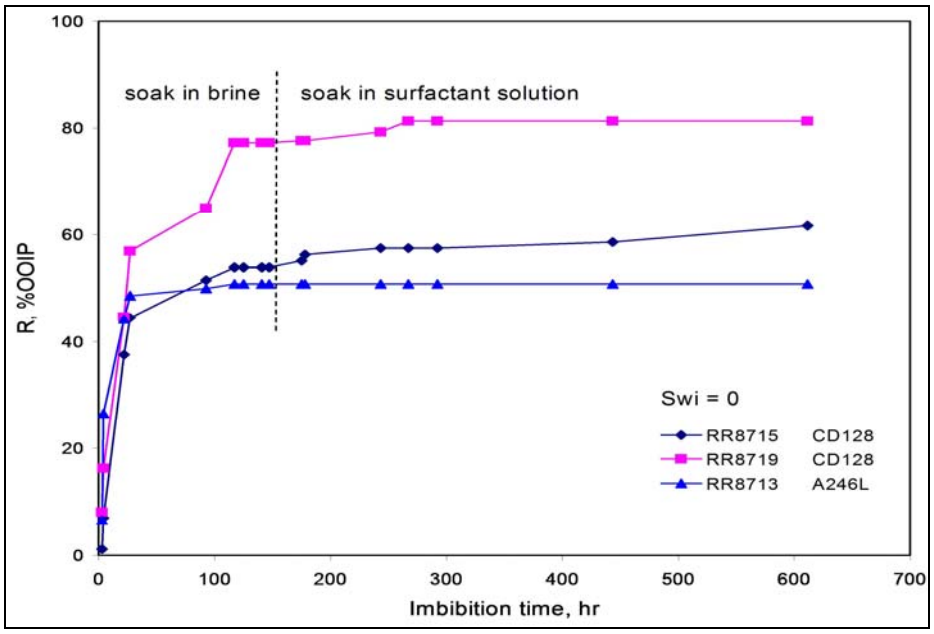

Figure 36. Spontaneous imbibition of Red River cores for $S_{wi} = 0$.

For the cleaned cores, initial water saturation ranged from 1–13.2%, and oil recovery by brine imbibition ranged from 2–21%. Imbibition of the CD128 solution improved oil recovery by 4–8%, whereas the A246L solution improved oil recovery up to 3% as shown in Figure 37.

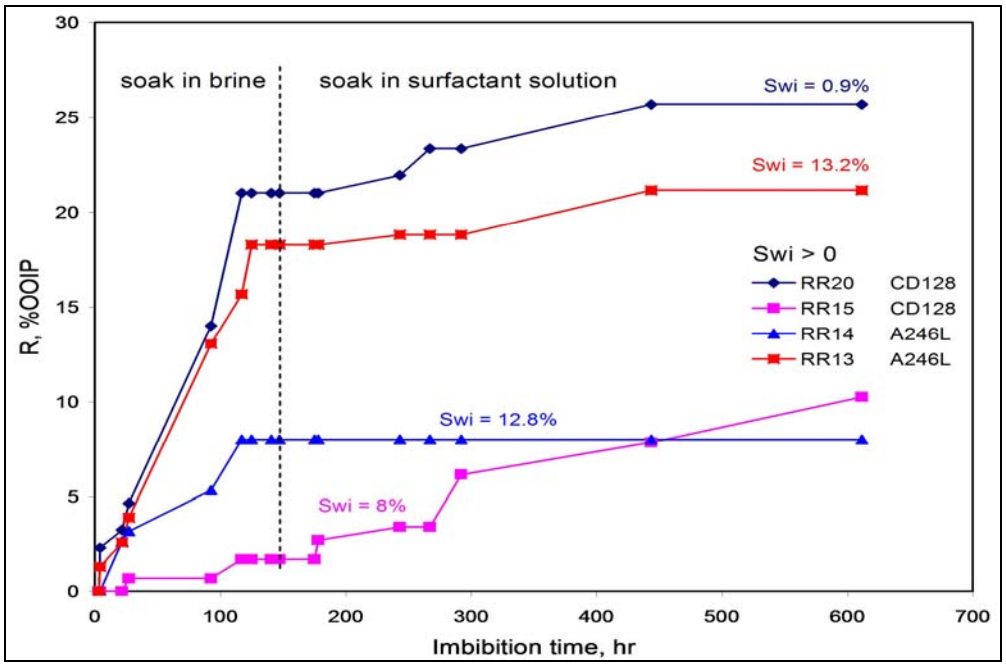

Figure 37. Spontaneous imbibition of Red River cores for $S_{wi} > 0$.

Interlake Cores

Non-cleaned Interlake core samples were cut from slabbed Interlake core (Pennel Well 34-10). The two Interlake cores had much higher permeability than those from Stony Mountain and Red River formations. Imbibition curves for Interlake cores are plotted in Figure 38.

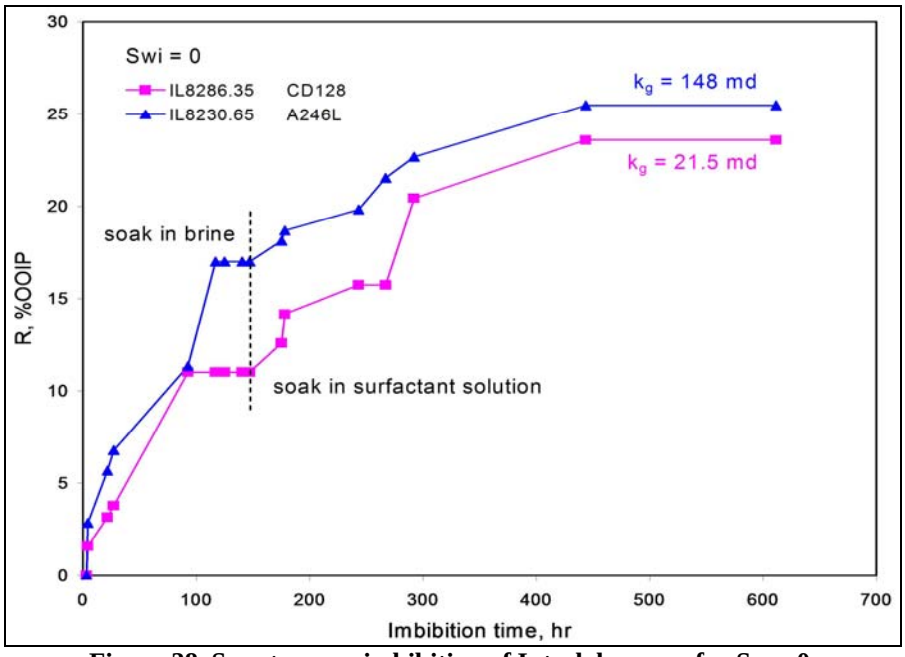

Figure 38. Spontaneous imbibition of Interlake cores for $S_{wi} = 0$.

Oil recovery from the two cores by Interlake brine imbibition was 11% and 17%, respectively. After the cores soaked in CD128 and A246L solutions, improved oil recovery was

12.6% and 8.5%, respectively, indicating that both surfactants were very effective in improving oil recovery of the Interlake cores.

As shown in Figure 39, core permeability can affect oil recovery by spontaneous imbibition, both for brine and surfactant solutions. Usually higher permeability allows the aqueous phase to imbibe more efficiently, therefore resulting in higher oil recovery. BVO in the cores also had a similar effect on oil recovery, though not as obvious as that of permeability.

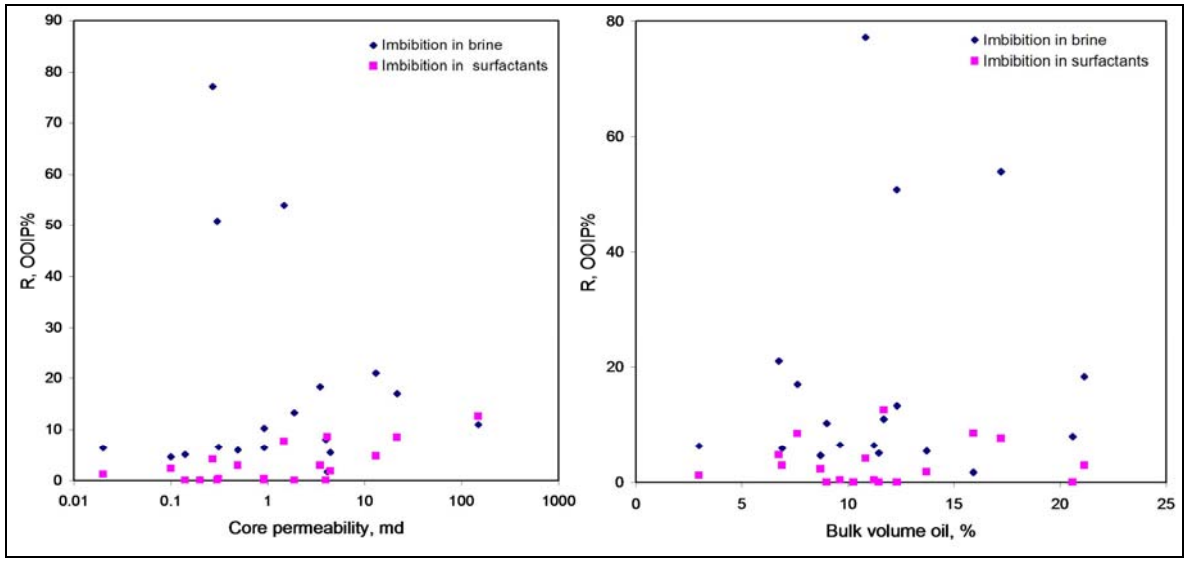

Figure 39. Effect of permeability and BVO on imbibition oil recovery.

Nuclear Magnetic Resonance Carr–Purcell–Meiboom–Gill Measurements

From saturation and displacement measurements, porosity and initial water saturation varied widely in range, from 7–24% and up to 13.2%, respectively. The NMR population density vs. resonance time T2 curves for all the cores is plotted in Figures 40–43. The NMR scans were taken prior to brine imbibition, after brine imbibition, and after surfactant imbibition.

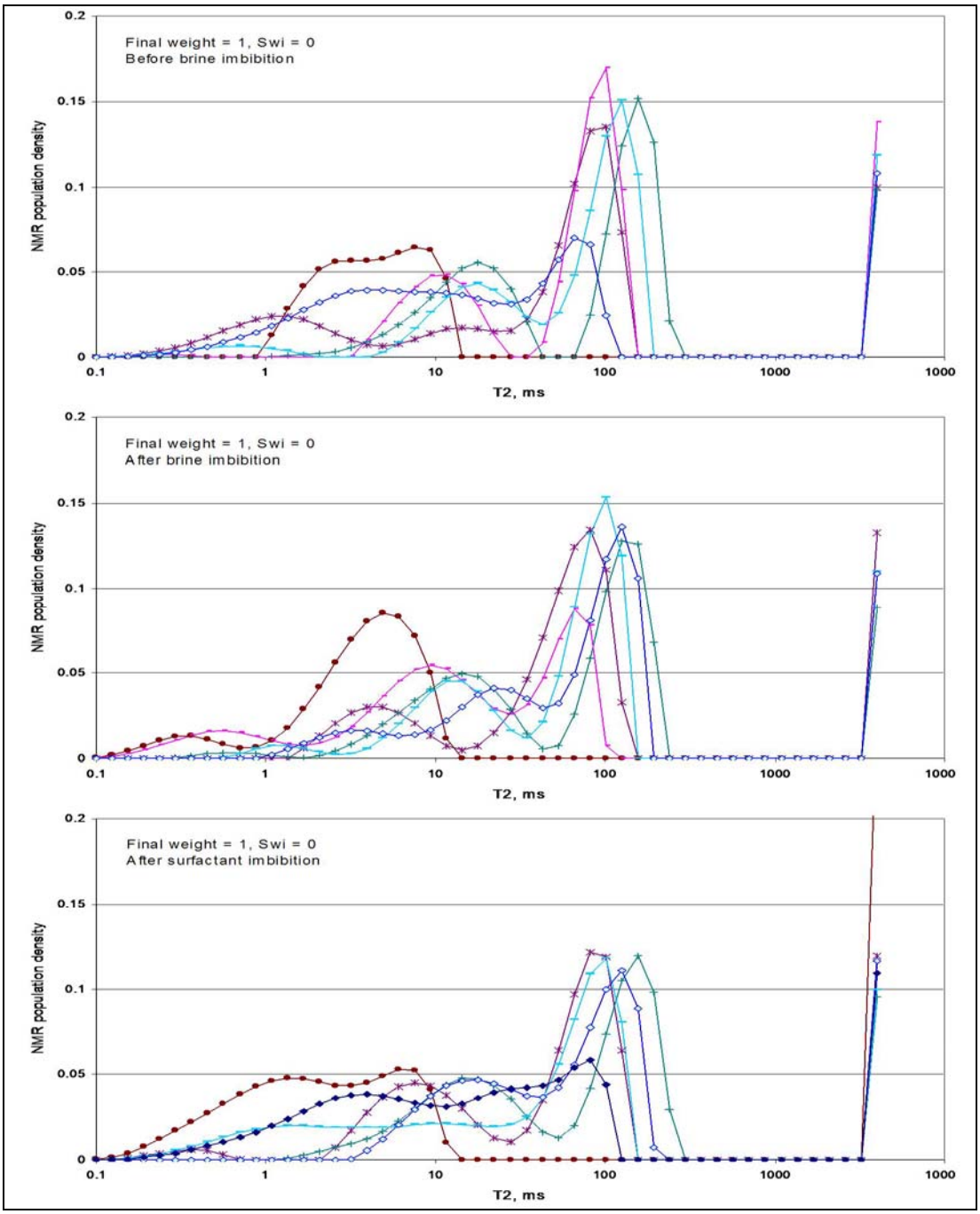

Figure 40. NMR scanning curves for Stony Mountain cores with S_{wi} = 0.

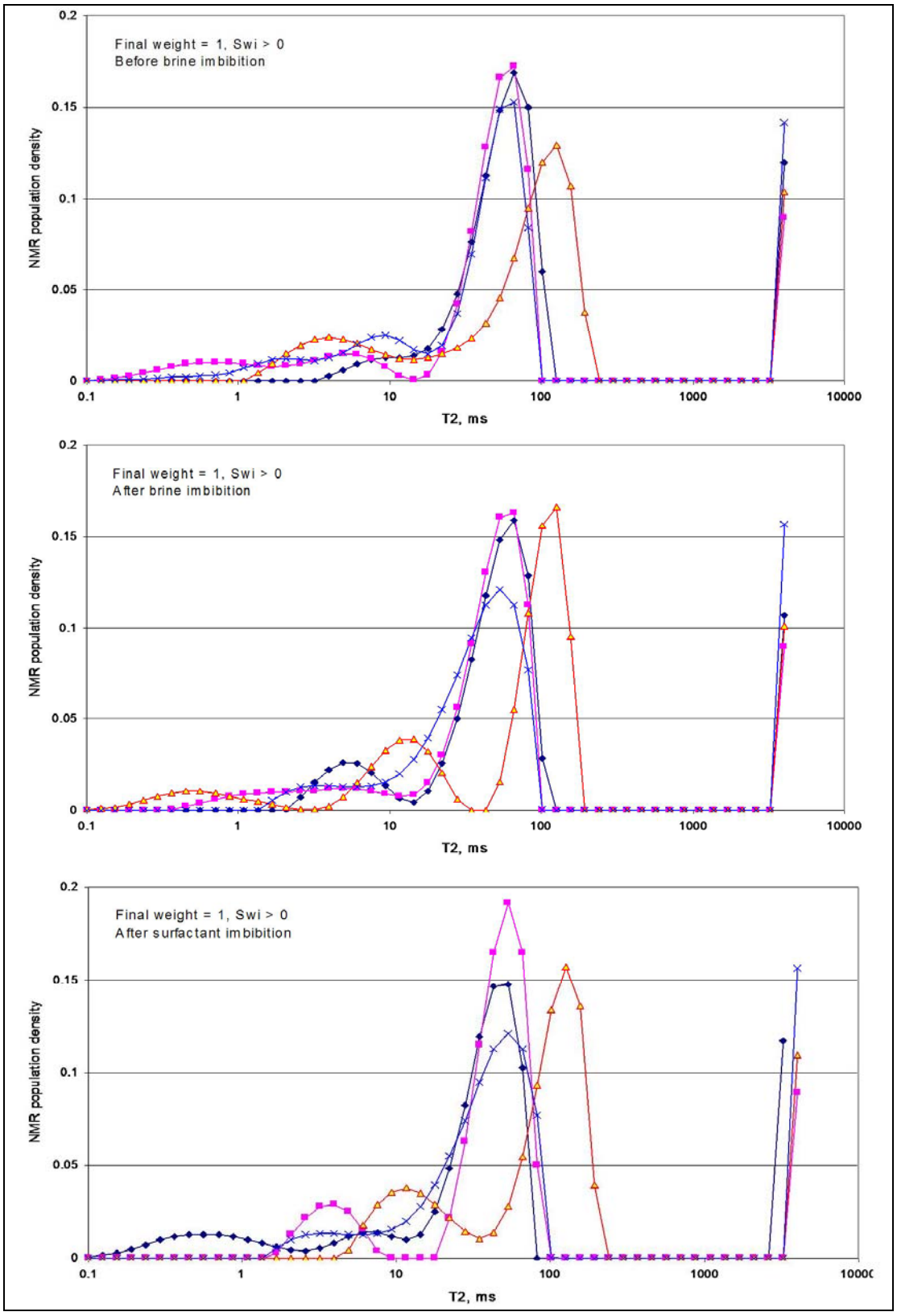

Figure 41. NMR scanning curves for Stony Mountain cores with $S_{wi} > 0$.

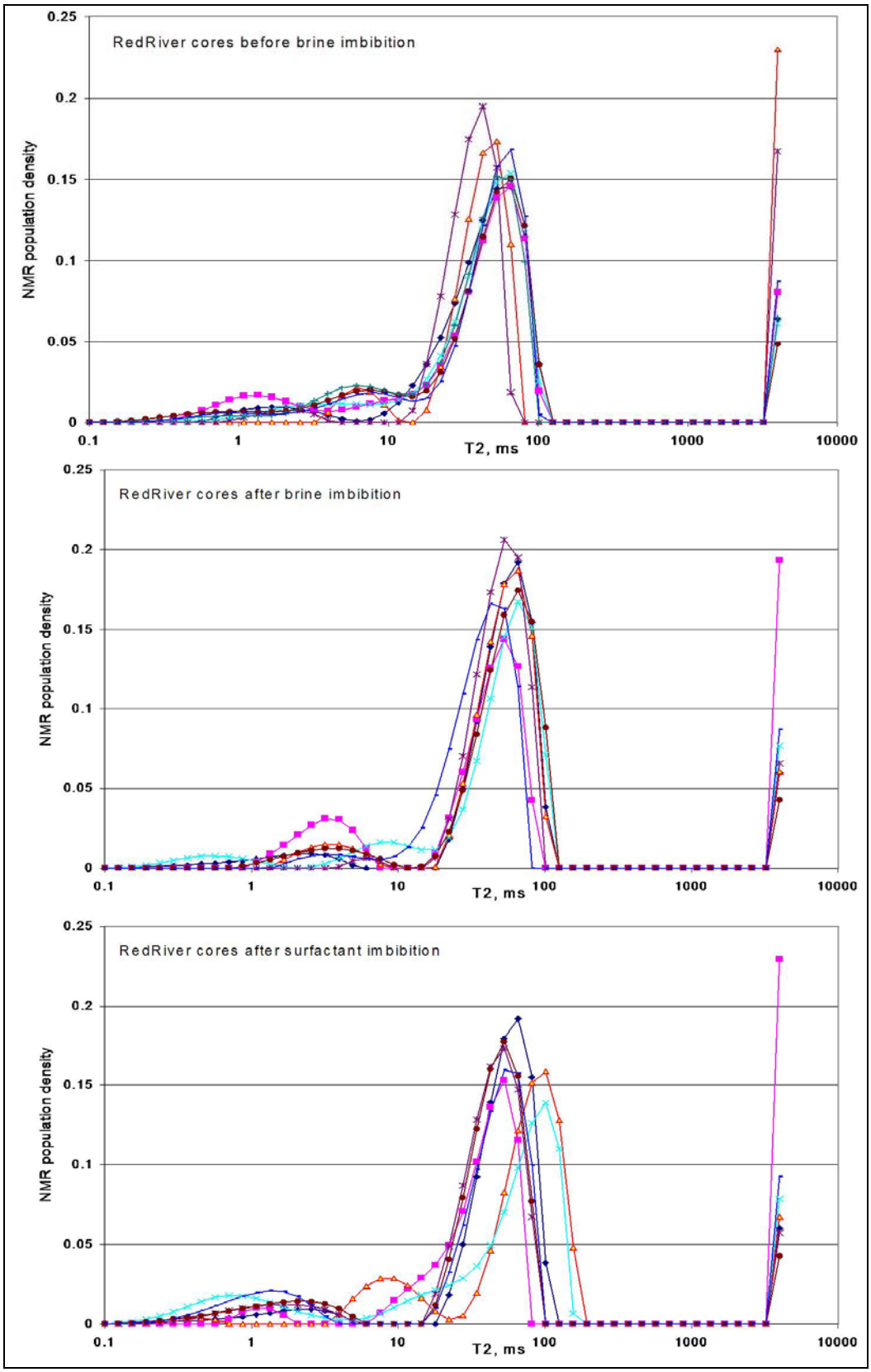

Figure 42. NMR scanning curves before and after imbibition for Red River cores.

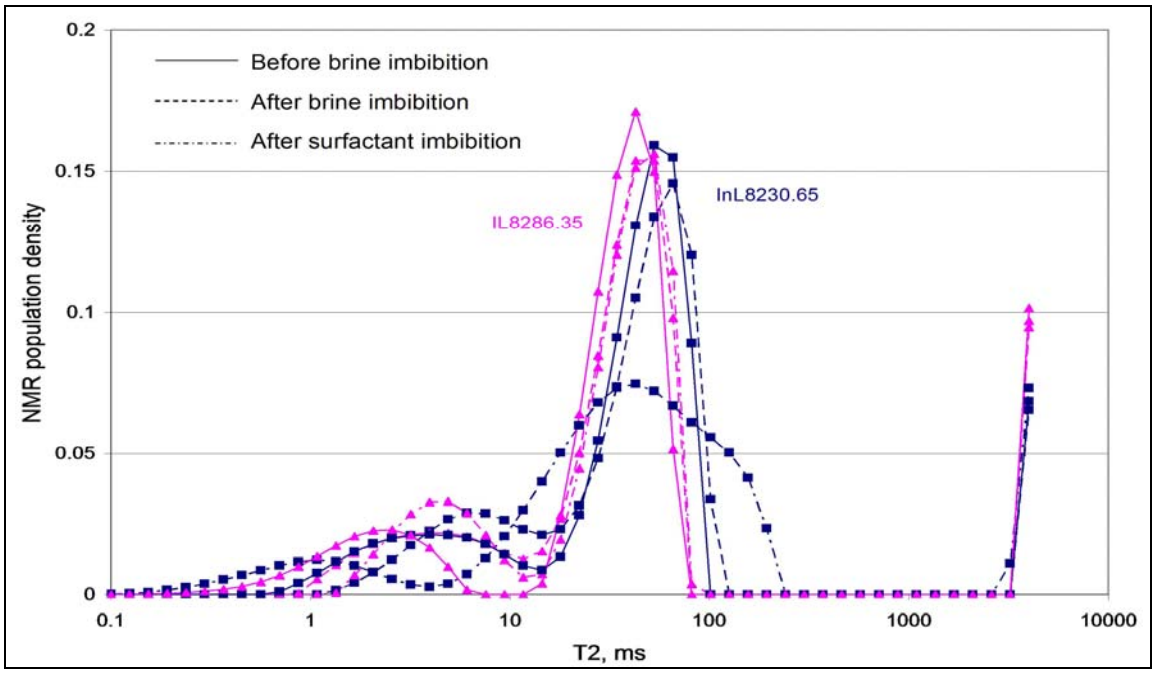

Figure 43. NMR scanning curves before and after imbibition for Interlake cores.

As seen from the figures, most of the curves have very distinct peaks for water and oil contained in the cores. The porosities derived from the size of NMR and water saturations derived from the CPMG curve peaks and spans are plotted against those measured with the volumetric method (Figures 44 and 45).

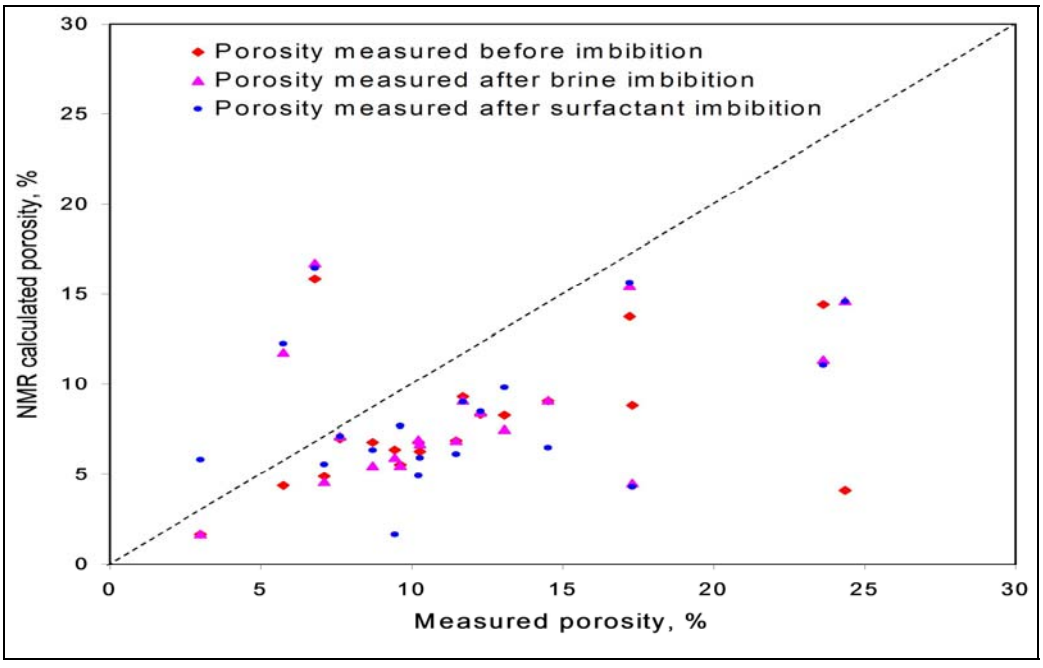

Figure 44. Comparison of porosity between measured and NMR derived.

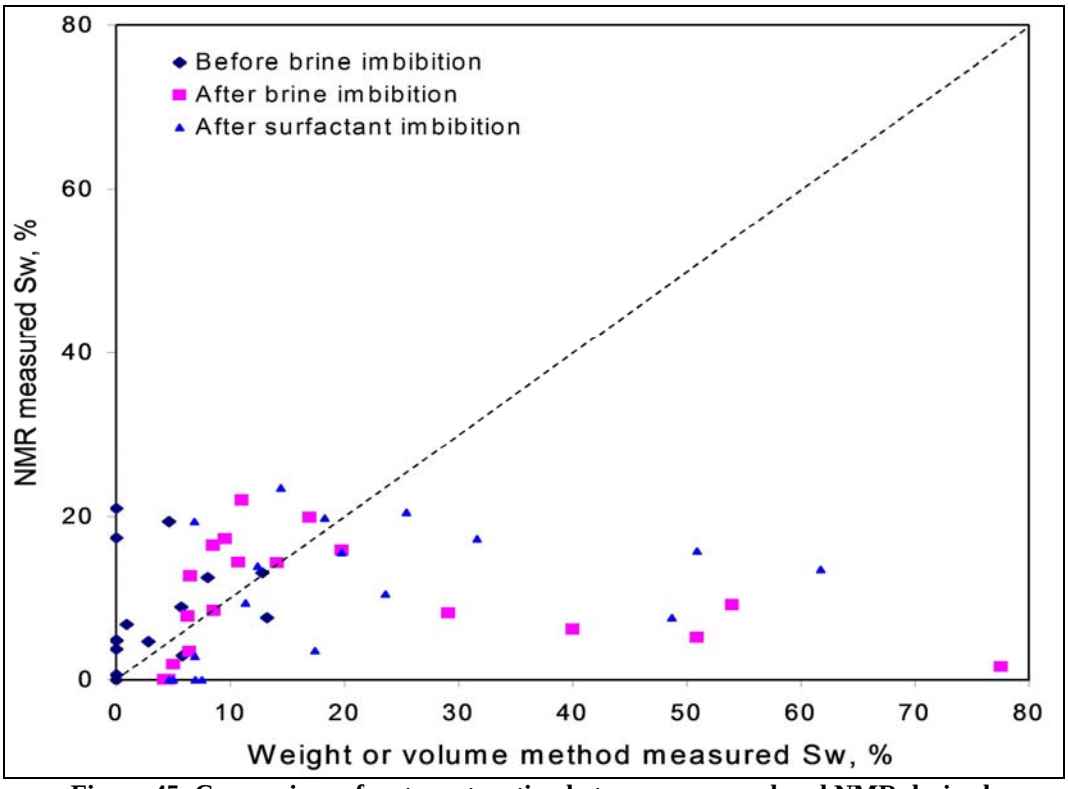

Figure 45. Comparison of water saturation between measured and NMR derived.

Some of the NMR calculated porosities and water saturations closely match the volumetric (or weight) measurements. The mismatches may have been caused by the heterogeneity of the rocks.

NMR CPMG measurements have been effective in measuring porosity and water saturation for homogeneous rocks such as Berea sandstone.[14] However, these Cedar Creek anticline carbonate cores are not amenable to the NMR method of determining porosity and water saturation.

Summary

The anionic surfactants CD 128 and A246L had a small effect on cores from the Stony Mountain formation due to the extremely low permeability (in the range of 0.2–4 md). For the three non-cleaned Red River cores, oil recoveries by spontaneous imbibition in formation water were 51, 54, and 77%, respectively. Those recoveries were very high for spontaneous imbibition, indicating the strongly water-wet nature of the cores. Imbibition of the CD128 solution increased oil recovery by another 4%, but the A246L solution did not improve oil recovery. For cleaned Red River cores, initial water saturation S_{wi} ranged from 1–13.2%, while oil recovery by brine imbibition ranged from 2–21%. Imbibition of the CD128 solution improved oil recovery by 4–8%. The two Interlake cores had much higher permeabilities than those from the Stony Mountain and Red River formations. Oil recovery by imbibition of formation brine was 11% and 17%, respectively. After the cores imbibed CD128 and A246L solutions, oil recovery was improved by 12.6% and 8.5%, respectively.

The brine pH and ionic strength had a minor effect on IFTs between oil and brine from the Cedar Creek Anticline. NMR measurements were not accurate for porosity and initial water saturation measurements.

The laboratory work supports field tests of the surfactant soak process in the San Andres dolomite formation in fields near the Fuhrman Masho. While not as dramatic as the San Andres results, the Stony Mountain and Interlake dolomites also responded to the improved imbibition oil recovery with surfactants. The Red River water-wet results were not expected since this formation is widely believed to be oil-wet. A discussion with the operator supports the water-wet nature of the cores from that well. The oil production and oil cut from the well are abnormally high, and special core analyses with cores from the well also suggest that the Red River dolomite is water-wet. Production from other Red River wells on the Cedar Creek anticline does not support a water-wet reservoir. The NMR measurements performed in conjunction with the Cedar Creek imbibition study were not confirmed by the physical laboratory measurements. The NMR technique could not be used as a substitute for the physical measurements of porosity and water saturation obtained from the dolomite cores.

The shallow San Andres formation on the northwestern edge of the Permian Basin proved to be too tight/oil-wet to facilitate spontaneous imbibition of water and resulting oil production. Core material from the Arbuckel formation in Kansas was received during the last month of the project; hence, this material was not included in the laboratory program.

The laboratory work demonstrated that alkyl ether sulfate, CD128, was stable at 200^{o}F. This chemical had been reported by others to suffer thermal degradation. Ionic strength and pH had only a minor affect on surfactant-oil IFTs measured in the Cedar Creek fluids.

The laboratory work convincingly demonstrates that chemical EOR screening needs to be conducted with real reservoir rock-fluid systems.

Part B Engineering

Overview

During the course of the 2-year project, the Cottonwood Creek Phosphoria surfactant soak treatments were revisited. The update included extended production history and the development of a neural network that included the oil-producing rate prior to the surfactant treatment. The inclusion of the prior oil rate as an input variable resulted from an evaluation of water-frac completions in a tight San Andres dolomite reservoir (Fullerton San Andres Unit). The evaluation demonstrated that a strong relationship existed between the prior oil rate and water-frac results. A 3-3-1 neural network was developed to correlate water-frac production response with the average and skew of the gamma ray log through the pay section plus the prior oil rate.

The Fullerton neural network was used to generate baseline water-frac predictions for use in evaluating the effectiveness of incorporating surfactant into water-fracs. The predicted response was quite impressive. Unfortunately, the operator of the Fullerton San Andres elected not to prove/disprove the predictions with field tests due to very high service company costs to mix surfactant into the frac water.

Although Cottonwood Creek is located in the Big Horn Basin of Wyoming, production is from a dolomite, and the dataset was used to predict surfactant response from three San Andres reservoirs in the Permian Basin.

The Cottonwood Creek dataset was used to predict surfactant soak performance in three wells in the West Fuhrman Masho Unit (WFMU). A 15 well dataset from the Cottonwood

Creek field tests was used to correlate the prior oil rate, the average of the neutron porosity log, and the pounds of surfactant per foot of pay with the oil rate following the treatment. The West Fuhrman Masho Unit, the Fullerton San Andres Unit, and the Cottonwood Creek Phosphoria Unit all produce from dolomite zones in limestone reefs. The WFMU operator conducted three field tests of the process to confirm the predictions. The field tests were precisely conducted with mechanical clean out of the wells, installation of new downhole pumps, and daily well tests for 1 month prior to pumping the surfactant treatments. The tests were conducted during October 2006. Daily well tests were conducted following the treatment. One of the treatments generated additional oil.

The Eagle Creek San Andres field is located on the northwest shelf of the Permian Basin. The Cottonwood Creek neural network suggested that wells in this very tight dolomite reservoir were excellent candidates for surfactant soak stimulation. Unfortunately, the laboratory results did not support the numerical predictions; thus, field tests were not conducted.

The boundaries of the public domain neural network used to evaluate the Cottonwood Creek dataset are constrained to the magnitude of the production response and the amount of surfactant used in the 23-well dataset. Commercial neural networks included in software packages such as *Matlab* can extrapolate beyond the limits of dataset domain. The neural network architecture developed with the public domain neural network was used to train an identical *Matlab* neural work. The training curve results are practically indistinguishable.

An analysis of the NMR scans collected during the high temperature imbibition tests conducted on core-fluid systems from Cedar Creek Anticline dolomite reservoirs was not beneficial. Scatter in the measurements prevented meaningful correlations using the conventional CPMG technique. Fuzzy curves and neural networks were investigated as pattern recognition tools to correlate the NMR scans with porosity and changes in water saturation during imbibition. The AI method generated improved correlations between NMR patterns and porosity. However, neither the AI nor the conventional methods of analysis generated meaningful correlations between the physical changes in saturation and changes in the scan patterns.

Cottonwood Creek Revisit

The production response of the 23 wells subjected to imbibition stimulation in the Phosphoria zone of the Cottonwood Creek field was revisited and updated.[9] Continental Resources, the field operator, provided the response through November 2005. The 23-well composite performance is shown in Figure 46. The noise in the production trend following the production of 110,000 bbl of oil is due to operational changes related to gas production. It is evident that these initial experimental treatments generated 15,000 bbl of incremental oil. The average incremental recovery was 680 bbl/well for a sum of 15,000 bbl. The total cost to treat the first 22 wells was $167,443 including acid and pulling unit cost. The cost of the surfactant treatment alone averaged $2512 per well (3063 lb/well). The recovery can be expressed as 4.5 lb of surfactant per barrel of incremental oil. The treatments were done during last half of 2002 and early 2003 when the cost of surfactant was about $0.80/lb. Today the surfactant cost is over $1.00/lb.

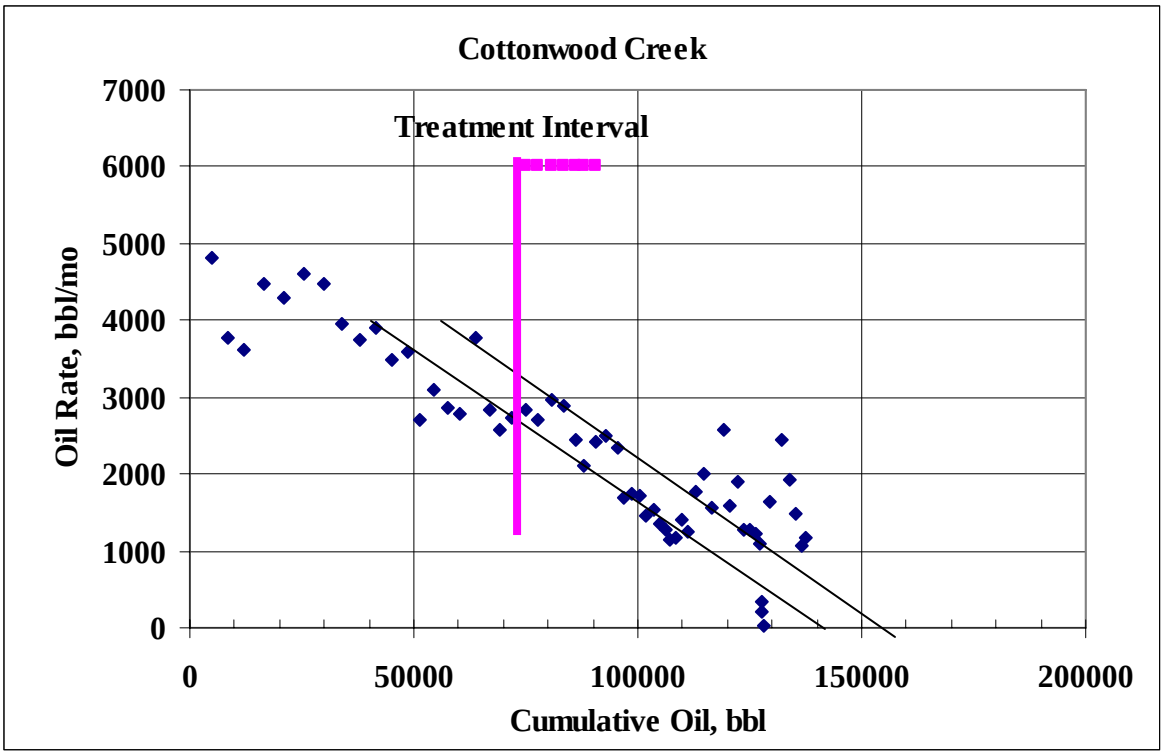

Figure 46. 23-well composite performance through November 2005.

The recovery-cost calculations are based on the average well performance. The response of well 218, shown in Figure 47, was superior to all others. The pink bar denotes the application date.

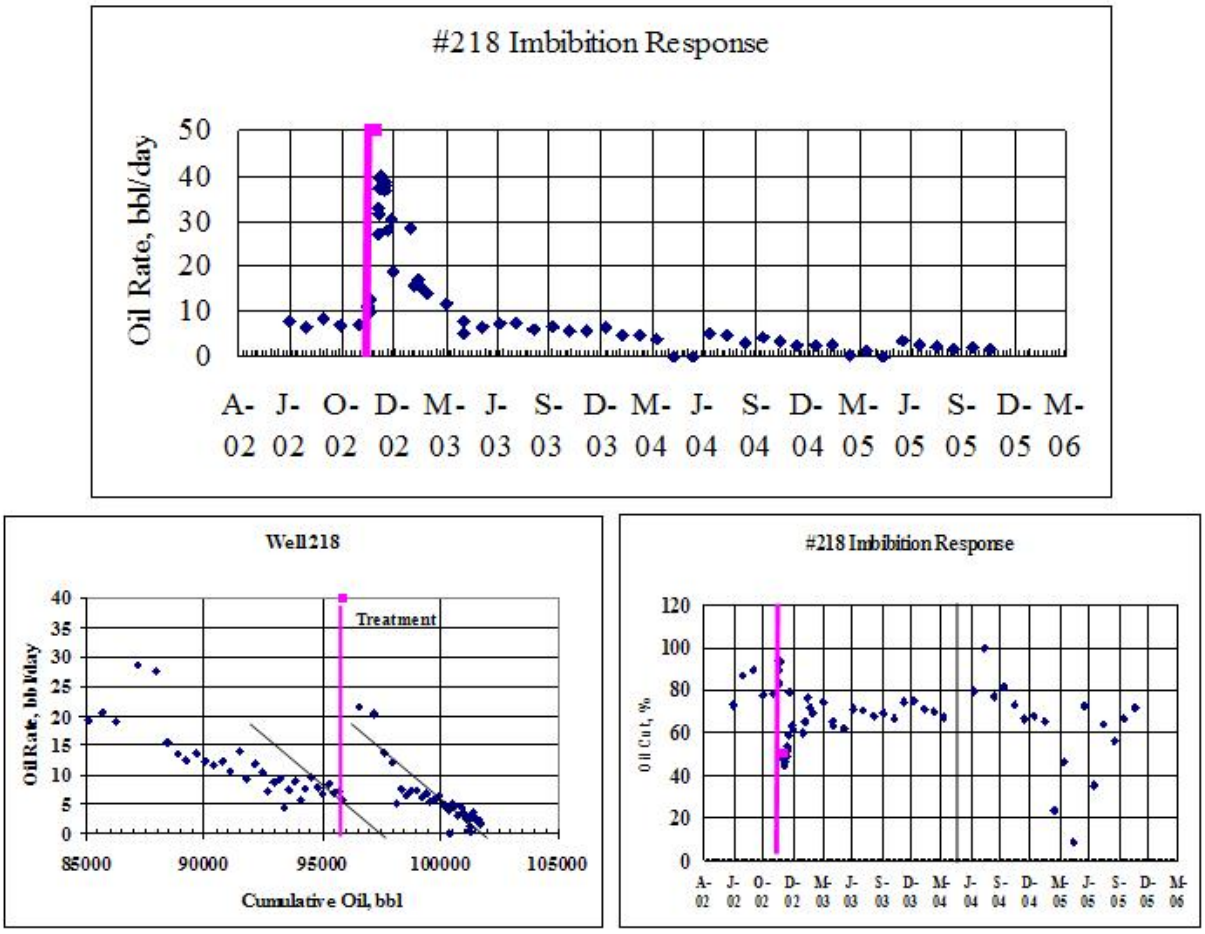

Figure 47. Cottonwood Creek well 218 performance through November 2005.

Well 218 produced 4500 bbl of estimated ultimate incremental recovery (EUIR). The goal of applying AI to the revisited and updated Cottonwood Creek dataset was to improve the average recovery from future well treatments.

An analysis of the Fullerton San Andres water-frac stimulations revealed that a strong correlation existed between the oil producing rates before and after treatment. The Fullerton analysis is presented later in this report. The correlation demonstrated that good wells are better water-frac candidates than poor wells. The same conclusion can be drawn from the Cottonwood Creek surfactant soak dataset as shown with the fuzzy curve in Figure 48.

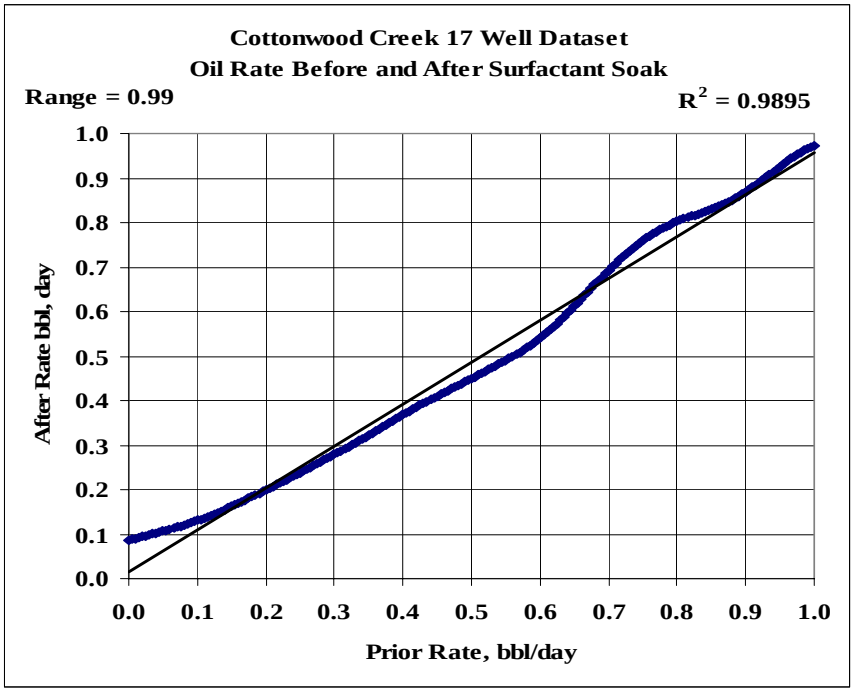

Figure 48. Cottonwood Creek fuzzy curve: before and after oil rates.

The benefit of a strong correlation between the before and after oil rates was incorporated into a 3-2-1 neural network using the before oil rate, the average of the neutron porosity, and the amount of surfactant as shown in Figure 49. The trained neural network was used to design surfactant soak treatments for San Andres fields.

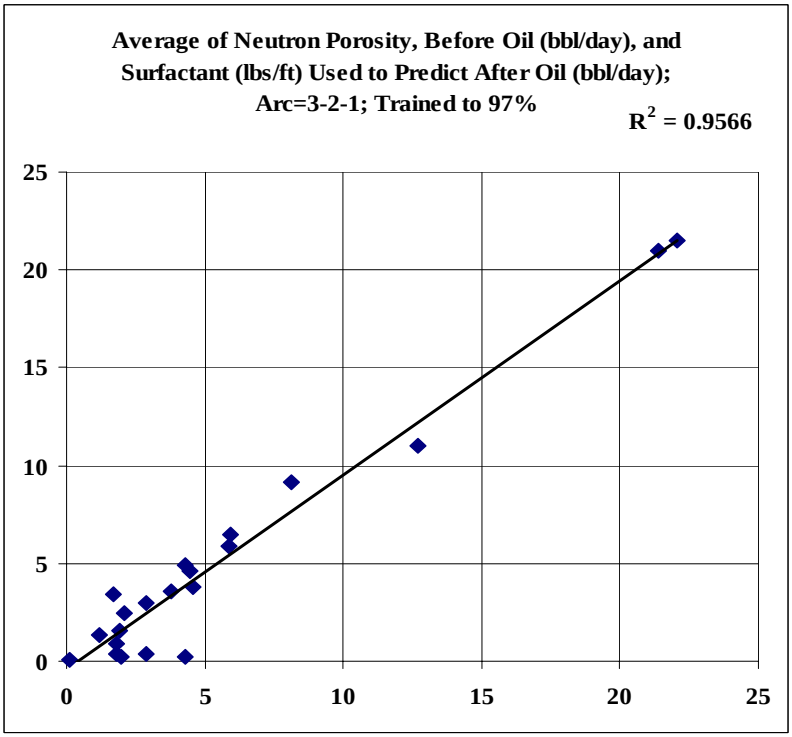

Figure 49. Results of the Cottonwood Creek neural network training.

San Andres Dolomite Reservoirs

West Fuhrman Masho Unit

The West Fuhrman Masho Unit is located near Andrews, Texas. Oil is produced from the same dolomite zone from which cores were cut for the laboratory imbibition tests described earlier. The information necessary to design surfactant soak treatments in the WFMU operated by Range Resources was provided and used to generate ~20 lb/ft of pay and ~75 lb/ft surfactant treatments for four wells. The wells are in an area of the field that has not met production forecasts. The trained neural network shown in Figure 49 was used with the average of the neutron porosity and the prior oil rate from WFMU wells 95, 152, 242, and 243 to predict the oil rate following treatment of the wells with 3000 lb of T91-8 surfactant. The quantity of surfactant was held constant and then increased to 9000 lb for a second set of predictions. The results are tabulated in Table 16.

Table 16. Neural network predicted response

	BOPD prior to treatment	BOPD after to treatment with 3000 lb	BOPD after to treatment with 9000 lb
WFMU95	17	22	22
WFMU152	8	12	**22**
WFMU242	8	**16**	13
WFMU243	10	**21**	22

Range Resources elected to test the laboratory results and the neural network predictions with three test wells in the WFMU highlighted in Table 16. Mechanical problems prevented a test in a fourth well. The Tomadol 91-8 surfactant soak field test procedure was as follows:

1. One month prior to treatment, pumps were pulled, and wells were mechanically cleaned to remove paraffin and scale. A new pump was installed, and the oil and water production rates were measured daily along with the pumping fluid level.

2. After the establishment of a 30-day baseline, surfactant was mixed in 1000 bbl fresh water (well 243) or 1000 bbl produced water (wells 152 and 242). The surfactant treatment for well 243 consisted of 3000 lb or 21 lb/ft of pay, 9000 lb or 75 lb/ft for well 152, and 3000 lb or 16 lb/ft for well 242. The treatments were followed by a displacement volume of 80-100 bbl. Both treatment and over-flush pumped into the wells at ~5 bbl/min at 130 psi pump pressure. Wells were shut-in for a 7-day soak period.

Well 152 averaged 5.0 BOPD prior to treatment and 7.8 BOPD for the first 27 producing days following the soak period. Well 152 produced a "chocolate milk" type emulsion that was difficult to break, but did clean up. Well 242 averaged 6.0 BOPD prior to treatment and 6.2 BOPD for the first 11 producing days following the soak period. Well 243 averaged 6.4 BOPD prior to treatment and 6.3 BOPD for the first 42 producing days following the soak period. Well 152 cost $29,383; Well 242 cost $18,783; and Well 243 cost $21,686.

The initial field test results are presented in a graphical format in Figures 50–52. The response period is too short to evaluate the effectiveness of the treatments. The initial oil rate response predicted by the neural network trained with Cottonwood Creek data is shown in Table 16 above. Mechanical problems prevented the well 95 treatment.

Well 152 was treated with 75 lb/ft of pay (9000 lb) and predicted to produce at a 22 BOPD rate.

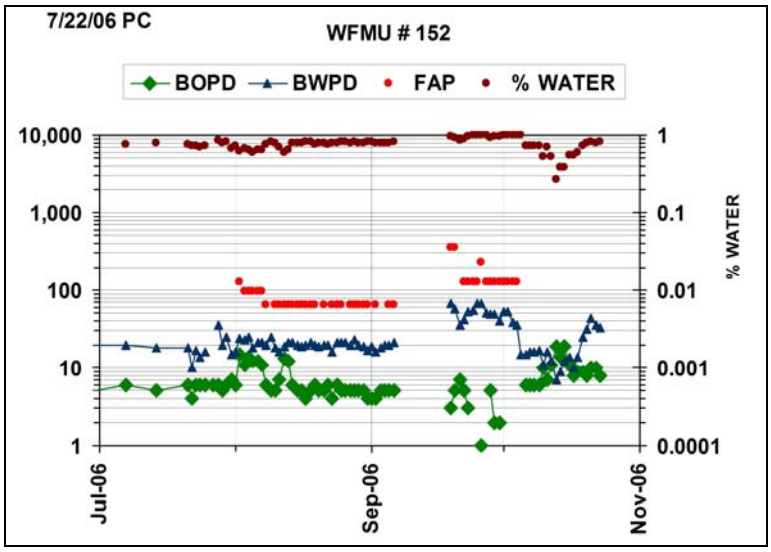

Figure 50. Well 152 initial response.

Well 242 was treated with 25 lb/ft (3000 lb) and predicted to produce at a 16 BOPD rate.

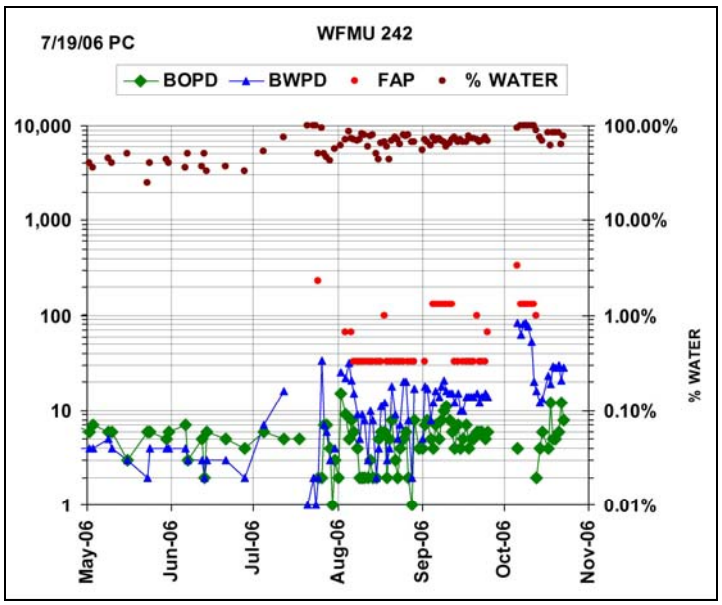

Figure 51. Well 242 initial response.

Well 243 was treated with 25 lb/ft (3000 lb) and predicted to produce at a 21 BOPD rate.

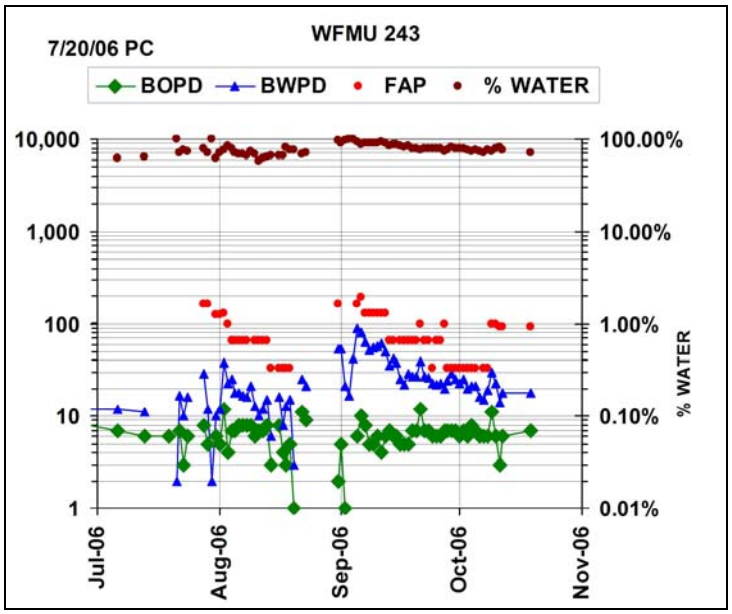

Figure 52. Well 243 initial response.

To date, well 152 has generated a positive response. All wells have demonstrated an increase in total fluid produced. The three wells produce from the equivalent of the B, C, and D zones in the Boner #40 well in the Fuhrman Masho field. Cores from the Boner #40 were used in laboratory tests where surfactant worked very well in the C zone, but not very well in the B zone.

Eagle Creek San Andres Field

The Eagle Creek San Andres field is located on the northwest edge of the Permian Basin near Artesia, New Mexico. The 7% porosity San Andres formation is found at 1300 ft. After an unsuccessful 1980s era waterflood, the 200+ wells in the field produced an average of less than one-half barrel of oil per day. The marginally economic tight oil reservoir now produces at extremely low bottom-hole pressures under primary conditions. Water salinity varies considerably throughout the field as a result of limited fresh water injection. The variation is shown in Figure 53. The variation resulted in the decision to test surfactant effectiveness in multiple salinity waters.

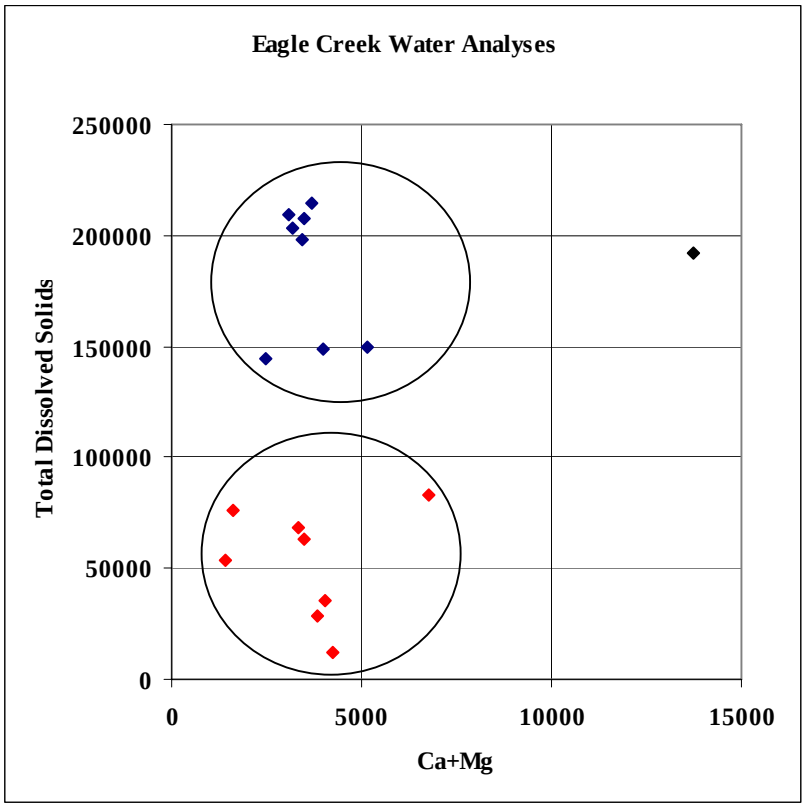

Figure 53. Variation in water hardness.

Optimum surfactant treatments were developed for Yates Petroleum following a presentation of the Fuhrman Masho San Andres laboratory results with information from prior field tests in the Cottonwood Creek Phosphoria field. The J-Lazy-J lease predictions were developed concurrently with the laboratory imbibition testing program.

Data from the Cottonwood Creek field were used to train a neural network to predict the performance of surfactant treatments in the Eagle Creek San Andres field. The training dataset was the result of surfactant treatments applied to 21 Cottonwood Creek Phosphoria wells. The gamma ray log and the quantity of surfactant expressed as lb/ft of pay were used to train the neural network to predict the percentage change in production after the surfactant.

Combinations of different statistical parameters of the gamma ray log pattern and bbl/ft of surfactant were used to train the neural network. The standard deviation of gamma ray and the lb/ft of surfactant generated the best training result. Figure 54 shows the neural net training result using the standard deviation of the gamma ray and lb/ft of surfactant as inputs.

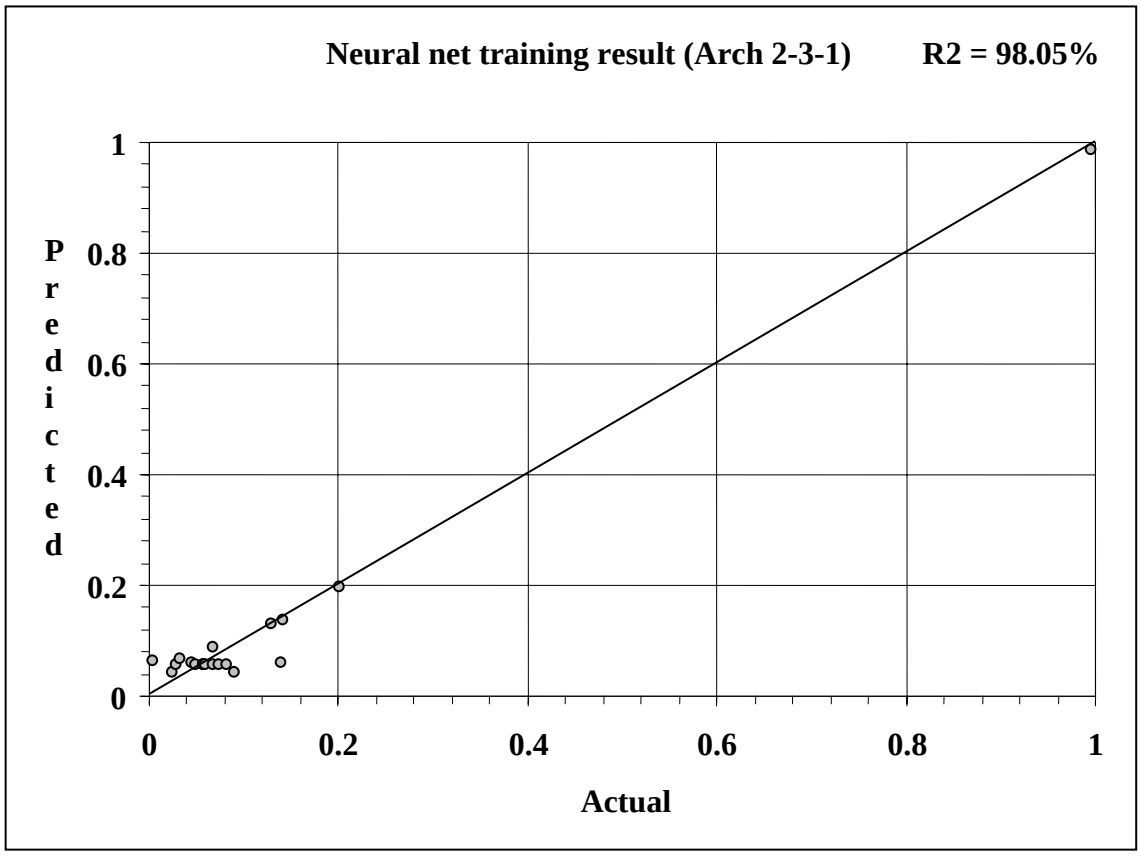

Figure 54. Neural network training result.

The neural network trained to 98%. Care was taken to avoid overtraining. The small dataset necessitated a simple training architecture. The trained neural network was used to predict the optimum surfactant treatment for the J-Lazy-J lease wells.

Eighteen wells are on the J-Lazy-J lease. Only 12 wells have the well logs required to make predictions. The optimum neural network predictions follow in Table 17.

Table 17. Optimum surfactant treatments

Well	Avg. production (before treatment), bbl/mo	Predictions (% change)	Production (increase/decrease)	Surfactant required (lb)
2	6.33	1492	94	1680
3	6.33	113	7	4170
4	15	78	12	1665
6	10	590	59	1680
7	3	1437	43	2790
8	6.3	91	6	2025
11	3	1508	45	950
12	3	1508	45	760
13	18.3	1249	228	1860
14	10	1508	151	1100
15	10	231	23	3840
17	8	1508	121	1580

These results were generated concurrently with the ongoing laboratory work. The completed laboratory work did not support the use of surfactant soak technology. The reservoir is either too oil-wet or too tight to imbibe either water or surfactant.

Fullerton San Andres Field

The Fullerton San Andres field is located in west Texas near the town of Andrews in the heart of the Permian Basin similar to the Fuhrman Masho field. The Fullerton operator, Texland Petroleum, has demonstrated that inexpensive water-fracs with very low sand concentrations are an economic method of stimulating the tight, low volume wells. The operator expressed an interest in incorporating the surfactant soak process in the water-frac design.

The operator's intention of including surfactant in the water-frac design dictates the development of a method of measuring the incremental oil response to surfactant. To date, about 80 wells have been water-fraced in this tight oil reservoir. Additional wells await stimulation; and the intention is to include nonionic surfactant in the stimulation fluid. The anticipated oil response to water-fracs only in the remaining wells is required to evaluate the effect of surfactants on enhanced oil recovery. Correlations based on the results of previous water-fracs were developed to predict the incremental oil from the stimulation treatments.

Since the correlating dataset shown in Table 9 is incomplete and sparse, AI tools, fuzzy logic, and neural networks were used to analyze the data. Fuzzy logic was used to find variables that bore a relationship to the incremental oil. Surprisingly, only the petrophysical log patterns correlated with the water-frac results. To date, prior production and pressure history have provided little insight to stimulation results. The petrophysical logs were digitized and the patterns described with statistical parameters. The dataset shown in Table 18 contains both open-hole and cased-hole logs with only the gamma ray common to both suites. The oil rate prior to the water-frac was available for all wells and provided the best correlation of the variables that were evaluated. The incremental oil response was based on the oil rate before and after the water-fracs.

Table 18. Available water-frac data summary

Variable	Number of records
Number of wells	84
API no.	19
Top of zone	84
Bottom of zone	84
Gamma ray logs	18
Sonic logs	14
Neutron logs	4
Resistivity logs	3
Frac size, lb/ft sand	69
Frac volume, gal/ft water	69
BHP prior to water frac	24
Incremental rate response	81

Initially, the well responses with open-hole logs were analyzed. Fifteen gamma ray and sonic logs from the Fullerton San Andres field were digitized. Fuzzy logic was applied to water-frac results to determine suitable parameters for correlations with production response. The production rate was the fuzzified variable that was crossplotted with the statistical parameter used to describe the log patterns. The parameters are prioritized in Table 19.

Table 19. Fuzzy ranking of well log statistical parameters with water-frac production response, BOPD			
Statistical parameter	Range	R^2	Goodness
DT- Kurt	0.30	0.96	1.26
GR- Skew	0.30	0.95	1.24
DT- VAR	0.30	0.92	1.22
DT- St Dev	0.20	0.92	1.12
GR- VAR	0.25	0.86	1.11
GR- Kurt	0.28	0.78	1.06
GR- St Dev	0.23	0.81	1.04
DT- Skew	0.24	0.43	0.67
GR- max	0.23	0.40	0.63
GR- Q3	0.22	0.19	0.42
GR- min	0.26	0.10	0.36
GR- median	0.27	0.08	0.35
GR- Trim (20%)	0.26	0.06	0.33
GR- Q1	0.30	0.00	0.30
GR- Ave	0.26	0.01	0.27
DT- max	0.12	0.14	0.26
DT- Q1	0.05	0.09	0.14
DT- Trim (20%)	0.05	0.07	0.12
DT- min	0.03	0.09	0.12
DT- median	0.06	0.06	0.12

The "Goodness" value in Table 19 was used to rank the log pattern statistical parameters. Kurtosis is the parameter that describes size of a distribution tail; skewness describes asymmetry in a random variable probability distribution, and variance measures the data spread of the gamma ray and sonic logs. These three parameters suggest that the log patterns are promising correlating variables.

The kurtosis and skew of the gamma ray water-frac log patterns were used as inputs to a 2-2-1 neural network that trained to 86% as shown in Figure 55. Additional training results are shown in Table 20. The comments about lines under "Note" column in Table 20 indicate that despite a satisfactory training value (R^2), predictions from the neural network are suspect due to assumed local minima problems.

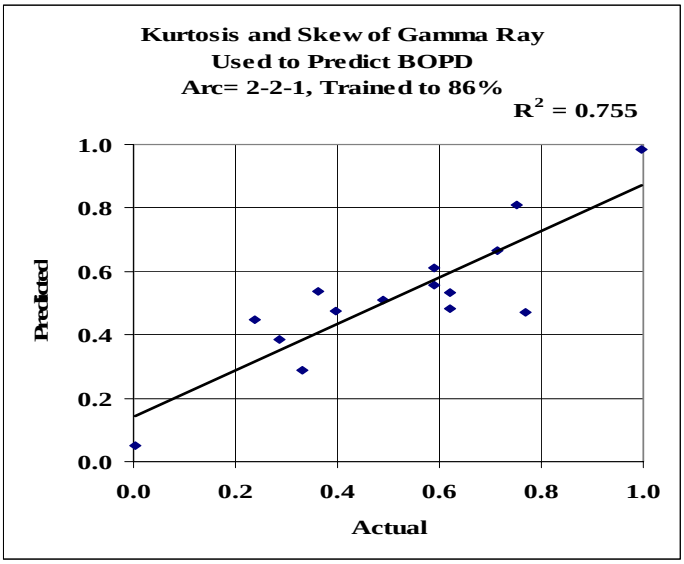

Figure 55. Water-frac neural network training results.

Table 20. Neural network open hole log training results			
Input #1	Input #2	R	Note
GRk	GRsd	0.37	
GRk	GRsk	0.86	OK
GRk	GRv	0.55	
GRsd	GRv	0.75	OK
GRsk	GRsd	0.67	Line
GRsk	GRv	0.01	
DTk	DTsd	0.82	OK
DTk	DTv	0.77	OK
DTsd	DTv	0.71	Line
GRk	DTk	0.83	Line
GRk	DTv	0.83	Line
GRsd	DTk	0.81	OK
GRsd	DTv	0.43	
GRsd	DTk	0.83	Line
GRsd	DTsd	0.78	Bottom Heavy
GRsd	DTv	0.84	Bottom Heavy
GRsk	DTk	0.71	Line
GRsk	DTsd	0.74	Line
GRsk	DTv	0.74	Line
GRsk	DTk	0.84	2 Lines
GRv	DTsd	0.86	2 Lines
GRv	DTv	0.84	2 Lines

The open-hole log dataset was small. Our experience with AI suggests that small datasets result in easily trained neural networks, which generate poor predictions. Larger datasets are more difficult to train, but confidence is greater in the predictions. Hence, an additional 45 through-pipe, gamma ray-neutron perforating logs and corresponding water-frac production responses were obtained for analysis. While the perforating logs are not appropriate for reserve calculations, the patterns of the cased-hole logs are believed to be suitable for AI analysis.

Initial work focused on the gamma ray log. The 45 logs were digitized, and the information reviewed for AI application. Thirty-four well logs with associated data were useful. The statistical parameters of the 34 well logs were calculated. The fuzzy rankings determined for the open-hole logs were used to select the inputs for the construction of the cased-hole neural networks. Again, the after water-frac production was the fuzzified variable. The statistical parameters used for neural network construction were as follows: Average, Kurtosis, Median, Minimum, Trim Mean, and Variance. The training results are shown in Table 21. All network architectures result in tie lines less than half the number of samples.

Table 21. Cased-hole gamma ray log training				
Architecture	Tie-lines	Inputs	Training CC, %	R^2, %
2-2-3-1	13	Kurt-Average	84	70.4
2-4-1	12	Kurt-Median	87	75.5
2-5-1	15	Kurt-Median	91	82.5
2-3-1	9	Kurt-Minimum	83	69.3
2-4-1	12	Kurt-Minimum	83	68.3
2-5-1	15	Kurt-Trim Mean	91	82.7

The value of R^2 is an indicator of the distribution of data along the 100%-45° actual versus predicted line. The greater the value of R^2, the better the forecasting ability of the trained neural networks. The cased-hole results are generally superior to the open-hole results shown in Table 20. The cased-hole dataset was extended to 37 wells as additional data became available. Analysis of the larger dataset was extended to include the neutron log patterns as correlating variables. The training results of 576 different neural network architectures with correlation coefficients of 70% or more are shown in Table 22. Seventeen of the tested architectures were found to have training correlation coefficients greater than 69%.

Table 22. GR-neutron log attributes used to predict water-frac response
Neural Network Training Results

Attributes		Architecture							
		2 2 1	2 3 1	2 4 1	2 5 1	2 2 2 1	2 2 3 1	2 3 2 1	2 2 2 2 1
		Correlation coefficient, %							
Avg GR	Avg Φ_N			**81**					
Avg GR	STD Φ_N							**86**	
Avg D GR	Avg D Φ_N				**83**				
Avg D GR	Med Φ_N				**79**				
Avg D GR	Var Φ_N			**85**	**80**				
D^2 GR	D^2 Φ_N				**79**		**78**		
D^2 GR	Kurt Φ_N			**73**					
Kurt GR	Med Φ_N		**72**						
Kurt GR	Max Φ_N			**76**					
Kurt GR	TrimM Φ_N							**71**	
Min GR	Min Φ_N				**80**				
Min GR	Quart 1 Φ_N				**89**				
Min GR	TrimM Φ_N				**75**				
Quart 1 GR	Quart 1 Φ_N				**83**				
Quart 1 GR	Max Φ_N		**77**						
Med GR	TrimM Φ_N							**86**	
Quart 3 GR	Var Φ_N		**80**						
Max GR	Avg Φ_N				**86**				
Max GR	STD Φ_N				**70**				
Skew GR	D^2 Φ_N				**76**				
Skew GR	Quart 3 Φ_N				**85**		**77**		
Skew GR	Max Φ_N						**71**		
Skew GR	STD Φ_N				**90**				
Skew GR	Var Φ_N				**74**				
STD GR	Min Φ_N				**77**				
STD GR	Avg D Φ_N							**77**	
STD GR	STD Φ_N				**73**				
STD GR	Var Φ_N				**90**				
TrimM GR	Quart 1 Φ_N				**79**				
Var GR	Avg D Φ_N		**75**		**82**				
Var GR	D^2 Φ_N							**81**	
Var GR	STD Φ_N			**92**					
Var GR	Var Φ_N				**93**				

It is evident that a 2-5-1 architecture with an assortment of statistical parameters as inputs generates satisfactory training results. The extended cased-hole water-frac dataset was analyzed with respect only to the gamma ray logs; the results are shown in Table 23.

Table 23. GR log attributes used to predict water-frac response Neural Network Training Results								
Attribute		2 2 1	2 3 1	2 4 1	2 5 1	2 2 2 1	2 2 3 1	2 3 2 1
Avg D GR	Skew GR				77			
Avg GR	Kurt GR			84	92			
Avg GR	Skew GR			73				
Kurt GR	Min GR		83	83				
Kurt GR	Med GR			87	91			
Kurt GR	Quart 3 GR				91			
Kurt GR	TrimM GR				91			
Kurt GR	Var GR				91			
Min GR	Skew GR			82	80			
Skew GR	STD GR			71	72			
Skew GR	TrimM GR				90			
Skew GR	Var GR				76			

The gamma ray open-hole logs were combined with the cased-hole gamma ray logs to generate a 50 water-frac well dataset. Only the gamma ray log was available in both the open-hole and cased-hole datasets. The open-hole logs occasionally included a sonic log, while the cased-hole logs included the neutron log.

Examination of Table 24 suggests that reasonable predictions can be made using only gamma ray log attributes in the combined dataset. Seven (2%) of 385 networks trained to a correlation coefficient of 70% or more without suspected local minima problems. Even though overtraining was not a problem with the 50 well dataset, the robustness of the neural network training shown in Table 24 could be inferior to the separate open-hole and cased-hole datasets because of numerous suspected local minima problems. Neural networks using the cased-hole gamma ray-only dataset generated training correlation coefficients greater than 70%, 18% of the time. Three percent of the neural networks using the cased-hole gamma ray-plus neutron log dataset trained to greater than a 70% correlation coefficient. The open-hole dataset had gamma ray and occasional sonic logs available as inputs, and the cased-hole dataset had gamma ray and neutron logs available. While the combined dataset had more wells in the training data, the neural networks were of poorer quality, indicating the value of multiple log patterns as inputs.

Table 24. Gamma ray log attributes used to predict water-frac response Combined Dataset Neural Network Training Results								
Attributes		Architecture						
		2-2-1	2-3-1	2-4-1	2-5-1	2-6-1	2-7-1	2-8-1
		Correlation Coefficient, %						
Avg GR	Kurt GR	37	37	37	37	37	37	0
Avg GR	Min GR	19	18	18	18	18	18	18
Avg GR	Quart 1 GR	32	9	5	4	9	2	9
Avg GR	Med GR	11	11	4	11	3	3	4
Avg GR	Quart 3 GR	24	24	1	24	24	2	24
Avg GR	Max GR	36	36	36	36	36	36	36
Avg GR	STD GR	36	28	27	29	26	15	16
Avg GR	Skew GR	29	35	36	36	36	36	36
Avg GR	TrimM GR	36	17	3	6	4	1	0
Avg GR	Var GR	27	26	25	15	26	13	11
TrimM GR	Var GR	27	26	26	24	6	15	13
Kurt GR	Min GR	**71**	39	**75**	39	39	39	39
Kurt GR	Quart 1 GR	37	38	38	38	38	38	0

Kurt GR	Med GR	38	38	38	38	37	38	0
Kurt GR	Quart 3 GR	37	37	37	38	37	37	37
Kurt GR	Max GR	63	64	64	**75**	35	35	0
Kurt GR	STD GR	67	67	**73**	**82**	**85**	35	**73**
Kurt GR	Skew GR	42	48	35	35	48	34	34
Kurt GR	TrimM GR	38	38	38	37	38	37	37
Kurt GR	Var GR	63	**71**	**74**	**74**	**76**	**78**	**73**
STD GR	TrimM GR	28	28	28	29	27	28	26
STD GR	Var GR	23	24	23	24	12	24	25
Min GR	Quart 1 GR	19	19	18	18	18	18	0
Min GR	Med GR	19	19	18	19	20	19	20
Min GR	Quart 3 GR	21	21	20	20	20	6	20
Min GR	Max GR	34	34	33	34	34	26	33
Min GR	STD GR	29	29	16	18	25	16	16
Min GR	Skew GR	60	36	36	36	36	36	36
Min GR	TrimM GR	20	19	20	20	20	19	19
Min GR	Var GR	28	26	19	15	23	16	16
Skew GR	STD GR	51	64	35	34	33	**80**	33
Skew GR	TrimM GR	36	36	36	36	36	36	36
Skew GR	Var GR	56	55	69	66	34	33	0
Quart 1 GR	Med GR	30	63	64	18	49	3	2
Quart 1 GR	Quart 3 GR	48	40	18	2	18	1	18
Quart 1 GR	Max GR	35	35	35	35	35	35	35
Quart 1 GR	STD GR	28	29	11	28	25	12	11
Quart 1 GR	Skew GR	36	36	36	36	36	36	36
Quart 1 GR	TrimM GR	50	58	3	3	17	2	1
Quart 1 GR	Var GR	27	28	25	28	25	16	0
Max GR	STD GR	56	31	41	32	32	34	**84**
Max GR	Skew GR	33	33	33	33	33	33	33
Max GR	TrimM GR	36	36	36	35	35	36	31
Max GR	Var GR	47	35	**71**	32	32	35	0
Med GR	Quart 3 GR	15	1	0	**72**	1	1	1
Med GR	Max GR	36	36	35	36	36	36	36
Med GR	STD GR	28	28	28	25	26	25	21
Med GR	Skew GR	36	36	36	36	36	36	36
Med GR	TrimM GR	5	4	3	2	5	2	2
Med GR	Var GR	26	28	19	27	14	17	27
Quart 3 GR	Max GR	36	36	36	36	36	36	30
Quart 3 GR	STD GR	28	29	27	25	22	**83**	26
Quart 3 GR	Skew GR	36	36	36	36	36	36	36
Quart 3 GR	TrimM GR	1	18	0	9	1	0	1
Quart 3 GR	Var GR	25	27	10	28	19	12	21

Neural network architectures were developed to predict water-frac incremental oil rates given either open- or cased-hole logs. These correlations will form the base line production in the evaluation of water-frac stimulations that incorporate surfactant in the frac fluid.

The water-frac incremental oil resulting from 69 of the well stimulations was evaluated in terms of frac size and incremental oil. Fuzzy curves were generated with volume in terms of gal/ft of pay and amount of sand in terms of lb/ft of pay. The normalized fuzzy curves are shown in Figures 56 and 57.

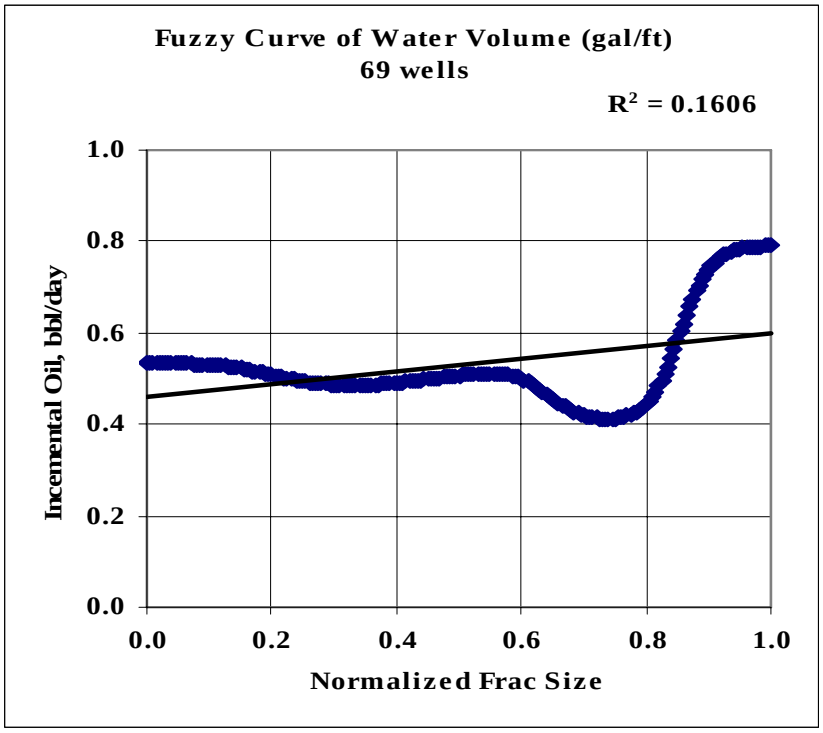

Figure 56. Volume fuzzy curve.

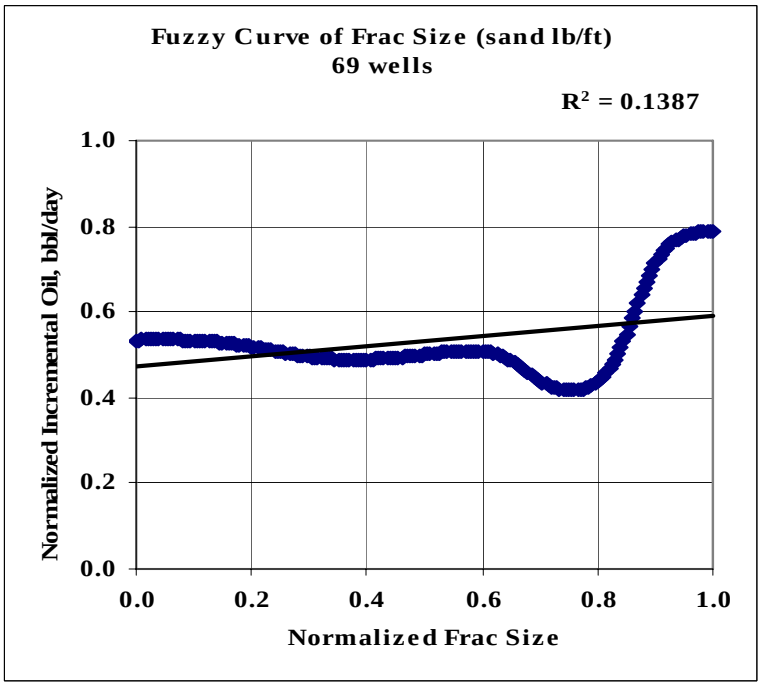

Figure 57. Quantity of sand fuzzy curve.

The normalized value of 0.9 equates to 1950 gal/ft for the volume of water and 350 lb/ft for the quantity of sand.

During the course of examining the Fullerton San Andres water-frac dataset, we observed that the oil rate prior to stimulation correlated well with the oil rate following the treatment as shown in a fuzzy curve (Figure 58).

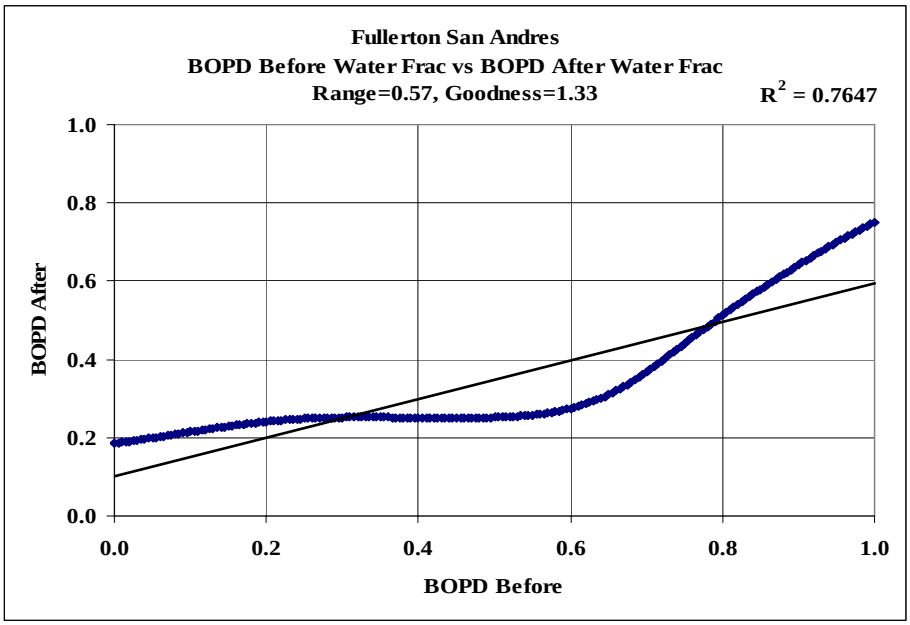

Figure 58. Fullerton San Andres before/after oil rate fuzzy curve.

The fuzzy relationship between the two oil rates is strong. Notice that the better the well, the better the response. However, the inverse applies to the incremental oil rate response. Normalizing the rates by feet of pay generates similar fuzzy curves.

Predictions made with the neural network used to generate Figure 49 are limited by the oil production rate limit of the dataset, about 25 BOPD. Since the predicted water-frac Fullerton San Andres wells exceeds 25 BOPD, commercial neural network software from *Matlab* was used to predict response to surfactant treatments with prior oil rates greater than 25 BOPD using the same input variables. The *Matlab NN* software was trained with the Cottonwood Creek dataset that includes the 25 BOPD limit, and the results generated with a 3-3-1 architecture are shown in Figure 59.

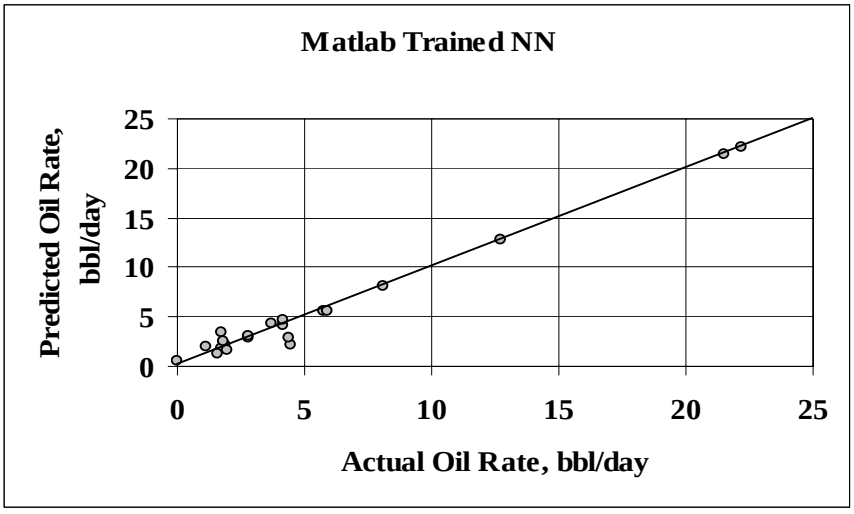

Figure 59. Matlab 3-3-1 NN training results with Cottonwood Creek dataset.

The cross plots shown in Figures 49 and 59 are quite similar. The *Matlab NN* software is not limited by the domain of the dataset, and the trained NN was used to generate the production forecasts shown in Table 25.

Table 25. Fullerton Field forecasted surfactant stimulation results

Well	Oil Rate Prior to Treatment bbl/day	Forecast Oil Rate bbl/day
Logsdon B 11	11	40
Logsdon C 51	12	29
Logsdon D 30	17	111
Logsdon E 19	13	57
Scarb. C 7	12	181
Scarb. C 8	6	192
SSAU 1128	5	10
SSAU 2024	3	12
SSAU 2045	11	121

The use of *Matlab* was driven by a recent report from an operator using neural network correlations to select drilling locations in the Red River formation in North Dakota. Luff Exploration Co. designed a *Matlab* neural network as part of an Intelligent Computing System to analyze a dataset, and generated excellent results.[15] Hence, Correlations Company was interested in comparing a *Matlab* neural network with the public domain network, SNNS NN[16] that we use. The *Matlab* software was evaluated using a dataset developed during this project.

Matlab Neural Network Toolbox

The *Matlab* NN toolbox consists of 15 different types of neural network algorithms. The Feed Forward Back-propagation was evaluated. All training parameters are user adjustable, making the training of networks totally user defined. The user can set parameters that stop training after a set number of cycles, at any given level of error, or when the cross validating error goes beyond a specified number. The GUI is fairly straightforward and very user friendly.

Layer terminologies are slightly different than the SNNS NN software. The *Matlab NN* includes the output layer in the network architecture design terminology. Various learning and training methods are available, each with its advantages and disadvantages. The transfer function for each layer can be individually selected for better results or faster training. The logarithmic sigmoid transfer function seems to generate the most robust networks. The tangent sigmoid function results in faster training. The transfer function for the output layer is usually a linear sigmoid function. The NN training results are consistently reproducible in *Matlab* as compared to the SNNS NN software. The *Matlab NN* software can generate extrapolated predictions as opposed to the SNNS NN that is confined to the domain of the dataset.

The training results of the *Matlab NN* toolbox are similar to the SNNS NN for a given neural network architecture. For example, a 50-well dataset from the Fullerton-San Andres was used to train both networks. The optimum network, using the SNNS NN, was 2-5-1 and trained to 82%. The cross plot is shown in Figure 60. Using the same architecture, the *Matlab NN* was trained. The *Matlab* training cross plot in Figure 61 shows that the network results in roughly the same correlations.

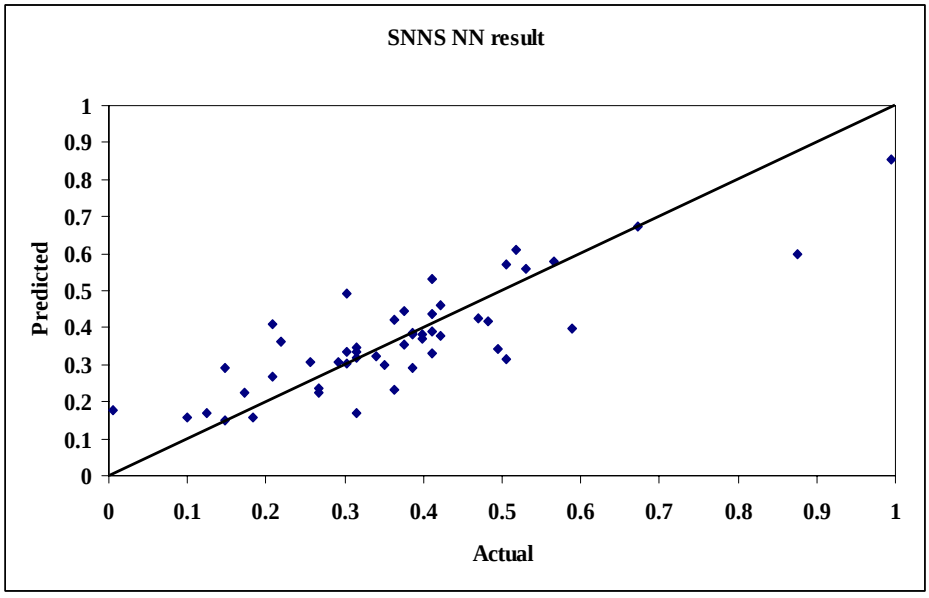

Figure 60. SNNS training result, 2-5-1 architecture.

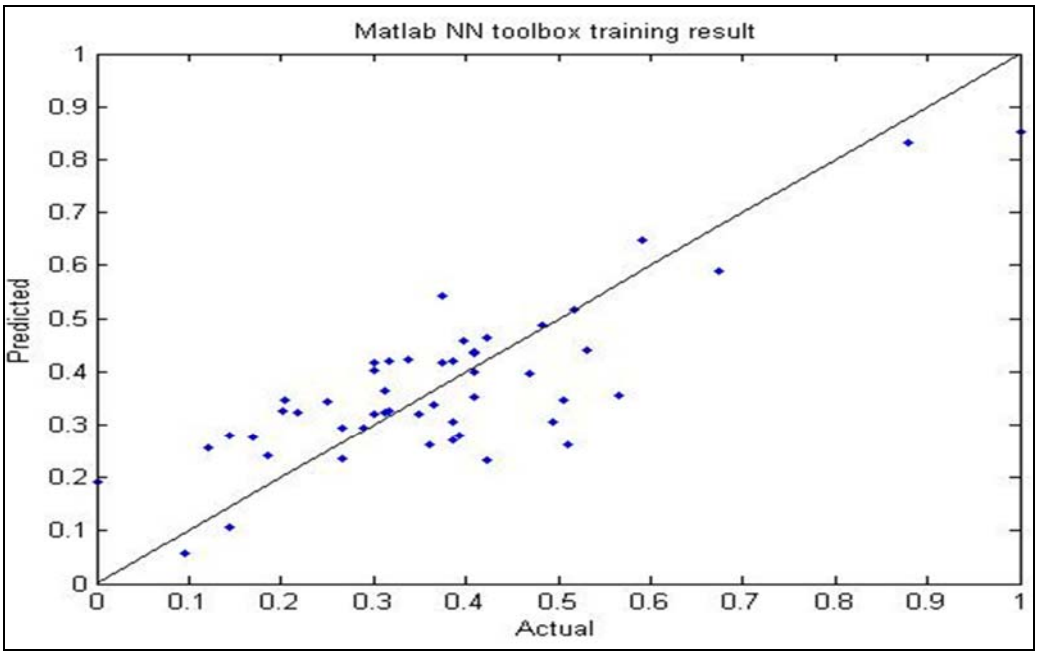

Figure 61. Matlab NN toolbox training result, 2-5-1 architecture.

The Matlab NN toolbox trained better than the SNNS NN when a 2-8-1 architecture was used as shown in Figures 62 and 63.

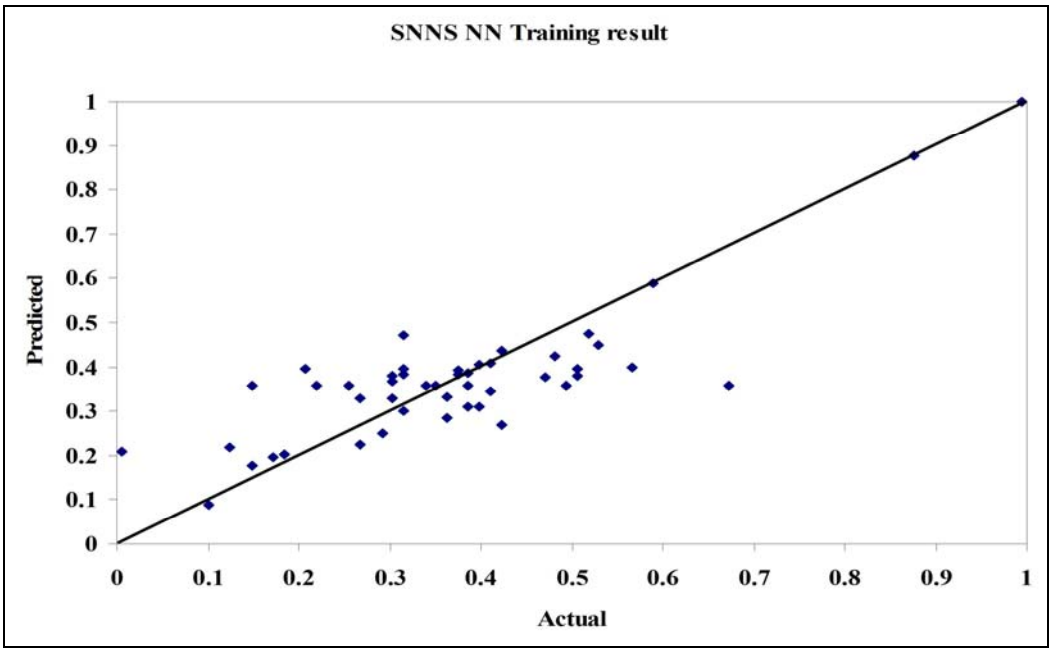

Figure 62. SNNS training result, 2-8-1 architecture.

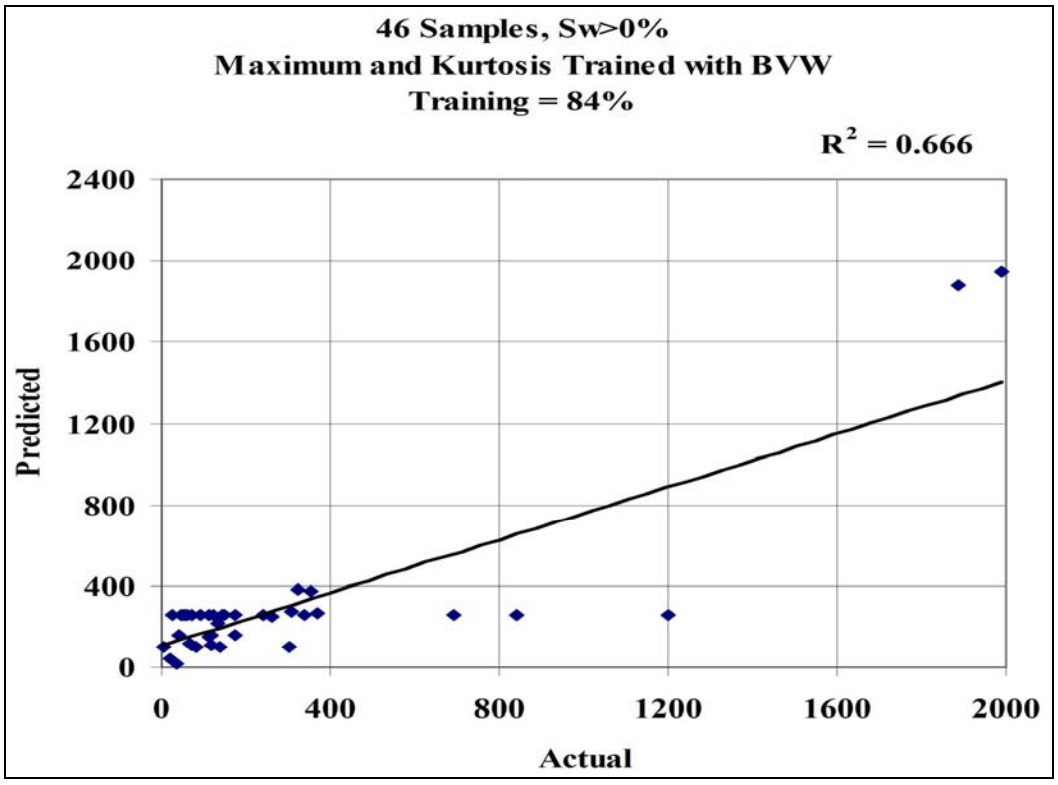

Figure 63. Matlab NN toolbox training result, 2-8-1 architecture.

Matlab in itself, a powerful mathematical tool, can be used in a variety of applications. It can perform most all functions available in Excel. However, *Matlab* cannot be used to work on database structures, a feature that is available with Excel. *Matlab* can be customized to perform calculations not originally provided with the software.

While training neural networks, the "flat line problem" can occur when the actual versus neural network values are cross-plotted. The flat lines are ostensibly related to local minima in the SNNS NN solver. *Matlab* technical support people attribute the flat lines to saturation of the neurons, and this most generally occurs primarily in the output layer. The range in the data is high, and the neuron fails to learn the pattern. The software then averages the input values and correlates the averaged input vector to the output. Then all input vectors lie with that range, and the trained neural network predicts one value resulting in a flat line. Unlike overtraining, this problem can be easily identified. The problem occurred when the network was repeatedly trained to get better results.

Fuzzy ranking is used to prioritize neural network inputs in order to enhance the neural network training results. The *Matlab* fuzzy logic toolbox was investigated as another tool to select inputs given a dataset with many possible variables that can affect the output. The *Matlab* fuzzy logic was found to be similar to the decision tree approach and very similar to the "Fuzzy-Expert system" designed by the REACT group at the Petroleum Recovery Research Center.

The *Matlab NN* toolbox is user-friendly. The user can choose the type of neural network and set any of the training parameters to obtain the best-trained neural network to solve the problem. Additional reading and training datasets are required to understand the applicability and usefulness of the various neural network algorithms.

The fuzzy logic toolbox is a very useful tool for decision-making problems. When the conditions of choice cannot be clearly defined, the toolbox is designed to solve such problems. However, it has little obvious value as a means of evaluating the "goodness" of variables thought to influence the output of a multi-variable problem.

AI Analysis of Cedar Creek NMR Dataset

An AI analysis of NMR scans conducted in conjunction with the high-temperature (200°F) imbibition tests performed at the ConocoPhillips Technical Center in Bartlesville, Oklahoma, was conducted in an effort to improve the correlation between the NMR scans and the physical laboratory measurements of water saturation and porosity as determined via the CPMG method provided by ConocoPhillips. The cores were scanned before brine imbibition, before surfactant imbibition, and after surfactant imbibition. The objective was to monitor imbibition via the NMR method with the first step being to correlate core porosity with the core scans.

T2 scans were taken of 19 high-temperature imbibition test cores. Their statistical parameters were calculated and normalized with the respective bulk volume of the core sample, e.g., the sum of the scan divided by the bulk volume of the core. The statistical parameters of the T2 scans prior to imbibition are shown in Table 26 along with the measured core porosity. The correlation coefficient that describes the goodness of the relationship between the measured core porosity and a statistical parameter is shown in the last row of Table 26.

Table 26. Statistical properties of T2 scans prior to imbibition normalized with core bulk volume

Core sample	Average	Sum	Maximum	Median	Skew	Kurt	Variance	Core Porosity, %
IL 8230.65	41.88	2094	333.2	0.000	0.0932	0.2152	182218	11.69
IL 8286.35	31.94	1597	219.8	6.151	0.0935	0.1479	84605	7.62
RR20	69.04	3452	501.8	2.664	0.1305	0.2261	315013	6.79
RR15	48.10	2405	335.5	16.956	0.1237	0.2301	137734	17.3
RR13	17.35	867	188.3	0.000	0.1610	0.5701	22972	24.35
RR14	64.84	3242	562.1	3.079	0.1449	0.3403	336468	23.62
RRU 8719.75	19.04	952	159.4	0.000	0.0939	0.1648	33666	5.74
RRU 8715.35	63.98	3199	585.2	10.471	0.1157	0.3138	441871	17.21
RRU 8713.5	36.78	1839	294.4	8.628	0.1107	0.2337	121228	12.27
St 8848A	30.96	1517	260.0	0.000	0.1300	0.2522	86389	13.07
St 8845A	40.13	1966	384.5	11.985	0.1481	0.4125	164893	14.51
St 8293	26.16	1282	208.5	0.000	0.0975	0.2427	63953	9.43
St 8831B	18.23	893	101.5	2.550	0.0711	0.0755	21786	7.1
St 8801A	28.30	1387	194.6	14.891	0.0993	0.2215	55821	8.7
St 8785	4.18	205	36.9	0.000	0.0911	0.3008	1358	3.0
St 8800	27.74	1359	248.5	0.000	0.0999	0.2582	82854	11.46
St 8188B	21.55	1056	145.2	0.990	0.0904	0.1787	31717	9.62
St 8831A	26.61	1304	154.5	4.125	0.0786	0.1039	40763	10.22
St 8801B	25.81	1265	75.7	13.188	0.0215	-0.0616	17574	10.26
Correlation Coefficient	18.5%	18.6%	28.8%	2.8%	38.7%	37.3%	18.0%	

NMR software was used to calculate the porosity values plotted versus the measured values (Figure 64). This figure is used as a baseline for the water saturation values calculated

from the T2 distributions following brine imbibition and surfactant imbibition. The two outliers (double size symbols) are the core plugs identified as Red River #13 and #20.

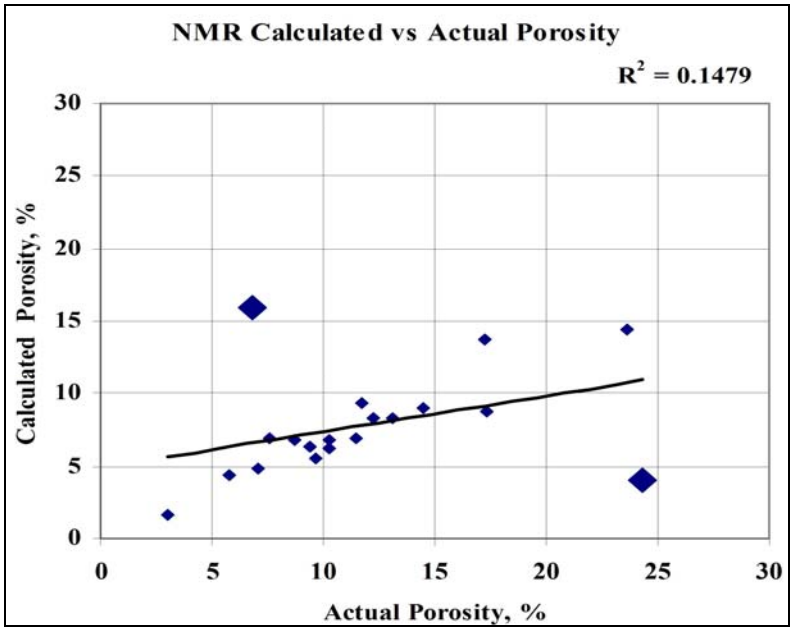

Figure 64. Calculated using NMR software vs. actual porosity.

For background purposes, the T2 distributions versus time of the two outliers seen in Figure 64 are shown in Figure 65.

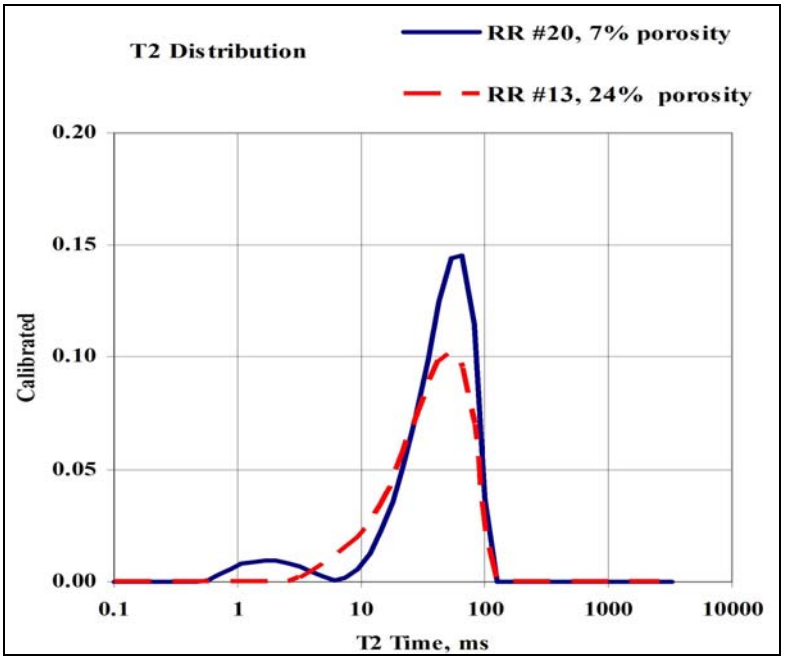

Figure 65. T2 distribution of the two outliers shown in Figure 64.

To improve the calculated porosity versus measured porosity correlation shown in Figure 64, we tested numerous neural network architectures with the statistical parameters shown in Table 26 as input variables. A 2-3-1 neural network trained to a 94% correlation coefficient with the scan statistical parameters Average and Maximum as inputs and Core Porosity as output (Figure 66). The correlation over-predicts (~11%) at the point where the actual value is about 7% (Interlake 8230). The correlation also includes a significant under-prediction at 10% actual porosity where the predicted value is about 5% (Stony Mountain 8188B). The outliers are the double-size symbols.

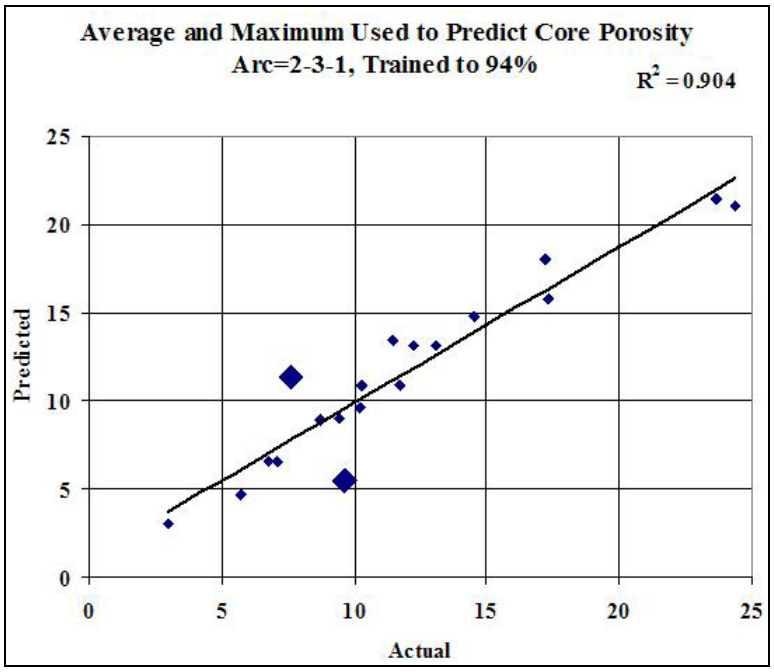

Figure 66. Porosity training results with a 2-3-1 neural network.

While the neural network predictions are not good, they are considerably better than the variation seen in the actual versus calculated porosity values generated with the NMR software (Figure 64). The improvement in the porosity correlation suggested that a similar AI approach could be used to generate water saturation correlations.

Shown in Table 27 are the statistical parameters generated from the T2 scans prior to imbibition, after water imbibition, and after surfactant imbibition. Included in Table 27 is a column entitled Bulk Volume Water, BVW. BVW was used as the neural network training output with the thought that the inclusion of porosity would improve the correlations. The bold values shown in Table 27 are after-water imbibition data. The first eight samples are those prior to imbibition with water saturations greater than 0%. The last 19 values are the after-surfactant imbibition results. Note the very poor correlation between any of the statistical parameters and BVW as shown in the last row of the table.

Table 27. Forty-six core samples with Sw >0%. All cores normalized with bulk volume							
Core sample	Average	Sum	Maximum	Skew	Kurt	Variance	BVW
RR20	69	3452	502	0	0	315013	6
RR15	48	2405	335	0	0	137734	138
RR13	17	867	188	0	1	22972	321
RR14	65	3242	562	0	0	336468	302
St 8848A	31	1517	260	0	0	86389	73
St 8845A	40	1966	385	0	0	164893	81
St 8293	26	1282	209	0	0	63953	43
St 8831B	18	893	102	0	0	21786	20
IL 8230.65	**39**	**1896**	**155**	**1**	**0**	**2672**	**370**
IL 8286.35	**29**	**1444**	**250**	**3**	**6**	**3851**	**151**
RR20	**71**	**3474**	**710**	**3**	**7**	**30572**	**118**
RR15	**14**	**687**	**136**	**3**	**6**	**1060**	**842**
RR13	**63**	**3084**	**523**	**3**	**6**	**17377**	**1988**
RR14	**49**	**2421**	**365**	**3**	**6**	**7593**	**1202**
RRU 8719.75	**53**	**2621**	**481**	**3**	**6**	**14774**	**354**
RRU 8715.35	**70**	**3445**	**637**	**3**	**6**	**24974**	**119**
RRU 8713.5	**36**	**1780**	**312**	**3**	**6**	**6216**	**56**
St 8848A	**32**	**1588**	**266**	**3**	**6**	**4332**	**90**
St 8845A	**37**	**1803**	**380**	**3**	**8**	**7965**	**72**
St 8293	**23**	**1149**	**203**	**3**	**7**	**2283**	**71**
St 8831B	**16**	**802**	**115**	**2**	**3**	**995**	**49**
St 8801A	**23**	**1126**	**156**	**2**	**5**	**1487**	**125**
St 8785	**8**	**380**	**28**	**1**	**-1**	**110**	**34**
St 8800	**28**	**1361**	**179**	**2**	**4**	**1918**	**142**
St 8188B	**25**	**1247**	**82**	**0**	**-1**	**704**	**176**
St 8831A	**31**	**1525**	**199**	**2**	**6**	**2059**	**241**
St 8801B	**26**	**1277**	**160**	**2**	**2**	**1766**	**261**
IL 8230.65	39	1890	295	2	5	5308	340
IL 8286.35	30	1447	246	3	6	3713	151
RR20	69	3370	666	3	6	28865	65
RR15	16	798	142	3	6	1195	692
RR13	61	3001	597	3	7	22297	1888
RR14	49	2379	431	3	7	10898	1202
RRU 8719.75	48	2368	523	3	7	16967	310
RRU 8715.35	66	3248	592	3	6	22835	112
RRU 8713.5	34	1677	305	3	5	6421	51
St 8848A	33	1611	287	3	6	5088	60
St 8845A	38	1865	333	3	6	6903	72
St 8293	27	1309	242	3	8	2938	59
St 8831B	16	802	115	2	3	995	46
St 8801A	22	1072	166	2	5	1711	74
St 8785	6	304	38	2	2	123	25
St 8800	30	1486	208	2	5	2624	123
St 8188B	25	1245	122	1	1	1021	136
St 8831A	28	1348	232	3	7	2834	112
St 8801B	28	1351	206	2	6	2260	174
Correlation Coefficient	9.3%	9.1%	8.8%	5.5%	5.6%	0.7%	

Using a trial and error method, 2-3-1 neural networks were evaluated based on the training correlation coefficient. All combinations of the 46 sets of statistical parameters shown in Table 27 were tested. One network, using sum and maximum as inputs and another using maximum and kurtosis, produced the best correlations. Both trained to 84%, but the distribution of the data points along the 45^{o} is poor in both cases (Figures 67 and 68).

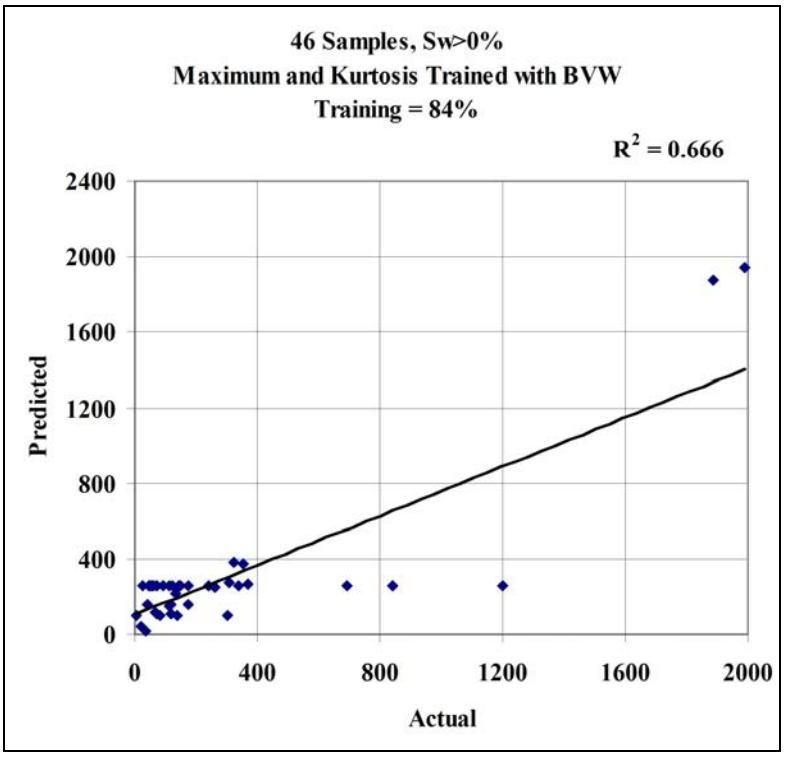

Figure 67. All samples with Sw > 0%, maximum and kurtosis as inputs.

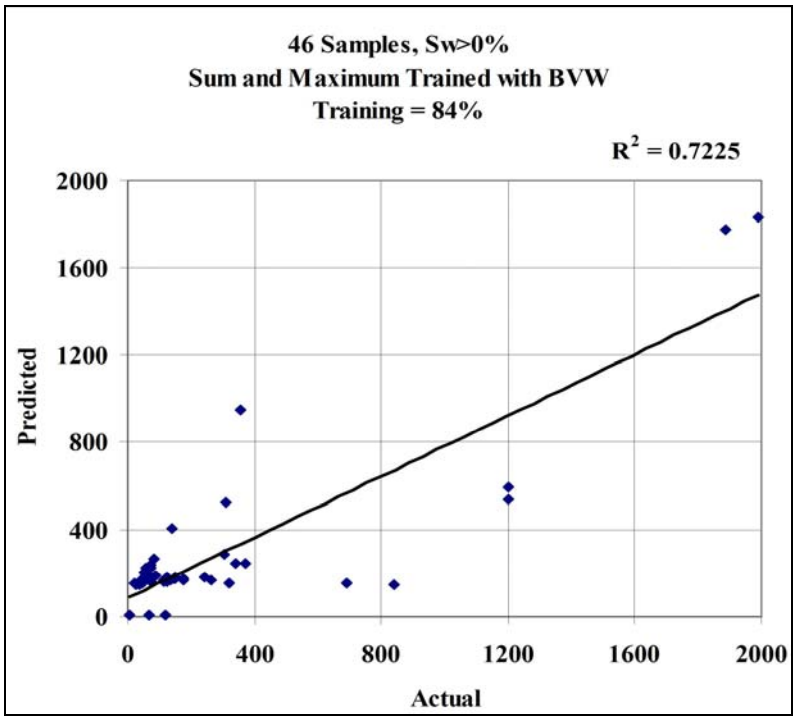

Figure 68. All samples Sw >0%, maximum and sum as inputs.

An attempt was made to generate useful BVW correlations based on the normalized dataset available from the NMR software. These software calculations are based on T2 scans normalized with the sum of the respective scan to generate a value for "Norm Ccalc" in the parlance of the NMR software. This normalizing procedure results in constant average value for each scan, and the sum always equals 1.0; thus, the statistical parameters skew, kurtosis, and maximum were evaluated as neural network inputs for multivariate correlations. The "Norm Ccalc" statistical datasets are shown in Tables 28–30 representing the scans prior to imbibition, after water imbibition, and after surfactant imbibition.

Table 28. Statistical parameters of 19 core samples, initial t2 scans

Sample	Maximum	Skew	Kurtosis	BVW
RR13	0.217	2.916	10.325	321.4
RR14	0.173	2.633	6.183	302.3
RR15	0.139	2.271	4.224	138.4
RR20	0.145	2.210	3.831	6.1
RRU 8719.75	0.167	2.131	3.740	0.0
RRU 8713.5	0.160	2.482	5.236	0.0
RRU 8715.35	0.183	2.863	7.763	0.0
St 8188B	0.137	2.171	4.295	0.0
St 8801B	0.060	0.500	-1.433	0.0
St 8801A	0.140	2.482	5.538	0.0
St 8800	0.183	2.621	6.773	0.0
St 8785	0.180	2.432	8.035	0.0
St 8831A	0.119	1.800	2.380	0.0
St 8293	0.163	2.638	6.566	43.4

St 8831B	0.114	1.752	1.860	19.9
St 8845A	0.196	3.006	8.375	82.7
St 8848A	0.171	2.386	4.628	75.8
IL 8230.65	0.159	2.537	5.855	0.0
IL 8286.35	0.138	2.165	3.427	0.0

Table 29. Statistical parameters of 19 core samples after brine imbibition t2 scans

Sample	Maximum	Skew	Kurtosis	BVW
RR13	0.187	2.668	6.196	769.7
RR14	0.167	2.563	5.796	466.6
RR15	0.193	2.656	6.735	300.9
RR20	0.186	2.628	5.978	330.6
RRU 8719.75	0.206	2.718	6.486	468.6
RRU 8713.5	0.166	2.369	4.507	624.4
RRU 8715.35	0.174	2.543	5.496	1062.5
St 8188B	0.098	1.397	1.234	66.6
St 8801B	0.152	2.414	5.744	47.2
St 8801A	0.155	2.393	5.083	59.9
St 8800	0.140	2.207	4.757	57.1
St 8785	0.123	1.908	2.331	22.5
St 8831A	0.172	2.609	6.572	69.9
St 8293	0.185	2.913	8.338	136.0
St 8831B	0.143	2.144	3.483	80.5
St 8845A	0.178	2.709	6.398	179.8
St 8848A	0.178	2.606	5.927	238.7
IL 8230.65	0.146	2.288	4.677	275.7
IL 8286.35	0.154	2.415	5.057	193.7

Table 30. Statistical parameters of 19 core samples after surfactant imbibition t2 scans

Sample	Maximum	Skew	Kurtosis	BVW
RR13	0.158	2.431	5.135	769.7
RR14	0.139	2.321	4.674	466.6
RR15	0.229	2.923	8.769	300.9
RR20	0.192	2.722	6.490	330.6
RRU 8719.75	0.173	2.553	5.594	468.6
RRU 8713.5	0.159	2.409	4.882	624.4
RRU 8715.35	0.177	2.650	6.147	1062.5
St 8188B	0.066	0.430	-1.370	66.6
St 8801B	0.125	1.687	2.233	47.2
St 8801A	0.138	2.174	4.527	59.9
St 8800	0.132	2.010	3.832	57.1
St 8785	0.072	0.841	-1.114	22.5
St 8831A	0.130	2.403	5.815	69.9
St 8293	0.177	2.646	6.641	136.0
St 8831B	0.143	2.144	3.483	80.5
St 8845A	0.211	2.906	7.742	179.8
St 8848A	0.167	2.716	6.484	238.7
IL 8230.65	0.075	1.129	-0.322	275.7
IL 8286.35	0.156	2.357	4.709	193.7

The purpose of generating the correlations is to predict the change in water saturation following water imbibition and surfactant imbibition. Water saturation was included in the output as BVW. The water saturation was 0.0 in 8 of the 19 initial core scans. If the "two samples per network tie-line rule" is imposed,[17] the number of permissible correlating samples (initial only) is reduced to 11, which in turn limits the available neural network architectures to 2-1-1. Thus, the initial neural network training was done with the NMR data obtained following brine imbibition plus the surfactant results. The statistical parameters skew, kurtosis, and maximum generated with this dataset are plotted versus BVW as shown in Figure 69. Note that the data points flatten following 200 BVW indicating poor correlation.

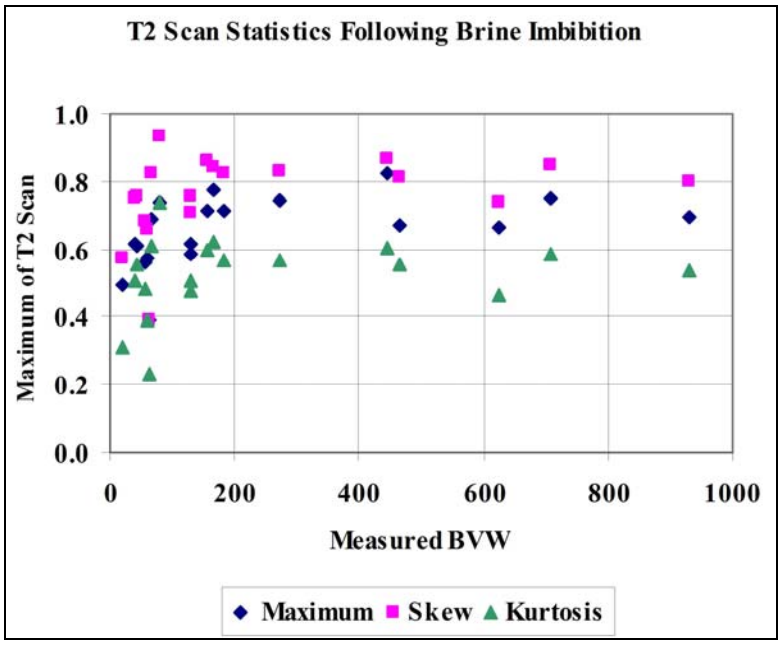

Figure 69. Statistical parameters generated from after-brine imbibition T2 scans dataset.

By trial and error, it was determined that a 2-3-1 neural network with maximum and kurtosis of the after-brine imbibition dataset trained to a 95% correlation coefficient, as shown in Figure 70. Table 31 shows the training results of the 13 network architectures that were tested.

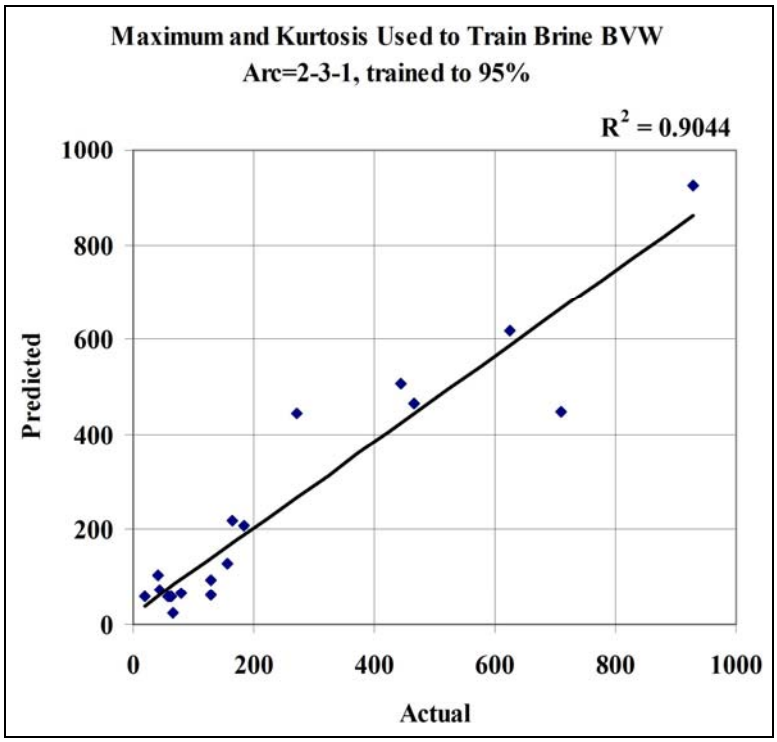

Figure 70. NORM Ccalc brine dataset training with maximum and kurtosis to predict brine BVW.

Table 31. Training results of the 13 network architectures						
	Input 1	Input 2	Input 3	2-2-1	2-3-1	3-2-1
Initial	Maximum	Skew		68	71	
Initial	Maximum	Kurtosis		61	69	
Initial	Skew	Kurtosis		75	75	
Initial	Maximum	Skew	Kurtosis			66
Brine	Maximum	Skew		**90**	**90**	
Brine	Maximum	Kurtosis		**86**	**95**	
Brine	Skew	Kurtosis		**87**	89	
Brine	Maximum	Skew	Kurtosis			**87**
Surfactant	Maximum	Skew		61	59	
Surfactant	Maximum	Kurtosis		58	0	
Surfactant	Skew	Kurtosis		**86**	59	
Surfactant	Maximum	Skew	Kurtosis			61

The maximum and the kurtosis values of the dataset prior to imbibition and after surfactant imbibition were used as a blind test of the Brine 2-3-1 architecture. The surfactant predictions shown plotted against the measured values are presented in Figure 71.

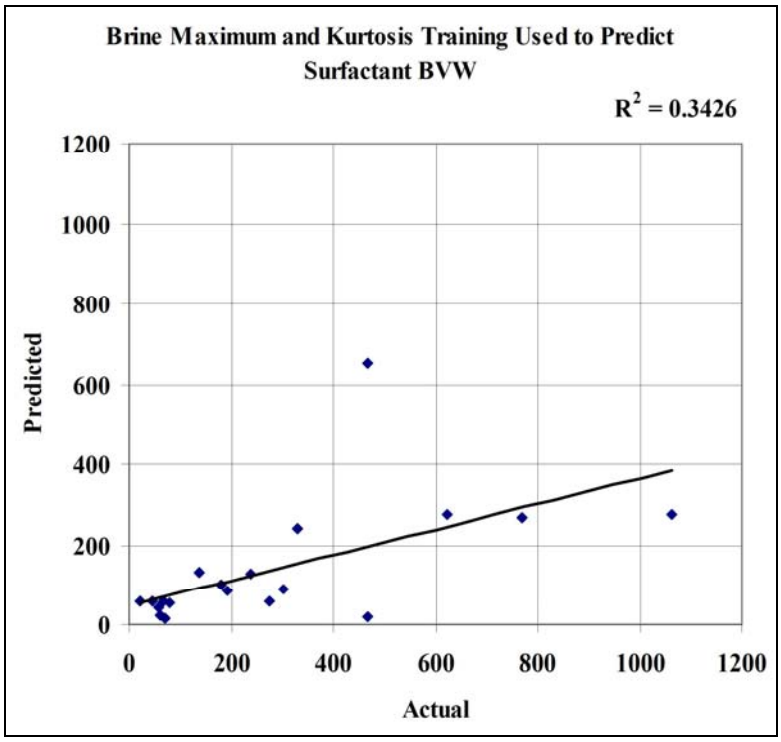

Figure 71. Predicted after-surfactant imbibition versus measured BVW.

Based on the least square fit line correlation coefficient, the neural network correlation improves upon the NMR (CPMG method) calculated values that are plotted versus the measured values in Figure 72.

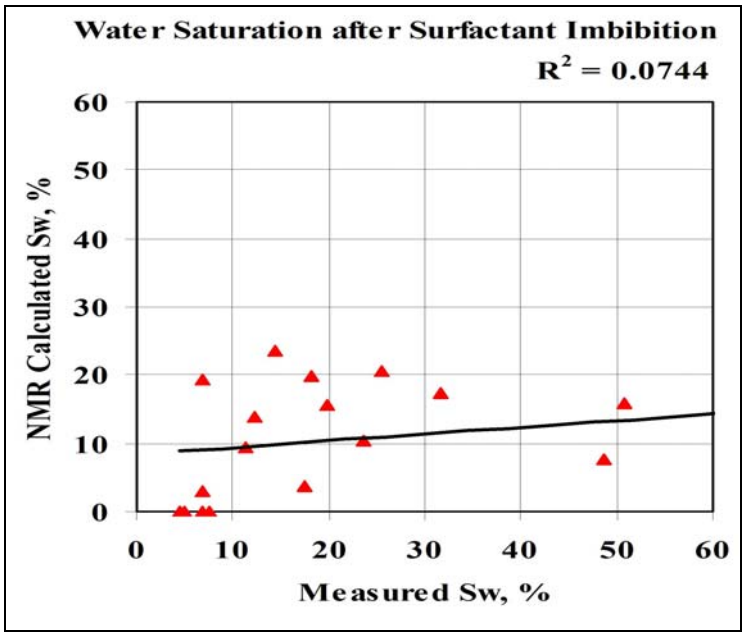

Figure 72. NMR calculated Sw following surfactant imbibition.

The trained brine 2-3-1 neural network was used to predict the initial water saturations. The predictions are compared to actual in Figure 73.

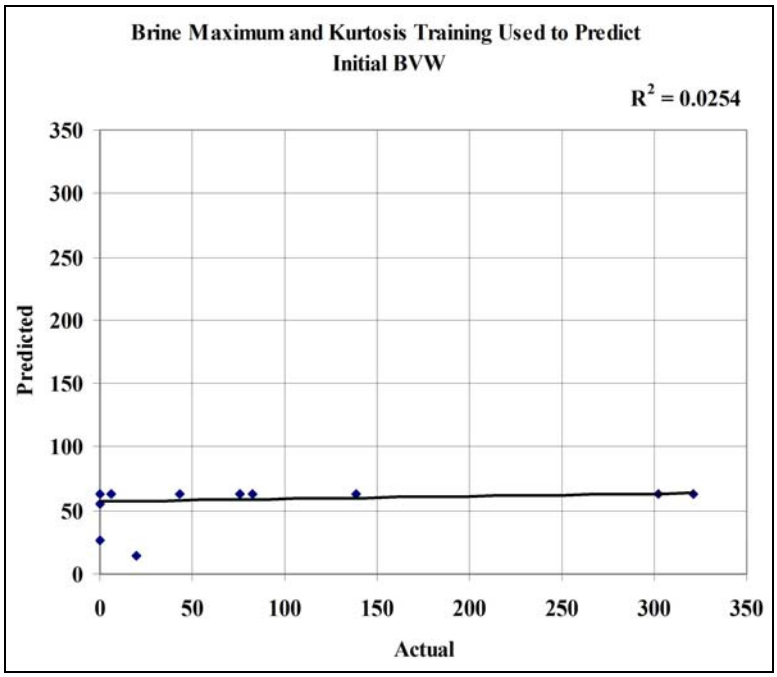

Figure 73. 2-3-1 neural network prediction versus measured values of Swi.

The neural predictions are less reliable than the NMR calculated values shown in Figure 74.

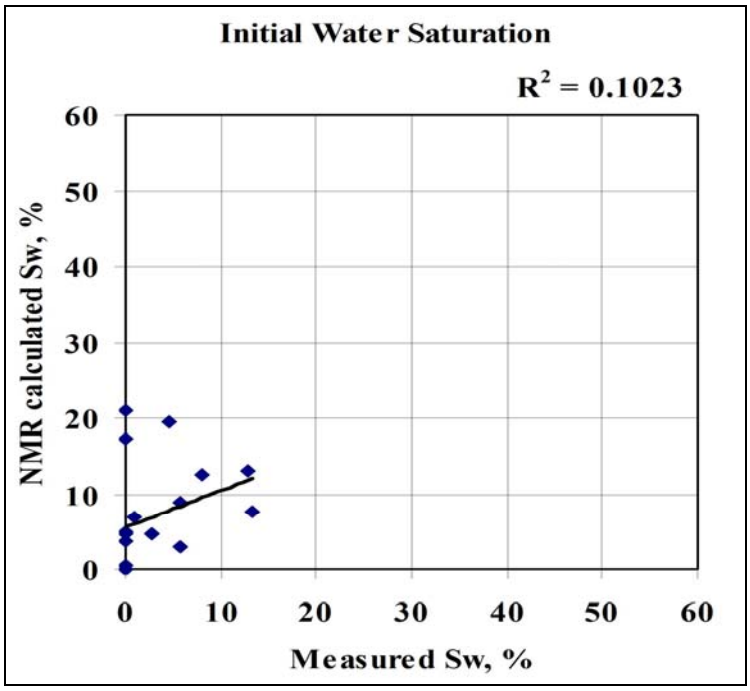

Figure 74. NMR calculated Swi versus measured Swi.

Cost and Schedule Status

The grant deliverable was completed on schedule and within cost as specified in grant contract.

Accomplishments

1. Five different reservoir systems were evaluated in the laboratory for enhanced oil recovery via surfactant imbibition.
2. High temperature (200^{o}F) laboratory tests support the surfactant soak process in the Interlake and Stony Mountain dolomite reservoirs on the Cedar Creek anticline. Future field tests are anticipated.
3. The Red River reservoir on the Cedar Creek anticline is not universally oil-wet as generally believed.
4. The San Andres laboratory work generated three field tests of the process.
5. An AI correlation was developed to predict water-frac results in a tight oil reservoir.
6. A review of 23 earlier surfactant soak field tests with updated production data showed that 4.5 lb of surfactant generated 1 bbl of incremental oil.
7. Four publications were generated during the course of the 2-year project:
    - Xie, X., Weiss, W.W., Tong, Z., and Morrow, N.: "Improved Oil Recovery from Carbonate Reservoirs by Chemical Stimulations." Journal of Petroleum Technology Vol. 57, No. 1, January 2005 (62-53).
    - Xie, X., Weiss, W.W., Tong, Z., and Morrow, N.: "Improved Oil Recovery from Carbonate Reservoirs by Chemical Stimulations." SPE Journal, September 2005 (276-285).
    - Weiss, W.W., Weiss, J.W., Subramaniam, V., and Xie, X.: "AI Applied to Evaluate Waterflood Response, Gas Behind Pipe, and Imbibition Stimulation Treatments," Journal of Petroleum Science and Engineering, Vol 49, Issues 3-4, December 2005 (110-121).
    - Weiss, W.W., Xie, X., Weiss, J.W., Subramanian, V., Taylor, A., and Edens, F.: "Artificial Intelligence Used to Evaluate 23 Single-Well Surfactant Soak Treatments," SPE Paper 89457, SPE Reservoir Evaluation & Engineering, June, 2006.

Actual Problems

Delays in conducting the field tests were the result of oil company priorities. In a similar vein, reservoir core and fluid samples were slow in arriving to the laboratory. Engaging the service companies in this project led to one presentation to Occidental Petroleum. Many more were envisioned.

Technology Transfer Activities

As the laboratory results became available, they were presented to Encore Acquisition, ConocoPhillips, Yates Petroleum, Range Resources, Texland Petroleum, Cano Petroleum, and Kinder Morgan. Additionally results of the San Andres laboratory work geared toward service company needs were presented to Tiorco and Gel-Tec, small niche-type service companies located in Denver, Colorado and Midland, Texas.

Gel-Tec requested a sample of T91-8 for a bench scale study of the handling properties of the surfactant. They will investigate potential mixing and foaming problems of the viscous surfactant when applied in the field. It is expected that Gel-Tec and Tiorco will generate field tests of the technology in the San Andres and Phosphoria formations as well as create interest in the process among producers in the Arbuckle formation.

The laboratory and field results were used in the four publications mentioned above. Additionally the concepts developed during this research effort are being utilized in an effort to improve gas deliverability from natural gas storage reservoirs.

Conclusions

Three of the five different reservoir systems evaluated in the laboratory suggested that oil recovery via spontaneous imbibition is a promising technique. An update of previous field tests in the Phosphoria dolomite of the surfactant soak process demonstrated that the process can be profitable. However, three field tests conducted in the West Fuhrman Masho San Andres dolomite were not successful. Poor results were not anticipated based on the laboratory tests and a published report[2] by Marathon of a successful San Andres test.

Additional tests in dolomite producing zones on the Cedar Creek anticline are anticipated, and the results of these tests will be incorporated into a database consisting of field tests conducted in a Big Horn Basin Phosphoria reservoir, a Permian Basin San Andres reservoir, and the Interlake and Stony Mountain reservoirs on the Cedar Creek anticline.

There is some evidence that a more detailed analysis of the gamma ray logs might correlate with surfactant soak performance. Similar partial correlations were seen in the laboratory work. To date, none of the evidence supports robust correlations; however, as the size of the database increases, it is expected that correlations will be developed using AI tools such as fuzzy logic and neural networks. Additionally future work may improve the surfactant selection process.

High temperature imbibition tests were successfully conducted, demonstrating that spontaneous imbibition is a viable recovery process in the 200°F reservoirs on the Cedar Creek Anticline. Unfortunately the measurement of porosity and saturations using NMR imaging techniques was not successful.

Due to the current state of activity in the domestic oil and gas business, long lead times are required to gather information and conduct field tests. The high rate of activity affects both producing and service companies in their ability to meet non-contractual obligations.

References

1. Standnes, D.C. and Austad, T.: "Wettability alteration in chalk 2. Mechanism for wettability alteration from oil-wet to water-wet using surfactants," J. Petr. Sci. Eng., 28 (2000), 123-143.
2. Chen, H.L., Lucas, L.R., Nogaret, L.A.D., Yang, H.D. and Kenyon, D.E., "Laboratory monitoring of surfactant imbibition using computerized tomography," SPE 59006, presented at the International Petroleum Conference and Exhibition, Villahermosa, Mexico, February 1-3, 2000.
3. Hirasaki, G. and Zhang, D.L., "Surface chemistry of oil recovery from fractured, oil-wet, carbonate formation," SPE 80989, presented at the SPE International Symposium on Oilfield Chemistry, Houston, Texas, February 5-8, 2003.

4. Graham, J.W., McCardell, W.M., Osoba, J.S. and Richardson, J.G., "Method of increasing oil production," US patent 2792894, 1953.
5. Putra, E., Fidra, Y. and Schechter, D.S.: "Study of waterflooding process in naturally fractured reservoirs from static and dynamic imbibition experiments," Proceedings of the International Symposium of the Society of Core Analysts, Golden, CO, August 1999.
6. Craig, M.D., "Oil recovery process employing cyclic wettability alteration," US patent 4842065, 1988.
7. Stone H.L., Graham, J.W. and Blackwell, R.J., "Oil recovery from fractured matrix reservoirs," US patent 3498378, 1970.
8. Spinler, E.A., Zornes, D.R., Tobola, D.P. and Moradi-Araghi, A.: "Enhancement of oil recovery using a low concentration of surfactant to improve spontaneous and forced imbibition in chalk," SPE 59290 presented at the SPE/DOE Improved Oil Recovery Symposium, Tulsa, OK, April 3-5, 2000.
9. Austad, T., et al., "Seawater as IOR fluid in fractured chalk," SPE 93000, presented at the SPE International Symposium on Oilfield Chemistry, Houston, TX, Feb. 2-4, 2005.
10. Xie, X. and Weiss, W. W.: "Chemical stimulation of oil wells producing from carbonate reservoirs," Phase II annual report, Contract No.DE-FG03-01ER83226, U.S. DOE SBIR Program, May 2003.
11. Strand, S., Hognesen, E. and Austad, T., "Wettability of carbonates–effects of potential determining ions (Ca2+ and SO42-) and temperature. Colloids and Surface A: Physicochemical and Engineering Aspects 275, Issue 1-3 (2006) 1-10.
12. Porter, M.R., "Handbook of surfactants," second edition, Blackie, Chapman & Hall, 1994.
13. Hung, I., Rossini, A. J., and Schurko, R.W.: "Application of the Carr-Purcell Meiboom-Gill Pulse Sequence for the acquisition of solid-state NMR spectra of spin-1/2 nuclei," J. Phys. Chem. A, 108 (34), 7112 -7120, 2004.
14. Howard, J.J., Personnel Communication, ConocoPhillips Laboratories, Bartlesville, OK,.
15. Sippel, M.A., Carrigan, W.C., Luff, K.D. and Canter, L.: "Intelligent computing system for reservoir analysis and risk assessment of the Red River Formation," DE-FC26-00BC15123-3, Luff Exploration Company, Denver, CO, November 2003.
16. www-ra.informatik.uni-tuebingen.de/SNNS
17. Du, Y., Weiss, W.W., Xu, J., Balch, R.S., and Li, D.: "Obtain an optimum artificial neural network model for reservoir studies," SPE 84445 presented at the SPE Annual Conference, Denver, CO, 5-8 October 2003.